SCIENCO

SOUTHERN BRAZILIAN JOURNAL OF CHEMISTRY

ISSN 0104-5431

AN INTERNATIONAL FORUM FOR THE RAPID PUBLICATION OF ORIGINAL SCIENTIFIC ARTICLES DEALING WITH CHEMISTRY AND RELATED INTERDISCIPLINARY AREAS

VOLUME TWO, NUMBER TWO

DECEMBER 1994

SOUTHERN BRAZILIAN JOURNAL OF CHEMISTRY

ISSN 0104-5431

VOLUME TWO, NUMBER TWO DECEMBER 1994

CONTENTS / CONTEÚDO

SOUTHERN BRAZILIAN JOURNAL OF CHEMISTRY
Vol. 2, No.2, 1994.

XORGE ALEJANDRO DOMINGUEZ, MEXICO'S FOREMOST ORGANIC CHEMIST

Xorge Alejandro Dominguez, Mexico's Foremost Organic Chemist was born in Orizaba, State of Veracruz, Mexico on November 12, 1926 and died of heart attack in Mexico City on May 26, 1991, only hours after he had been awarded by President Carlos Salinas de Gortari the *Lázaro Cárdenas Medal* for his contributions and dedication to the scientific advancement of Mexico.

He attended primary and secondary schools in his native city (Escuela Primaria Cantonal and Escuela Secundaria Federal Obrera de Orizaba). He continued his studies in Mexico City and obtained the Bachelor Degree in Biological Chemistry from the Instituto Politécnico Nacional in 1950. In 1952 he obtained a Master of Science Degree from Harvard University and in 1964 he was awarded a Ph.D. Degree in Chemistry from the University of Texas. In 1970, Professor X.A. Dominguez received an Honorary Doctoral Degree from the Universidad Autónoma de Guadalajara.

His first faculty appointment (1946-47) was in the National School of Biological Sciences of the National Polytechnic Institute of Mexico in Mexico City. From 1948 until his death he was Professor of Chemistry at the Instituto Tecnologico y de Estudios Superiores de Monterrey - ITESM, in Monterrey, Nuevo León, Mexico. From 1957 to 1991 he acted as Chairman of the Chemistry Department of ITESM. Prof. Dr. X.A. Dominguez taught as Visiting Professor at many universities in different countries, including Mexico, United States, Costa Rica, Guatemala, El Salvador, Nicaragua, Colombia and Argentina.

Professor X.A. Dominguez had research interests that dealt mainly with the chemistry of natural products. He discovered,isolated and identified many new chemical substances from Mexican plants and organized many international symposia and conferences dealing with phytochemistry. He has published over 250 articles and several books dealing with this subject. During the 44 year period as professor and researcher at the Instituto Tecnologico y de Estudios Superiores de Monterrey, ITESM, he acted as research advisor of more than 200 students at the graduate and undergraduate levels. More than 100 graduate students completed their master's theses or doctoral dissertations under his supervision.

We first met Prof. Dr. Xorge A. Dominguez in December of 1975 during the First Chemical Congress of the North American Continent in Mexico City. At the time, he was already one of the most respected chemists in Mexico. Wherever he went, he was the center of attention, appreciation and esteem.

Professor Xorge A. Dominguez was a very educated and erudite man, a scientist aware of his social responsability and a patriot. He firmly believed that the main purpose of the true scientist was the search for truth and its application to the improvement of the conditions of man. He was also a great educator. Like all good teachers,he believed in the power of example and thought that a teacher can teach the most by his own example.

According to many of his students and collaborators who used to call him "Doctor", Prof. X. A. Dominguez was not only a professor, educator, chairman, co-worker, researcher, but also a guide, source of inspiration and example, father, friend and a lot more.Many recollect their peripatetic walks with him on the various floors of the Chemistry Building, then to the Post Office, Administration Building Library of ITESM, etc. and back to his office. During these journeys or peregrinations with him they learned about a lot things while accompanying the teacher. The knowledge gained could be philosophy, chemistry, politics, a new chapter of the history of Mexico, world history or about the poverty oath of the true scientist. Sometimes he would tell a lot of jokes. His office was a true "Temple of Entropy". Mountains of books, journals, articles, papers and all kinds of other "things" (cosas). There, almost in a strike of magic, he always found what he was looking for.

Professor Xorge A. Dominguez was preoccupied with the teaching of science at all levels. He was the author of more than 35 chemistry books aimed for university and secondary school instruction. Among them we cite *Fundamentos y Problemas de Química Orgánica*, Limusa-Wiley, 1970; *Fitoquímica*, Limusa-Wiley, 1975; *Química Orgánica Fundamental*,Limusa, 1980; *Química Orgánica Experimental*, Limusa, 1982 and *Cromatografia en Papel y en Capa Delgada*, OEA, Washington, D.C., 1975. He also translated about a dozen books dealing with chemistry or other areas of science, mainly from English.

Professor X. A. Dominguez was widely respected in the scientific community. He was a member of the Mexican Chemical Society, American Chemical Society, Swiss Chemical Society, Phytochemical Society of America, National Academy of Scientific Research of Mexico and a fellow of the Royal Chemical Society. He was President of the Northeast Section of the Mexican Chemical Society from 1976 to 1978 and gave many invited lectures throughout Europe and the Americas.

He received many awards for excellence in teaching or research in chemistry. Among them we cite the Romulo Garza Prize for Research in 1974 and for Teaching in 1975, National Scientific Prize Luis Elizondo in 1976, National Education

SOUTHERN BRAZILIAN JOURNAL OF CHEMISTRY
Vol. 2, No.2, 1994

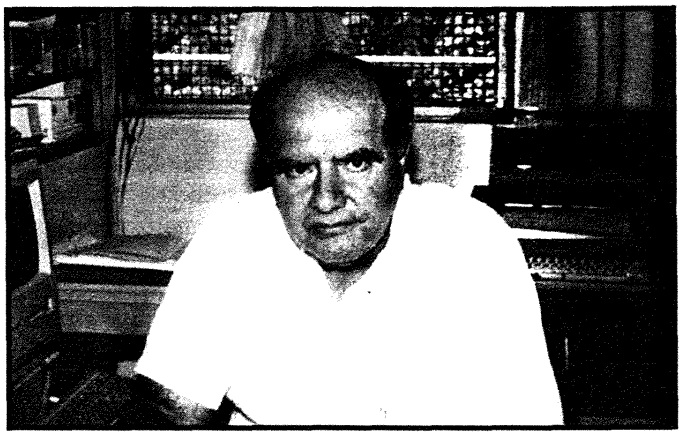

XORGE ALEJANDRO DOMINGUEZ

AZTEC CALENDAR. SYMBOL OF PERIODIC ONDULATORY BEHAVIOR OF THE UNIVERSE AND TOKEN OF THE ETERNITY OF KNOWLEDGE.

Award in 1982, Andrés del Rio National Award in Chemistry in 1984, National Chemical and Pharmaceutical Sciences Award in 1986 and the Lázaro Cárdenas Medal in 1991.

He was Regional Editor (1970-1972) and Editor in Chief of the *Revista Latinoamericana de Química* from 1972 to 1991 and member of the Editorial Board of other journals and periodicals including the *Revista de la Sociedad Química de México* and *Revista Iberoamericana de Educación Química*.

Prof. Xorge A. Dominguez was also a Member of the Editorial Board of the *Southern Brazilian Journal of Chemistry* and he gave us very valuable advice during the initial stages of this Journsl. He was always ready to help, collaborate and fulfill his responsabilities. *¡Adiós muy distinto compañero y amigo !*

Lavinel G. Ionescu

ACKNOWLEDGEMENT. We express our sincere thanks to Dra. Elsa M. Guajardo Touché, Directora del Depto. de Química, ITESM, Monterrey, N.L., Mexico for her assistance and consideration.

SOUTHERN BRAZILIAN JOURNAL OF CHEMISTRY
Vol. 2, No.2, 1994

EXPERIMENTAL AND PREDICTED ISOELECTRIC POINTS FOR NIOBIUM AND VANADIUM PENTOXIDE

Gaspar González* and Sandra M. Saraiva
Petrobrás Research Center, Cidade Universitária, quadra 7,
Ilha do Fundão, CEP 21949-900, Rio de Janeiro, Brazil

Washington Aliaga
Departamento de Minas, Facultad de Ciencias Físicas y Matemáticas,
Universidad de Chile, Casilla 2777, Santiago, Chile

ABSTRACT

The isoelectric points for niobium and vanadium pentoxides were determined through electrophoretic measurements and the experimental results were compared with three alternative procedures to predict this parameter. Experimental and predicted results show good agreement for Nb_2O_5 that presents a well defined value for the isoelectric point but they do not correlate well in the case of V_2O_5 that presents a rather high solubility in the isoelectric pH region.

RESUMO

Os pontos isoelétricos de pentóxido de niobio e vanádio foram determinados experimentalmente através de medidas eletroforéticas e comparados com valores calculados teoricamente usando tres métodos diferentes. Para Nb_2O_5, que apresenta um ponto isoelétrico muito bem definido, os valores experimentais concordam muito bem com os valores calculados. Por outro lado, para V_2O_5, que tem uma solubilidade alta na região do pH isoelétrico, a correlação é menos satisfatória.

Key words: Niobium pentoxide, vanadium pentoxide, electrophoresis, isoelectric points.

---

*Author to whom correspondence should be addressed.

INTRODUCTION

The knowledge of the point of zero charge (zpc) or the isoelectric point (iep) of the individual components of complex particulate materials dispersed in aqueous electrolyte solutions permits, in many cases, a characterization of the solids in terms of their surface composition. For the case of supported catalysts for instance, Gil-Llambias et al.[1] developed a method to estimate the apparent surface coverage of the particles by equating the isoelectric point of the catalyst with the weighted average of the iep of each component, i.e., the support and the supported oxide.

Niobium and vanadium pentoxide are extensively used in the preparation of new materials like high electric conductivity or dielectric ceramics[2], support material for metallic catalysts[3] or as catalysts when dispersed on the surface of support oxides like Al_2O_3, TiO_2 or SiO_2[4]. However, there is still very little information available on the surface properties of these oxides, when dispersed in aqueous electrolyte solutions. In this paper, the isoelectric points for Nb_2O_5 and V_2O_5 obtained using electrophoretic measurements are reported and the experimental results are compared with the predicted values obtained using three different procedures to estimate this parameter theoretically.

EXPERIMENTAL PROCEDURE

Two samples of niobium pentoxide were used in this work. One of them was prepared by calcination of niobic acid (Nb_2O_5 x nH_2O) at 550°C. Through X-ray diffraction, the solid was identified as Nb_2O_5 presenting a monoclinic structure. The sample was polydisperse containing particles from 1 to 100 μm in diameter and a surface area of 34 m^2g^{-1}. The other sample was kindly supplied by the Companhia Brasileira de Metalurgia e

Mineração and presented an orthorhombic structure. This preparation was fairly monodisperse, containing predominantly 1 μm particles and a surface area of 3 m^2g^{-1}. The vanadium pentoxide was a commercial sample obtained from Merck and presented an orthorhombic structure. Most of the particles were 2 μm in diameter but a small fraction presenting sizes up to 20 μm was also present. The BET surface area for this oxide was 4 m^2g^{-1}. Copper oxide was an analytical grade commercial sample obtained from Merck, Al_2O_3 was obtained from Catalysts Chemical Industry (CCI, USA) and Fe_2O_3 was a sample of pure mineral produced in the region of Minas Gerais, Brazil.

Water was deionized using a Millipore Milli-Q columns system and its resistivity was about 10 MΩ.cm. Potassium nitrate, nitric acid and sodium hydroxide were reagent grade products and were used without further purification.

The electrophoresis of the solid particles was measured using an electrophoresis apparatus provided with a thin walled cylindrical cell (Rank Bros. UK). The polarity of the electrodes was reversed between consecutive measurements to avoid polarization. The dispersions were prepared in KNO_3 solutions and the pH was modified using HNO_3 and KOH. Mean values resulting from at least twelve measurements for each point were the reported values. For V_2O_5 a few measurements were also carried out using a Malvern Zetasizer IIc particle electrophoresis analyzer; the results obtained using both techniques were practically identical.

RESULTS AND DISCUSSION

Experimental Isoelectric Points

The electrophoretic mobility versus pH diagrams obtained for the two samples of niobium pentoxide in potassium nitrate solutions are presented in Figure 1. The curves were drawn fitting the experimental

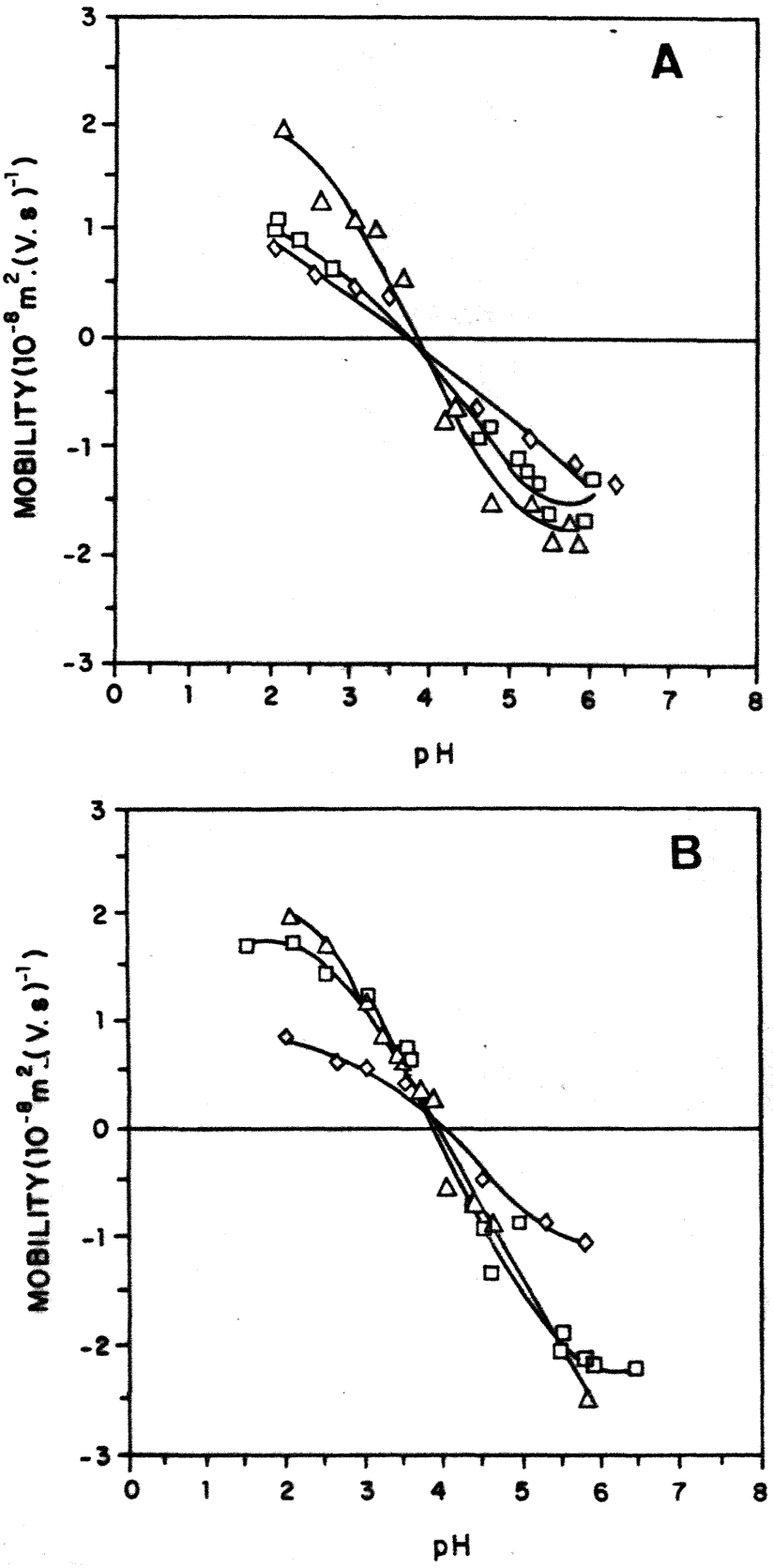

FIG. 1 - Eletrophoretic mobility-pH diagrams for Nb_2O_5 calcinated at 550°C (A) and commercial sample (B) in KNO_3 solution. -Δ- $5x10^{-4}$; -□- $5x10^{-3}$ and -◇- $5x10^{-2}$ mol dm^{-3}.

points to a fourth-order polynomial. For both samples, the electrophoretic mobility is zero at the same pH value for the three electrolyte concentrations employed as expected for particles dispersed in an indifferent electrolyte solution[5]. An isoelectric point of 3.8 was therefore obtained for this oxide.

The behavior of the vanadium pentoxide dispersions was different. The solid particles presented a rather high solubility in acid as well as in alkaline solutions. For this reason, experimental measurements were difficult to carry out in this system due to the high conductivity of the aqueous dispersions. As a result, it was not possible to determine the mobility of particles under low pH conditions, at which positively charged species should be expected to be present, even using the zeta sizer apparatus that detects particles in the submicron range. The experimental results, when extrapolated to low pH values, showed isoelectric points between pH 1 and 1.5 depending on the concentration of electrolyte. The isoelectric point obtained by Gil Llambias[6] for a different sample of V_2O_5 also falls in this pH region. In their study, only one point was presented for positively charged particles, which confirms the experimental difficulties in this pH region. The small increment in the extrapolated iep for higher electrolyte concentration may be attributed to specific adsorption of ions by the solid but may also correlate with the formation of highly charged isopoly-vanadates in solution and its subsequent reprecipitation on the particles as described by Healy for other oxides[7].

Predicted Isoelectric Points

When an insoluble metallic oxide is suspended in water, the hydroxylated surface groups undergo amphoteric dissociation according to the reactions:

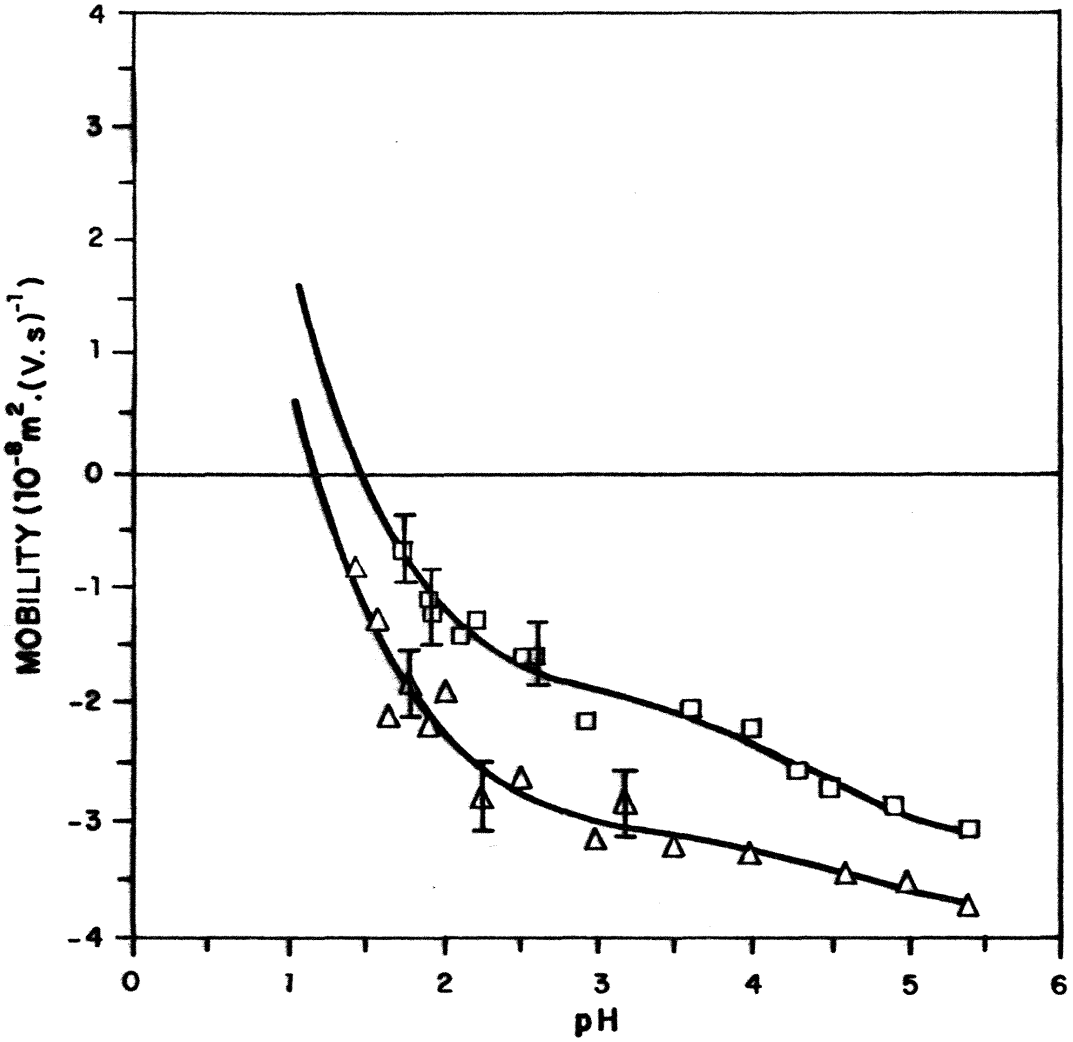

FIG. 2 - Eletrophoretic mobility-pH diagrams for V_2O_5 in KNO_3. -Δ- $5x10^{-4}$ and -□- $5x10^{-3}$ mol dm^{-3}. The points containing deviation bars were obtained using the Zetasizer apparatus.

$$\text{...MOH} + H^+ \underset{}{\overset{K_b}{\rightleftharpoons}} \text{...MOH}_2^+$$

$$\text{...MOH} \overset{K_a}{\rightleftharpoons} \text{MO}^- + H^+$$

Where MOH, MOH_2^+ and MO^- are the neutral, positively and negatively charged species on the solid surface and K_b and K_a are the basic and acid dissociation constants, respectively.

At a particular pH value the concentration of positive sites equals the concentration of negative sites. This condition is defined as the point of zero charge[8] which, in the absence of specific adsorption, should coincide with the isoelectric point. From the previous equations, it is possible to show that the point of zero charge may be defined by the following relationship:

$$ZPC = \frac{1}{2}\,(pK_a - pK_b) \qquad (1)$$

A simple method to estimate the point of zero charge for metallic oxides was suggested by Tanaka and Ozaki[9]. They used a parameter called generalized electronegativity of the metal ion, X_i, defined as:

$$X_i = (\delta I/\delta z) \qquad (2)$$

Where z is the charge on the metal ion and I is the ionization potential of the atom. I may be approximately expressed as a quadratic function of z:

$$I = Az + Bz^2 \qquad (3)$$

Obtaining the derivative of I in Equation (3) as:

$$X_i = A + 2Bz \qquad (4)$$

for z = 0, X_i is equal to the Pauling's electronegativity[10] of the

neutral atom, X_0, hence,

$$X_i = (1 + 2 \frac{B}{X_0} z) X_0 \quad (5)$$

The ratio B/X_0 was assumed to be unity by the authors and a good linear relationship between pK_a and X_i was obtained. As expected from equation 1, the zpc also correlates with the generalized electronegativity and when all the zpc and iep values compiled by Parks[11] were plotted against this parameter a fair linear correlation was also obtained.

We selected thirteen oxides for which there are reasonably reliable zpc and/or iep data in the literature and calculated the corresponding X_i using the electronegativity values reported by Gordy and Thomas[12], the values are presented in Table I.

The equation obtained by least-squares fitting the data to a straight line (Figure 3) was:

$$ZPC = 14.43 - 0.58 X_i \quad (6)$$

In Table 1 are also presented the zpc values obtained using equation 6. A reasonable agreement is observed between the experimental and predicted data. An equally acceptable agreement was obtained for other oxides not included in Table I.

The electronegativities for niobium and vanadium are 1.7 and 1.9. Introducing these parameters in equation 6, the zpc values of 3.6 and 2.3 are obtained for Nb_2O_5 and V_2O_5, respectively. The results show a good agreement with the experimental data in the case of niobium but the value predicted for vanadium pentoxide is higher than the value obtained from the extrapolation of the experimental data.

One way to improve the predicted results would be to calculate the ratio B/A (or B/X_0 in equation 5) assumed to be one, by Tanaka and Ozaki. This constant may be obtained from the first and second ionization potentials of the metal ion. However, the use of these parameters did not improve the predicted zpc values for these oxides.

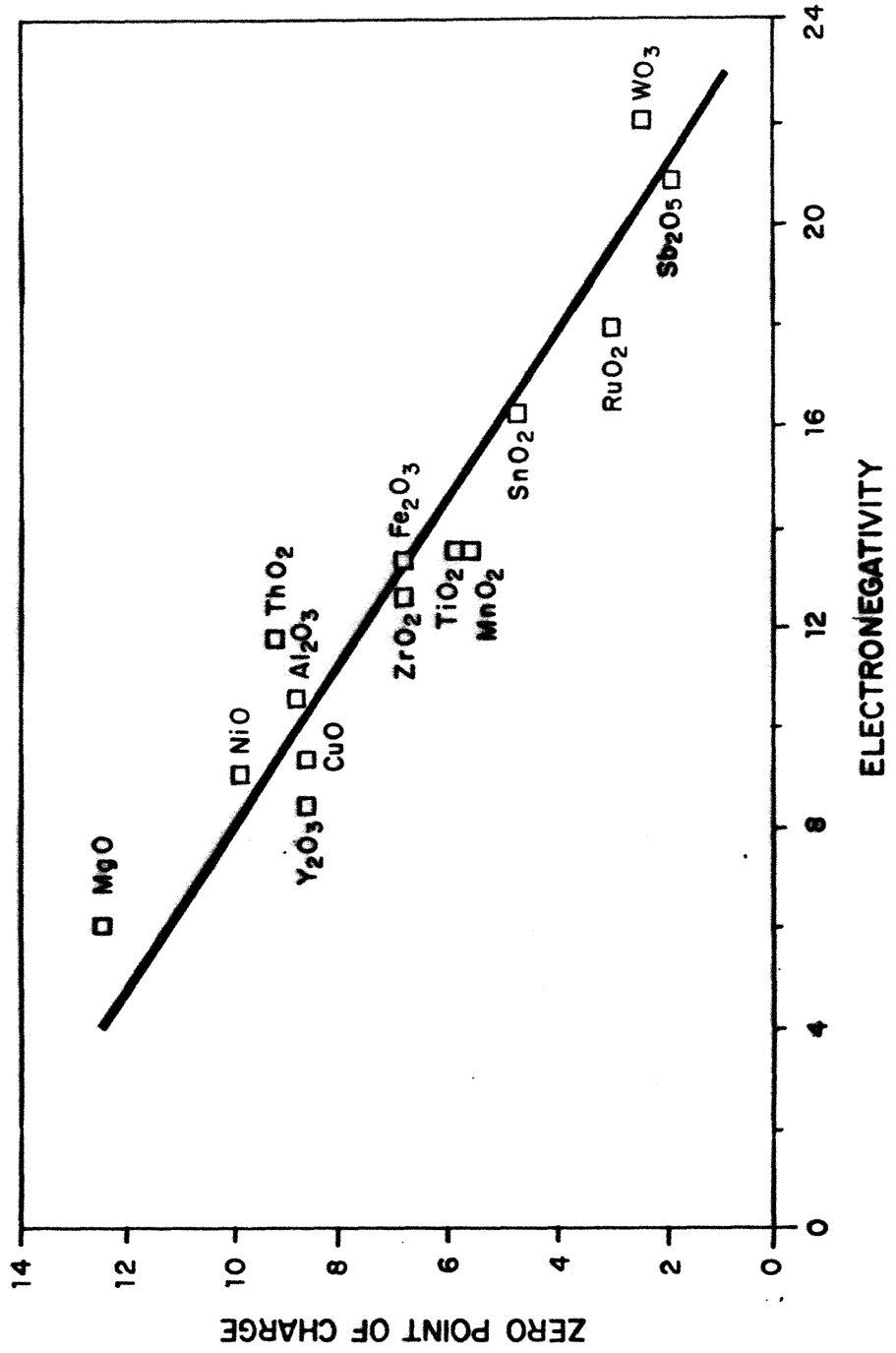

FIG. 3 - Experimental zpc versus generalized electronegativity for several metal oxides.

TABLE I

Points of Zero Charge and Generalized Electronegativity of the Various Oxides Used in Figure 3

Oxide	Experimental zpc	Reference	X_i	zpc predicted by equation 6
WO_3	0.3	13	26.0	-0.5
Sb_2O_5	1.9	14	19.6	3.0
SnO_2	4.7	15	16.2	5.0
RuO_2	5.1	16	18.0	4.0
MnO_2	5.6	17	13.5	6.6
TiO_2	5.8	18	14.4	6.1
Fe_2O_3	6.8	this work	12.6	7.1
ZrO_2	6.8	19	13.5	6.6
CuO	8.5	this work	10.0	8.6
Y_2O_3	8.6	20	8.4	9.0
Al_2O_3	8.8	this work	10.5	8.3
NiO	9.8	21	8.5	9.5
MgO	12.4	22	6.0	11.0

An alternative procedure to predict isoelectric points was introduced by Parks[11] and further developed, more recently, by Yoon et al.[23]. The authors used a model similar to that already described for the amphoteric dissociation at the mineral surface and derived an expression for the free energy involved in the process of approaching two protons to the metal oxide. The equation obtained for the zero point of charge was:

$$ZPC = 18.43 - 53.12\ (\frac{v}{L}) - \frac{1}{2}\log\ (\frac{2 - v}{v}) \qquad (7)$$

Where v represents the charge on the metal ion divided by its coordination number in the oxide, L is the distance between the metal ion and the proton in the protonated oxide, defined as the O-H distance in the ice (1.01 Å) plus the M-O distance in the oxide crystal. The numerical constants in equation 7 were calculated by the authors using 12.4 and 9.1, respectively, for the zpc of MgO and α-Al_2O_3 and the corresponding crystallographic metal-oxygen distances in these oxides.

Niobium pentoxide presents octahedral coordination with a niobium oxygen distance of 1.95 ± 0.01 Å and a coordination number of 6[24]. When this data were introduced in equation 7, a value of 3.4 was obtained for the zpc of Nb_2O_5. Vanadium pentoxide has an orthorhombic structure with a coordination number of 5. The V-O distance reported by Wickoff[25] is between 1.54 and 2.02 Å and the values 1.93, 1.97, 1.95 and 1.67 Å were reported by Pope and Dale[26] for the five V-O bonds. Using these data, predicted values in the range -2.4 to 0.9 were obtained for the iep of V_2O_5. Therefore, the predicted value for V_2O_5 in this case was lower than the iep's obtained by the extrapolation of the experimental electrophoretic mobility data, but a good fit was obtained for Nb_2O_5.

A third method to estimate the point of zero charge of oxides was also introduced by Parks[8] and subsequently applied to oxides[27] and to salt type minerals[28]. The partial dissolution of the oxide results in the formation of metal hydroxy complexes in solution presenting different charges. When the free energies of formation for these species are known, it is possible to draw a diagram showing the logarithm of the concentration of the different species as a function of pH. The isoelectric point of the solution is defined as the pH at which the concentration of the two oppositely charged dominant ionic species of the same central ion, are equal. Considering that the solution is in equilibrium with the solid-solution interface it seems reasonable to assume that this pH also corresponds to the isoelectric point (or point of zero charge) of the solid.

Table II presents the free energies of formation for a few hydroxo complexes for niobium (V) and vanadium (V) ions[29,30].

Using these data, it was possible to plot the log concentration - pH diagrams presented in Figures 4 and 5. The zpc's for Nb_2O_5 and V_2O_5 obtained using this method were 3.4 and 2.2, respectively. There are several different negatively charged species in the alkaline pH, specially in the case of vanadium, however they do not affect the determination of the iep by this procedure.

TABLE II
Free Energy of Formation for Some Hydroxo-Complexes of Pentavalent Niobium and Vanadium[29,30]

Compound	ΔG_f (kcal.mol^{-1})
$Nb_2O_{5\ (s)}$	-422.6
$Nb(OH)_4^{+}{}_{(aq)}$	-288.9
$NbO_3^{-}{}_{(aq)}$	-222.8
$Nb(OH)_{5\ (aq)}$	-346.1
$V_2O_{5\ (s)}$	-339.3
$VO_2^{+}{}_{(aq)}$	-140.3
$H_3V_2O_7^{-}{}_{(aq)}$	-445.5
$H_3VO_{4\ (aq)}$	-248.6
$H_2VO_4^{-}{}_{(aq)}$	-244.0
$H_2V_{10}O_{28}^{4-}{}_{(aq)}$	-1847.3

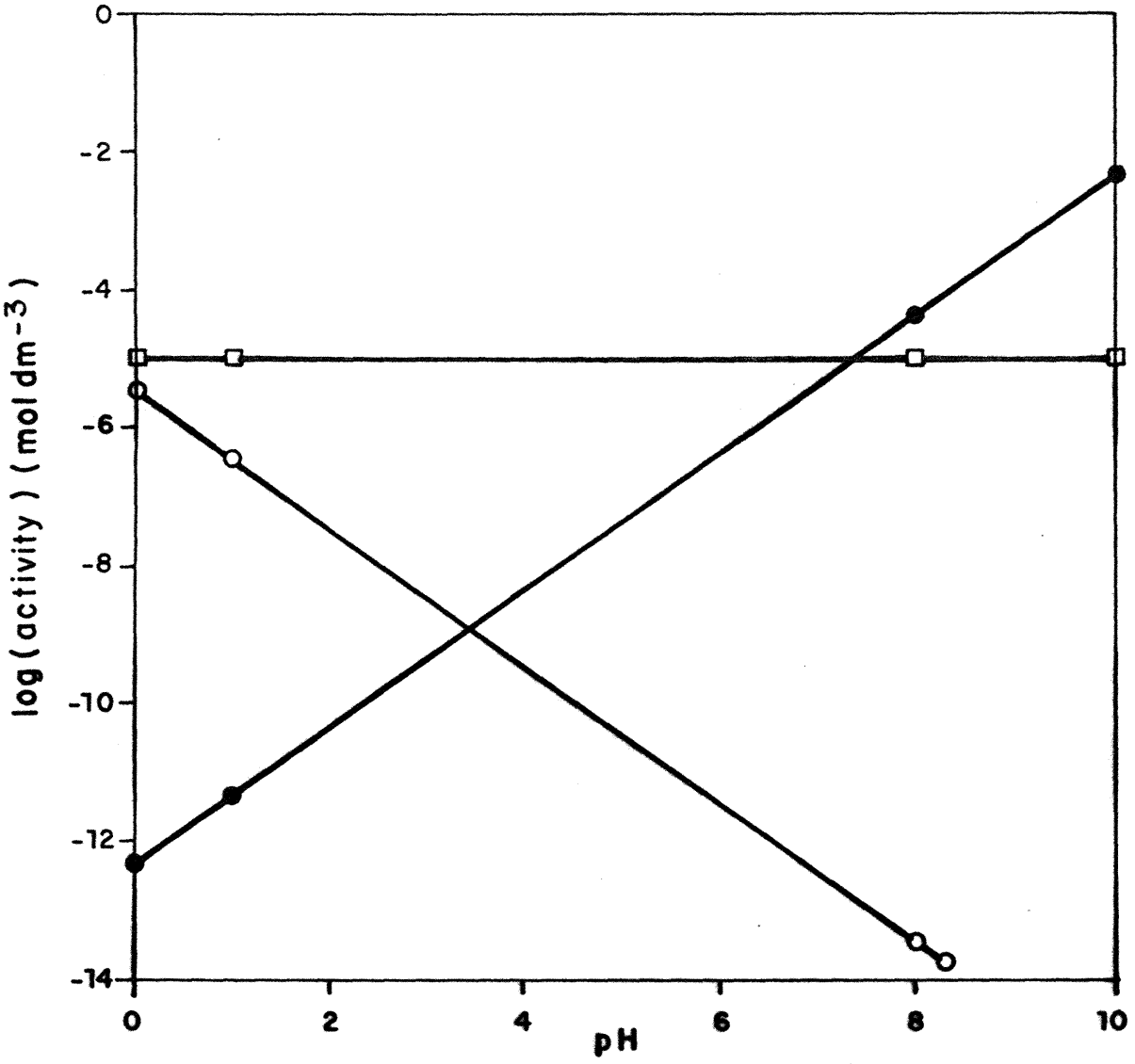

FIG. 4 - Logarithm of activity versus pH for Nb^{+5} dissolved species in equilibrium with Nb_2O_5 -□- $Nb(OH)_5$; -o- $Nb(OH)_4^+$; -●- NbO_3^-.

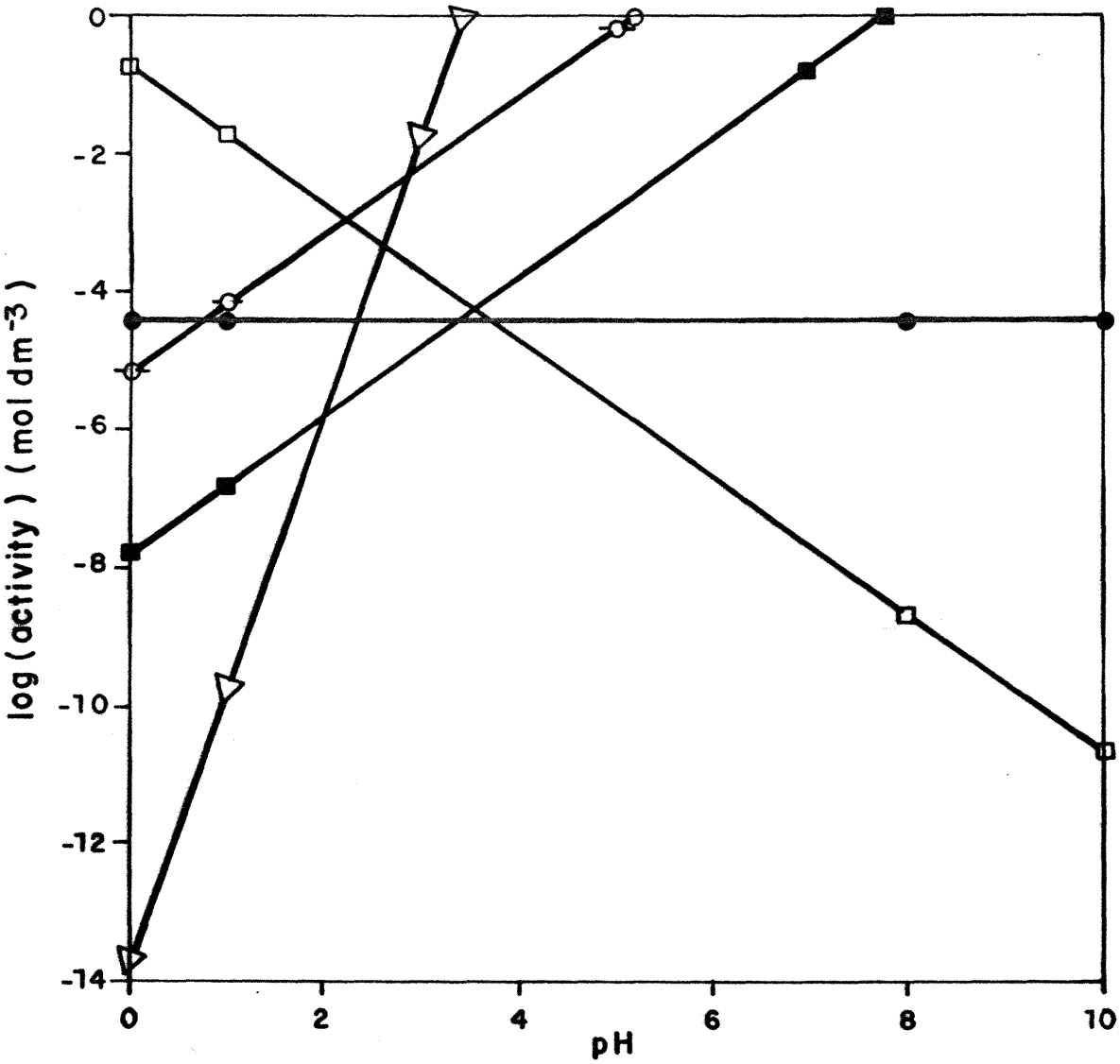

FIG. 5 - Logarithm of activity versus pH for V^{+5} dissolved species in equilibrium with V_2O_5 -□- VO_2^+ -o- $H_3V_2O_7^-$; -●- H_3VO_4; -■- $H_2VO_4^-$; -▽- $H_2V_{10}O_{28}^{-4}$.

TABLE III

Experimental and Predicted Isoeletric Points for Niobium and Vanadium Pentoxide

	Nb_2O_5	V_2O_5
Experimental values:	3.8	≅ 1.5*
Predicted values, method:		
Electronegativities:	3.6	2.3
Crystallographic data:	3.4	-2.4 to 0.9
Thermodynamic data:	3.5	2.3

* Extrapolated value

Table III summarizes the experimental isoelectric points as well as the values obtained by the three alternative procedures used to predict this parameter. It may be concluded that the experimental value obtained for niobium pentoxide i.e. 3.8, shows good agreement with the predicted values. For vanadium pentoxide it was not possible to obtain a well defined iep due, most likely, to an ill-defined interface caused by the high solubility of this oxide in the isoelectric pH region. The extrapolated values were around pH 1.5 and the correlation with the predicted values was less satisfactory in this case. It is interesting also to emphasize that the simplest predicting procedure, using the generalized electronegativity, conduces to results equivalent to those obtained using other more elaborated procedures.

REFERENCES

1. F. J. Gil-Llambías and A. M. Escudey-Castro, *J.C.S. Chem. Commun, 478* (1982).
2. T. O. Ota, I. Y. Yamai and J. Takanashi, *Adv. Ceram. Mater., 1, 4,* 371 (1986).
3. T. Isuka, T. Tanaka and K. Tanabe, *Mol. Catal., 17,* 381 (1982).
4. S. Okazaki and T. Okuyama, *Bull. Chem Soc. Jpn., 56,* 2159 (1983).
5. R. J. Hunter, *"Zeta Potential in Colloid Science - Principles and Applications"*, Academic Press, London (1981), pp. 229.
6. F. J. Gil-Llambías, A. M. Escudey, J. L. G. Fierro and A. López Agudo, *J. Catal., 95,* 520 (1985).
7. R. O. James and T. W. Healy, *J. Colloid Interface Sci., 40,* 53(1972).
8. G. A. Parks and P. L. de Bruyn, *J. Phys. Chem., 66,* 967 (1962).
9. K. I. Tanaka and A. Ozaki, *J. Catal. 8,* 1 (1967).
10. L. Pauling, *"The Nature of Chemical Bond"*, 3rd Ed., Cornell University Press, Ithaca, New York (1960).
11. G. A. Parks, *Chem. Rev., 65,* 177 (1965).
12. W. Gordy and W. J. Orville Thomas, *J. Chem. Phys., 24, 2,* 439, (1956).
13. F. J. Gil LLambias, *Bol. Soc. Chil. Quim., 28,* 7 (1983).
14. L. Xiao, P. Liao and W. Hu, *Colloids Surfaces, 26,* 273 (1987).
15. D. W. Fuerstenau and R. Herrera-Urbina *in "Surfactant-based Separation Processes", J. F. Scamerhorn and J. H. Harwell (eds.)*, Marcel Dekker, Inc. New York (1987).
16. S. Ardizzone, P. Siviglia and S. Trasatti, *J. Elecroanal. Chem., 122,* 395, (1981).
17. D. W. Fuerstenau and R. Herrera-Urbina *in "Cationic Surfactants, Physical Chemistry"* , Eds.: P. Holland and D. Rubingh, Marcel Dekker, New York (1991).
18. G. R. Wiese and T. W. Healy, *J. Colloid Interface Sci., 51,* 427 (1975).
19. J. Randon, A. Larbot, L. Cot, M. Lindheimer and S. Partyka, *Langmuir, 7* , 2654 (1991).
20. E. Kawahashi and E. Matijevic, *J. Colloid Interface Sci., 143* (1), 103, (1991).
21. S. Kittaka and T. Marimoto, *J. Colloid Interface Sci., 75,* 398 (1980).
22. M. Robinson, H. A. Pask and D. W. Fuerstenau, *J. Amer. Ceram. Soc., 47,* 516 (1964).
23. R. H. Yoon, T. Salman and G. Donnay, *J. Colloid Interface Sci., 70* (3), 483 (1979).
24. *"International Tables for X-Ray Crystallography"*, Published by The International Union of Crystallography by The Kynoch Press, vol. III (1968).
25. R. W. G. Wyckoff, *"Crystal Structures"*, 2nd Ed., Interscience Pub., New York (1963).
26. M. T. Pope and B. W. Dale, *Quart. Rev., 22,* 527 (1968).
27. J. Laskowski, P. W. Fuerstenau, G. González and R. Herrera-Urbina, *Min. Process. Technol. Review, 1,* 1 (1985).
28. P. Somasundaran and G.E. Agar, *J. Colloid Interface Sci., 24,* 433, (1967).
29. A. J. Bard, R. Parson and J. Jordan, *"Standard Potentials in Aqueous Solutions"*, Marcel Dekker Inc., New York (1985), pp 508 - 515.
30. H.E. Barner and R.V. Scheuerman, *"Handbook of Thermodinamical Data for Compounds and Aqueous Species"*, John Wiley and Sons, New York (1978), p 87.

SOUTHERN BRAZILIAN JOURNAL OF CHEMISTRY
Vol. 2, No.2, 1994

MICRO–HPLC SEPARATION OF SOME THENOYLTRIFLUOROACETONATES

Florentin TACHE, Andrei MEDVEDOVICI and George-Emil BAIULESCU

Department of Analytical Chemistry, Faculty of Chemistry, University of Bucharest, Blvd. Republicii no. 13, 70 346, Bucharest, Romania.

ABSTRACT

Micro-HPLC separation and UV detection of some metal thenoyltrifluoroacetonates has been achieved. Cyano, octadecyl and HTTA modified silica gels were used as stationary phases. Data about separation and detection parameters optimization are also described.

RESUMO

Alguns tenoiltrifluoroacetonatos metálicos foram separados por microcromatografia líquida de alta pressão e detectados com métodos ultravioletas.As fases estacionárias usadas forma silica gels modificados com ciano, octadecil e HTTA. A otimização dos parâmetros de separação e detecção foi descrita em termos dos dados experimentais.

Keywords:

micro-HPLC separation; UV detection; thenoyltrifluoroacetonates (Cr (III), Al(III), Fe (III), Cu (II), Pb (II), Mn (II), Zn (II), Cd (II), Co (II), Ni (II), Mg (II), Ca (II), Ba (II), Na (I), K (I)); process parameter optimization; HTTA bonded stationary phases.

INTRODUCTION

Separations of metal complexes using liquid chromatography are often preferred, compared to gas chromatographic techniques, due to the restriction withdrawing adopt volatility and thermal stability of analytes[1-3].

The advantage related to the higher selectivity of liquid chromatography is compensated, however, by lower efficiencies. The use of packed micro columns in HPLC is related to continuous effort in increasing the separation efficiency.

Liquid chromatography offers a variety of ways to differentiate partition of metal complexes between phases (adsorption [4-7], polarity [8-11], ionic association [12-14], ion exchange[15,16], ligand exchange [2], size exclusion[17-20]).

Particularities of the organic ligand (thenoyltrifluoroacetone -HTTA) allows the use of different kinds of stationary phases and mobile phase mixtures, respectively, according to normal- or reversed-phase elution mode.

EXPERIMENTAL PROCEDURE

Separations were performed on a Hewlett Packard HPLC 1090 liquid chromatograph, modified for micro column use, fitted with an internal loop injection valve (40 nL). The mobile phase flow was splitted before the injection valve by a T connection throughout a 360 mm x 4.6 mm i.d. column filled with RP8, 5 μm stationary phase (as flow rate regulator for the analytical micro column). A pneumatic pump Haskel, model DST-15, was used for the slurry packing of the column.

The UV detection was done with an Kontron Instruments 433 capillary UV-Vis detection system (with variable wavelength) equipped with a Z shaped quartz flow-cell (dead volume of 90 nL and 2 cm pathway). Working wavelength was 355 nm and 222 nm, respectively.

Response time was 0.5 sec.

The micro columns were 500 mm x 0.32 mm i.d. fused silica capillaries, home

packed with:

A. N-5-100 C_1/CN, 5 μm particle size, cyano modified silica gel stationary phase;

B. Nucleosil N-7-100 C_{18}, 7 μm particle size, octadecyl modified silica gel stationary phase;

C. HTTA chemically modified BioSil 90D 5S silica gel, 5 μm particle size, home synthesized (see **Figure 1**).

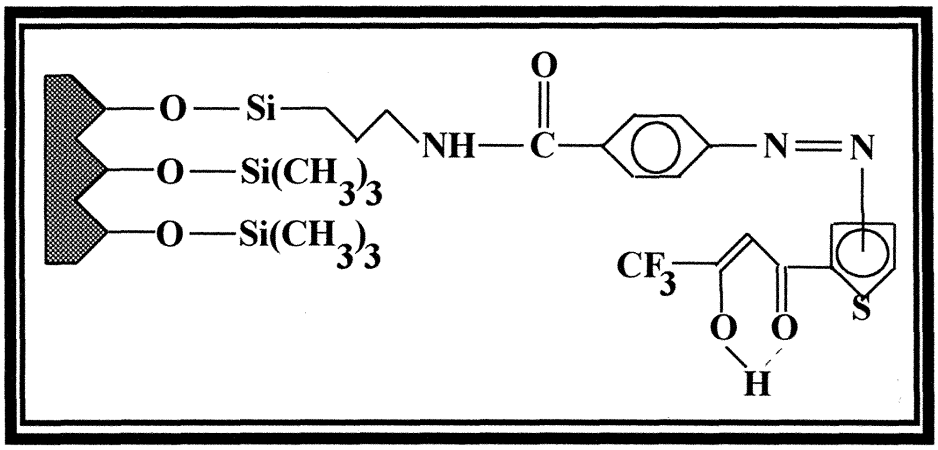

Figure 1. THE STRUCTURE OF THE HTTA CHEMICALLY MODIFIED BioSil 90 D 5S.

The packing of the stationary phases was performed by slurry packing method: 100 mg stationary phase was dispersed in a mixture of carbon tetrachloride :methanol (1:1, v/v). The packing was obtained at 500 bars during 4 hours, with acetonitrile as pumping solvent.

Flow rates through micro columns were selected in the range of 2 - 3 μL/min.

Mobile phase compositions were:

I. for stationary phase A, hexane:dichlormethane binary system, in variate proportions;

II. for stationary phase B, acetonitrile:water binary system, in variate proportions;

III. for stationary phase C, HTTA 1% in acetone.

Samples are represented by chloroform solutions (2 μg/μL) of HTTA complexes with Cr(III), Al(III), Fe(III), Cu(II), Mn(II), Pb(II), Zn(II), Cd(II), Co(II), Ni(II), Mg(II), Ca(II), Ba(II), Na(I) and K(I).

RESULTS AND DISCUSSION

Due to the fact that HTTA is an asymmetrically substituted organic ligand, for those complexes with trivalent metallic ions which are exhibiting an octahedral structure, the relative positions of the organic reagent substituents around the metallic ion leads to different forms, assimilated as geometrical isomers. It is expected, for selective chromatographic systems, to observe the splitting of the peaks for such kind of complexes .

The only possible separations of geometrical cis-trans isomers is effective for $Cr(TTA)_3$.

Cis-trans isomers of $Cr(TTA)_3$ are separated (also from the free ligand) in both systems A/(I) and B/(II), respectively.

In the first case, the resolution between the two isomers is increasing with the increasing of hexane percentage in the mobile phase (see **Figure 2**). **Figure 3** shows the typical chromatogram obtained with such elution system.

In the second case, the resolution between isomers is decreasing with the increasing of water percentage in the mobile phase (see **Figure 4**). **Figure 5** is showing the typical chromatogram obtained with B/(II) system.

The cis isomer is obtained in a lower yield from the synthesis step. Thermodynamically, the lower energy state for the molecule corresponds to the trans isomer (similar substituents of the ligand spatially distributed around the metallic ion, resulting in low repulsive effects). It is normal to be expected that the most stable state should be obtained with higher probability.

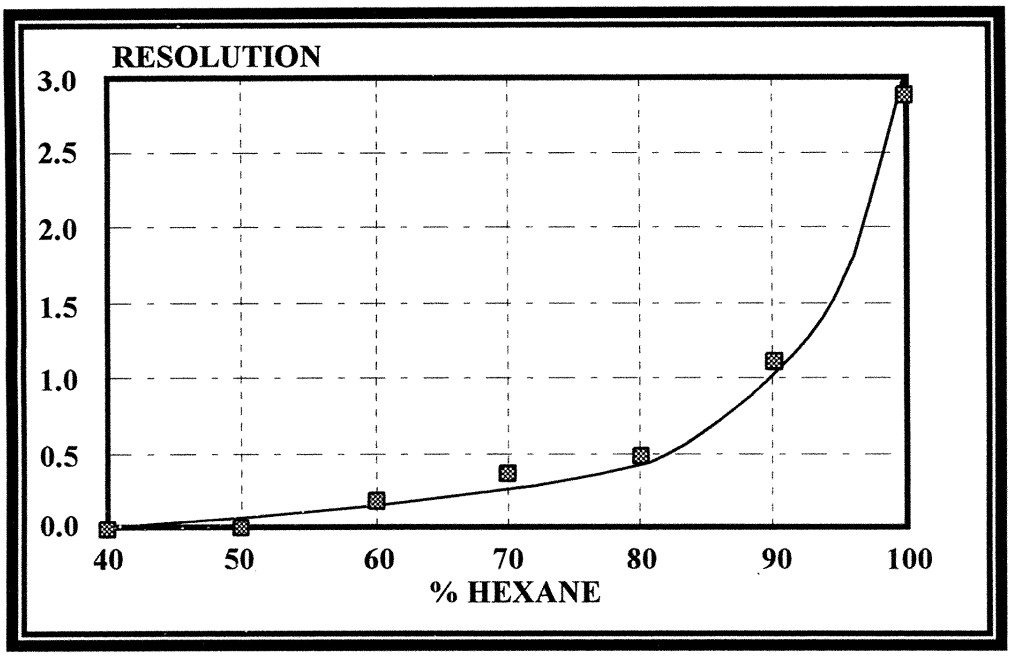

Figure 2. THE RESOLUTION VARIATION OF THE CIS-TRANS ISOMERS OF THE $Cr(TTA)_3$ AS A FUNCTION OF THE HEXANE PERCENTAGE IN THE MOBILE PHASE.

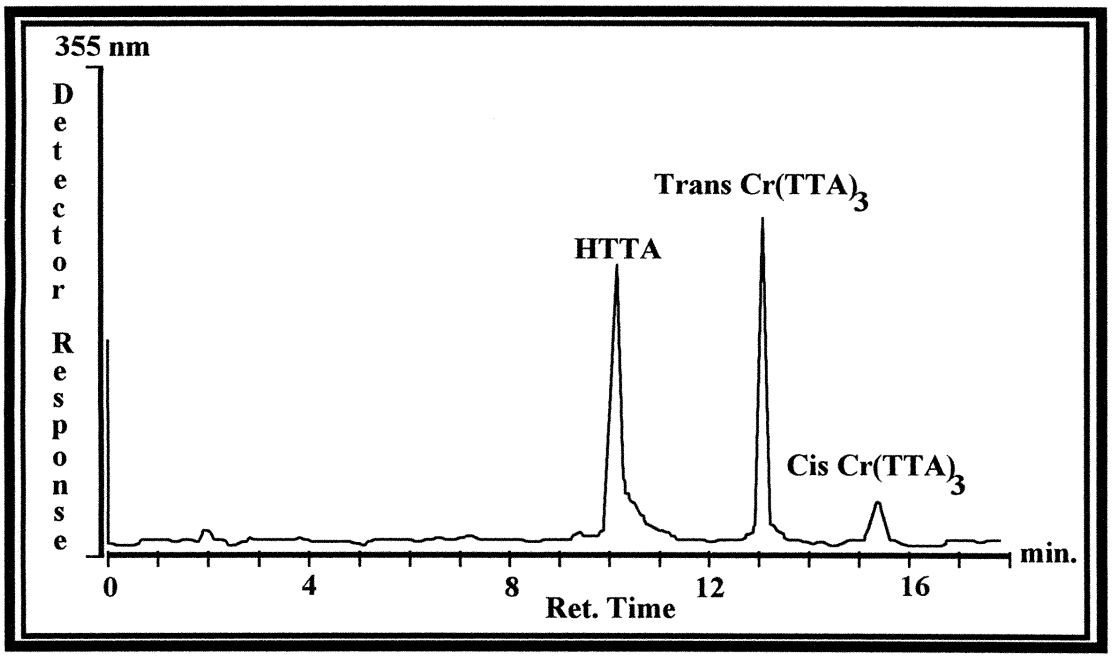

Figure 3. THE SEPARATION OF THE CIS-TRANS ISOMERS OF THE $Cr(TTA)_3$ ON A CYANO STATIONARY PHASE AND HEXANE AS MOBILE PHASE.

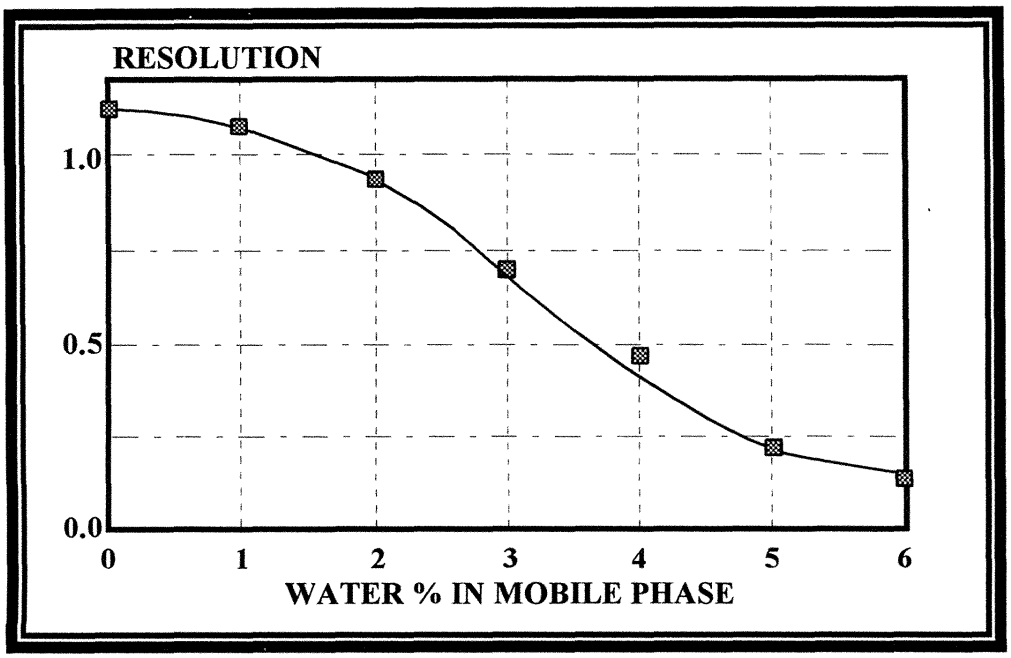

Figure 4. THE DEPENDENCE OF THE SEPARATION RESOLUTION OF THE CIS-TRANS ISOMERS OF THE $Cr(TTA)_3$ AS A FUNCTION OF THE WATER PERCENTAGE IN THE MOBILE PHASE.

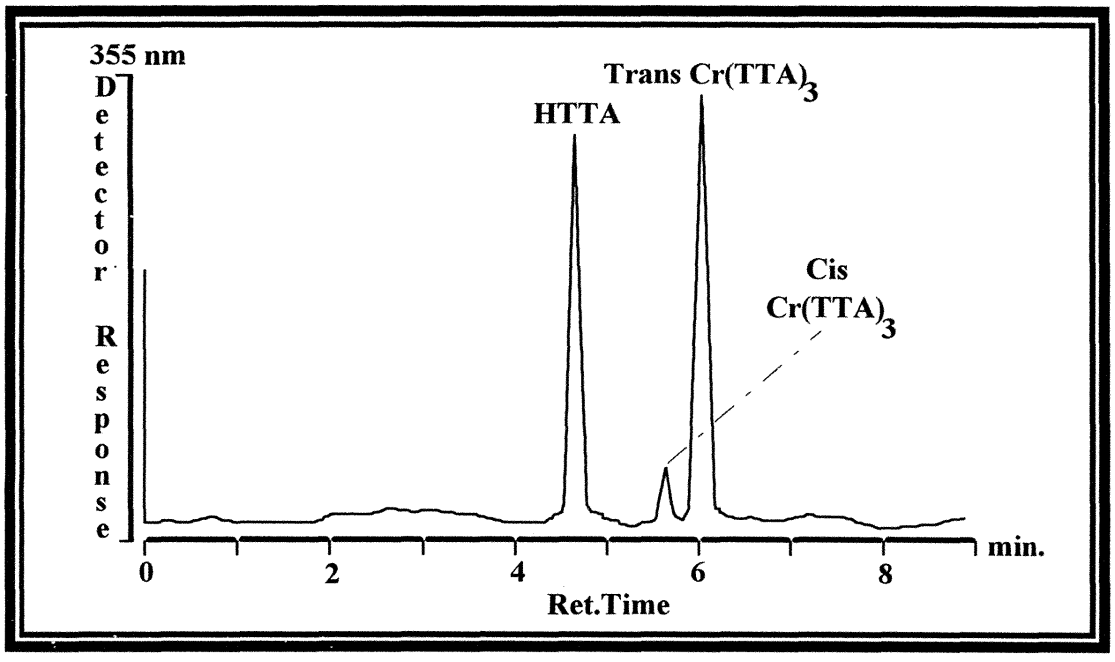

Figure 5. THE SEPARATION OF THE CIS-TRANS ISOMERS OF THE $Cr(TTA)_3$ ON THE OCTADECYL STATIONARY PHASE WITH ACETONITRILE/WATER MOBILE PHASE.

The tighter arrangement of similar substituents of the organic ligand around the metallic ion (the case of cis isomer) is probably responsible for the molecule polarization. The higher polarity of the cis isomer is observable from the elution order (second eluted in A/(I) system and first eluted in B/(II) system, respectively).

For the A/(I) separation system, the mobile phase components are not important, it is not possible to obtain the separation of the HTTA complexes from the free ligand. Only the Cr(III) complex exhibits a different chromatographic behavior in comparison to all the other metallic chelates, being retained a longer period.

For the B/(II) separation system, notable results were obtained only for the mixtures $Cu(TTA)_2$ + $Pb(TTA)_2$ + $Cr(TTA)_3$ and $Fe(TTA)_3$ + $Cr(TTA)_3$ + $Al(TTA)_3$, respectively. However, resolution between Cu(II) and Pb(II) HTTA complexes, Al(III) and Cr(III) HTTA complexes, respectively, did not show optimum values. Resolution remains lower, even for optimized programmed gradient elution.

For C/(III) separation system, differentiation between analytes is presented in **Table 1**, where the capacity factors characterizing elution of HTTA metal complexes are reviewed. **Figure 6** shows some typical chromatograms obtained with this system.

When the mobile phase contains the free ligand, UV detection becomes generally inoperant and the post-column derivatization step is necessary. Due to the fact that HTTA complexes are exhibiting major hyperchromic displacements in UV spectral region, it is possible to observe the elution of analytes from the chromatographic column, even in the presence of the free ligand into the mobile phase. The derivatization step is no necessary anymore in such a case.

Figure 7 shows the resulting UV spectrum obtained from an acetone 4 mg/L $Al(TTA)_3$ solution, compensated with 1% HTTA acetone solution. 222 nm and 379 nm signals could be used for monitoring metal complexes elution. Such a

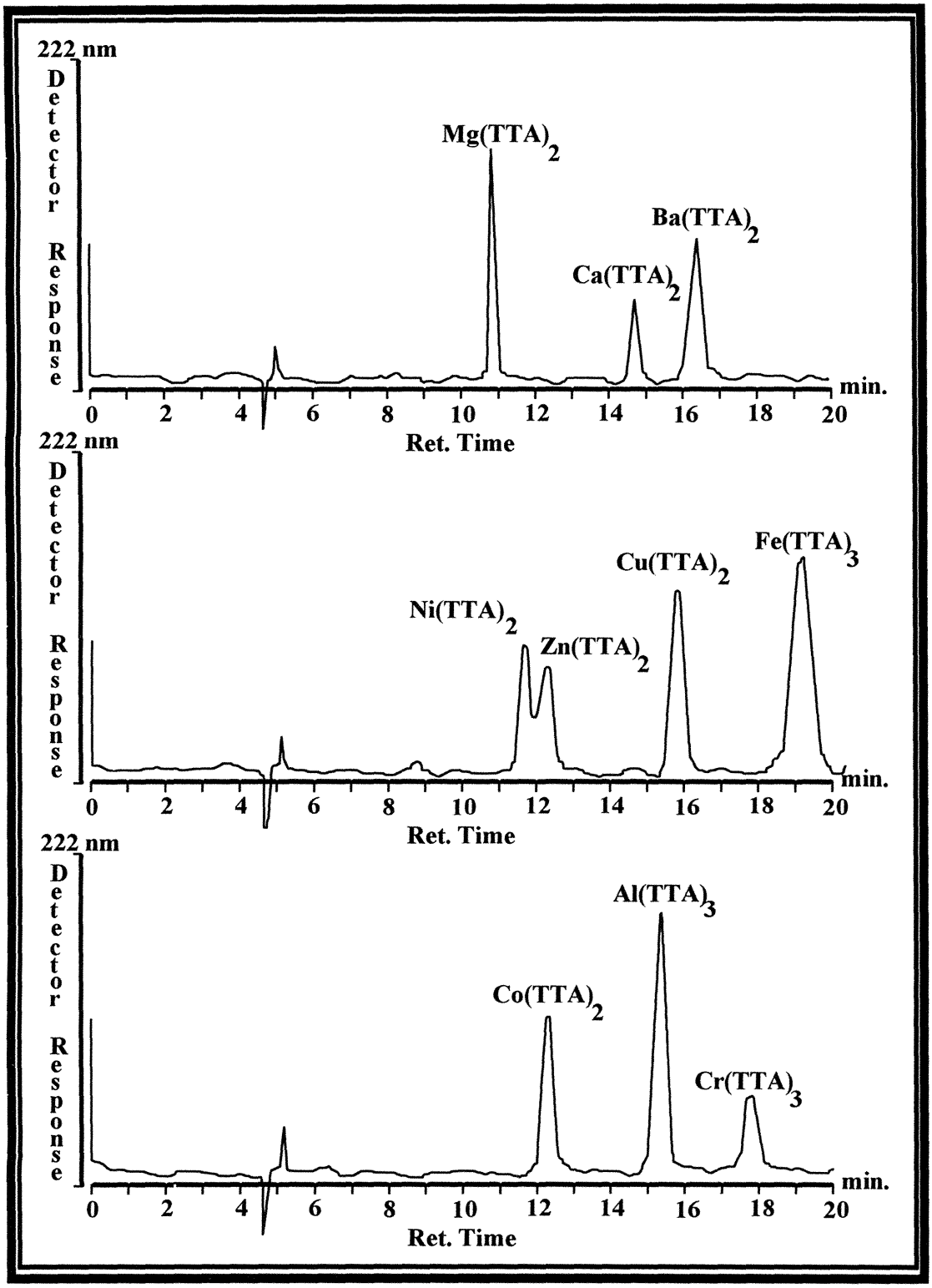

Figure 6 TYPICAL CHROMATOGRAMS OBTAINED IN C/III SEPARATION MODE FOR HTTA METALLIC COMPLEXES.

Table 1. CAPACITY FACTORS (K) CHARACTERIZING ELUTION OF METALLIC COMPLEXES WITH HTTA, ACCORDING TO C/III SEPARATION SYSTEM.

	HTTA complex with:						
	Cr(III)	**Al(III)**	**Fe(III)**	**Cu(II)**	**Pb(II)**	**Mn(II)**	**Zn(II)**
k	**2.50**	**2.05**	**2.85**	**2.30**	**2.35**	**1.71**	**1.53**

HTTA complex with:							
Cd(II)	**Co(II)**	**Ni(II)**	**Mg(II)**	**Ca(II)**	**Ba(II)**	**Na(I)**	**K(I)**
2.79	**1.52**	**1.35**	**2.25**	**1.95**	**1.21**	**1.49**	**1.48**

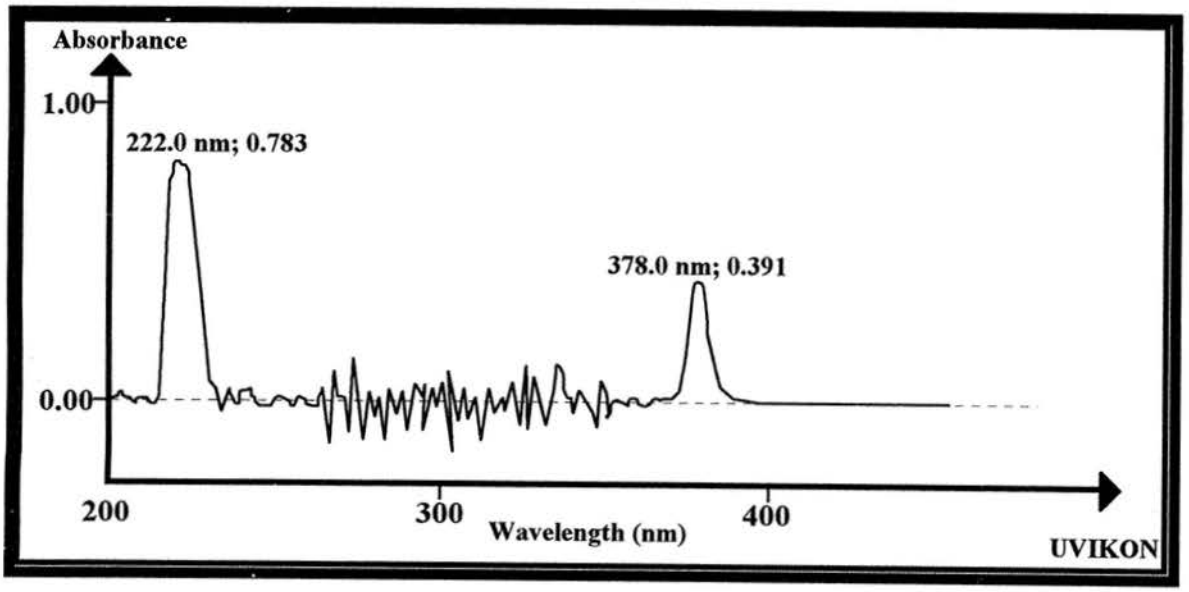

Figure 7 UV SPECTRUM OF AN ACETONE SOLUTION CONTAINING 4 mg/L $Al(TTA)_3$ COMPLEX, REGISTERED WITH 1 % HTTA IN ACETONE AS REFERENCE.

detection method is not related with a lack of sensitivity, when compared to a classical post-column derivatization step followed by Vis detection. Detection limits are similar to those obtained after pyridyl-azoresorcinol (PAR) post-column derivatization reaction and Vis detection. Z shaped flow cells are not recommended for use, due to the high energy looses during compensation for extremely long pathlengths.

Conclusions

It can be concluded that LC separation of thenoyltrifluoroacetonates is hard to be achieved when the mechanisms are based on the differentiation of the polarity of solutes. Probably, ligand molecules are "packed" around the metallic ion in a similar way, resulting in a low differentiation from the polarity point of view.

The β - diketonic structure substituents (trifluoromethyl - polar, thyenyl - non polar) confer an intermediate polar character to metal complex molecule. When the basic mechanism of the chromatographic partition changes (ligand exchange mechanism), good results are obtained and μ - column techniques contribute to better efficiencies.

REFERENCES

1. K. Robards; P. Starr and E. Patsalides, *Analyst*, **116**, 1247-1273 (1991).

2. B.R. Willeford and H. Veening, *J.Chromatogr.*, **251**, 61- 88 (1982).

3. C.A. Tollinche and T.H. Risby, *J.Chromatogr.Sci.*, **16**,448 - 454 (1978).

4. Yu. Nikitin, M.B. Morozowa, S.L. Lanin, T.A. Bol'shova, V.M. Ivanov and E.M. Basova, *Talanta*, **34**, 223- 227 (1987).

5. Yu. A. Zolotov, O.M. Petrukhin, A.R. Timerbaev, M.V. Evstiferov, V.V. Salov and N.G. Vanifatova, *Analyst*, **114**, 1137- 1143 (1989).

6. L. Liodakis, A. Pappa and G. Parissakis, *J.Chromatogr.Sci.*, **27**, 147 - 153 (1989).

7. J. Hagan, S. Taylor, and M. Tweedlew, *Anal.Chem.* **60**, 514- 520 (1988).

8. Y. Nagaosa, T. Suenaga and A. Bond, Anal.Chim.Acta, **235**, 279 - 283 (1990).

9. S. Ichinoki and M. Yamazaki, *J.Chromatogr.Sci.*, **28** , 258 - 264 (1990).

10. J. Shofstahl and J. Hardy, *J.Chromatogr.Sci.*, **28**, 225 - 229 (1990).

11. K. Nakajima, T. Yasuda and H. Nakazawa, *J.Chromatogr.*, **502**, 379 - 383 (1990).

12. N. Hoshino, K. Nakano and T. Yotsuyanagi, *Analyst*, **115**, 133 - 137 (1990).

13. P. Haddad and N. Rochester, *Anal.Chem.*, **60**, 536 - 541 (1988).

14. Y. Zhao and C. Fu, *Anal.Chim.Acta*, **230**, 23 - 29 (1990).

15. G. Schwedt and P. Schneider, *Fresenius Z.Anal.Chem.*, **325**, 116 - 121 (1986).

16. D. Cox, G. Harrison, P. Jandik and W. Jones, *Food Technology*, **41**, 245 -251 (1985), .

17. K. Saitoh, M. Satoh and N. Suzuki, *J.Chromatogr.*, **92**, 291 - 297 (1974).

18. K. Saitoh and N. Suzuki, *J.Chromatogr.*, **109**, 333 - 339 (1975).

19.N. Suzuki, K. Saitoh and M. Shibukawa, *J.Chromatogr.*, **138**, 79 - 87 (1977).

20. H. Noda, K. Saitoh and N. Suzuka, *J.Chromatogr.*, **168**, 250 - 254 (1979).

SOUTHERN BRAZILIAN JOURNAL OF CHEMISTRY
Vol. 2, No.2, 1994

THERMOGRAVIMETRIC STUDY OF THE OXIDATION KINETICS OF COPPER

José Schifino and Matheus A.G. Andrade
Departamento de Físico-Química - Instituto de Química - UFRGS
Av. Bento Gonçalves, 9500 - CEP 91501-000 - Porto Alegre - RS

ABSTRACT

The oxidation kinetics of copper in air has been studied at various temperatures in the range 500 °C to 924 °C by thermogravimetry. In that range of temperatures the oxidation leads to copper I oxide and the system shows diffusion controlled kinetics according to Wagner's parabolic law. Plots of the square of the variation of the sample weight as a function of time show a good linear correlation and allow the rate constant to be determined. Experiments at various temperatures confirm that the system exhibits an Arrhenius behaviour and the frequency factor as well as the activation energy have been calculated.

RESUMO

A cinética de oxidação do cobre ao ar foi estudada a varias temperaturas na faixa de 500 °C a 924 °C por termogravimetria. Nesta faixa de temperaturas a oxidação conduz à formação de óxido de cobre I e o sistema apresenta uma cinética controlada por difusão de acordo com a lei parabólica de Wagner. Gráficos do quadrado da variação do peso da amostra em função do tempo apresentam uma boa correlação linear e permitem a determinação da constante de velocidade. Determinações a várias temperaturas confirmam que o sistema exibe um comportamento de Arrhenius e o fator de frequência, bem como a energia de ativação, foram calculados.

Key words: Oxidation Kinetics, Thermogravimetry

INTRODUCTION

Solid state chemistry has been of increasing interest in recent times because of its technological importance as well as the possibility of mathematical modeling for the description of the kinetic behaviour of systems.

Heterogeneous kinetics implies in phase transfer of substances during the chemical reaction. Thus, the reaction rate for an heterogeneous reaction may depend not only on the chemical step but also on other steps involving diffusion, adsorption, dessorption etc. The system behaviour under such

conditions depends of factors like: viscosity of the medium, surface characteristics, amount of products formed and others that may affect the reaction rate.

Metal oxidation kinetics is an example of a solid-gas heterogeneous reaction. Reactions occurring on metallic surfaces are frequently controlled by diffusion and the presence of defects in the product layer plays an important role in the kinetics.

In the present work the oxidation kinetics of copper has been studied in order to establish the mechanism and to analyze the factors that determine the reaction rate. When copper reacts with oxygen two oxides, with different stabilities may be formed. While copper I oxide (Cu_2O) can be formed in a large temperature range, copper II oxide (CuO) has its existence limited to a restricted temperature interval.

The copper oxidation kinetics was studied by Ebisuzaki and Sanborn[1], in the temperature range of 687 °C to 1000 °C. They confirmed the validity of Wagner's parabolic law[2,3] and calculated the Arrhenius parameters. A detailed study, including isothermal and non-isothermal assays, was presented by Garnaud[4]. The isothermal assays allowed the determination of the forming conditions for the copper II oxide and copper I oxide as well as the influence of the apparent activation energy of the system.

Copper II oxide can only be formed when the relation between the number of copper ions and the number of oxygen ions, present in the external surface of the film, is less than a certain critical value[5]. The critical value is not achieved while the metallic surface is not completely covered by a layer of oxide. The temperature is a paramount factor for the formation of copper II oxide and, at 1000 °C, when copper is oxidized in air, only copper I oxide is formed. The CuO is inexistent bellow 150 °C, reaches a maximum between 300 °C and 500 °C decreases again at higher temperatures becoming minimum above 900 °C.

EXPERIMENTAL

High purity metallic copper samples (99.92%, determined by electrogravimetry), in the form of square plates 0.5 mm thick and with a total area between 0.14 cm^2 and 0.16 cm^2, were used in all measurements. The

samples were treated, for 30 seconds, with HNO_3 1:1, rinsed in distilled water, ethanol and dried in an hot air stream. After treatment, each sample was weighted in a thermobalance (Perkin-Elmer, TGS-2, System DSC-4) at room temperature. The thermobalance was programmed to operate at constant temperature and the variation of the sample weight registered as a function of time for about 150 minutes. All measurements have been carried out with the samples in air.

OXIDATION KINETICS

Kinetic processes governed by diffusion comprise two fundamental steps[6]; the chemical reaction itself and mass transport to the reaction region. The latter step may be the slowest, and constitutes the rate determining step.

When diffusion occurs monodimensionally, as in the present experiment, the nuclear growing can be described by a parameter **h**, representing the thickness of the layer which has not reacted[7] in a time **t**. Fick's first law for the diffusion of fluids in solids allows to write:

$$\frac{d\alpha}{dt} = -D.A\left(\frac{dx}{dh}\right) \qquad (I)$$

where **A** represents the diffusion area; **x** is the concentration of the species which diffuses into the layer; **D** is the diffusion coefficient and $d\alpha/dt$ represents the thickness variation of the formed oxide layer with time.

Integration of Equation (I), under constant temperature, gives for **x** the value:

$$x = \frac{h_o \alpha}{A.D}\left(\frac{d\alpha}{dt}\right) \qquad (II)$$

where h_o represents the thickness of the layer which has not reacted in the time t=0. Making $k = A.D/h_o$ and considering that **x** is time independent[8], integration of Equation (II) leads to:

$$\alpha^2 = 2kt \qquad (III)$$

Equation (III) is the well known Wagner's parabolic law[9] which describes the behaviour of diffusion controlled kinetic systems.

The oxidation of copper in the temperature range of the present experiment can be represented by:

$$2\,Cu^{+} + 2e^{-} + \tfrac{1}{2}\,O_2 \rightarrow Cu_2O$$

When a sample of metallic copper is submitted isothermally to an oxidizing atmosphere a weight increase results due to the incorporation of an oxygen atoms per molecule of Cu_2O formed. The system obeys the parabolic law and the weight increase, measured as a function of time, allows the rate constant to be determined. The use of a thermobalance makes it possible to carry out the reaction with very small copper samples without loss of precision. Once the weight increase of the system, Δm, has been measured the amount of Cu_2O formed can be calculated from the stoichiometry by:

$$M_{Cu_2O} = \frac{\Delta m.\overline{M}_{Cu_2O}}{\overline{M}_O} \qquad (IV)$$

where M_{Cu_2O} is the weight of copper I oxide formed in the reaction, $\overline{M}_{Cu_2O}$ is the molecular weight of copper I oxide and $\overline{M}_{O_2}$ represents the atomic weight of oxygen.

The value of M_{Cu_2O}, obtained from Equation (IV), allows the thickness of the oxide layer to be calculated once the density of copper I oxide and the area are known. Supposing that the oxide layer grows uniformly, its area must coincide with that of the metallic sample subject to oxidation. Representing by ρ the copper I oxide density and by **A** the surface area of the sample being oxidized, one may write:

$$\alpha = \frac{\Delta m.\overline{M}_{Cu_2O}}{\overline{M}_O.\rho.A} \qquad (V)$$

Substituting the layer thickness, given by Equation (V), in the parabolic law (3), results:

$$\frac{\Delta m^2 . \overline{M}^2_{Cu_2O}}{\overline{M}^2_O . \rho^2 . A^2} = 2kt \qquad \text{(VI)}$$

Equation (6) shows that if the system obeys the parabolic law, a linear relation should be obtained when the square of the mass change is plotted against time. The slope of the linear fit allows the reaction rate to be determined.

RESULTS AND DISCUSSION

A total of eleven determinations at varying temperatures, in the range 500 °C to 924 °C, have been performed as described in the experimental section. Figure 1 shows typical values of Δm as a function of time for the temperature of 712 °C. A graph relating Δm^2 as a function of time at 712 °C is presented in Figure 2. The good linear fit observed in the latter indicates that the proposed model (equation 6) describes adequately the system behaviour. The slope of the straight line allows the rate constant for copper oxidation to be determined.

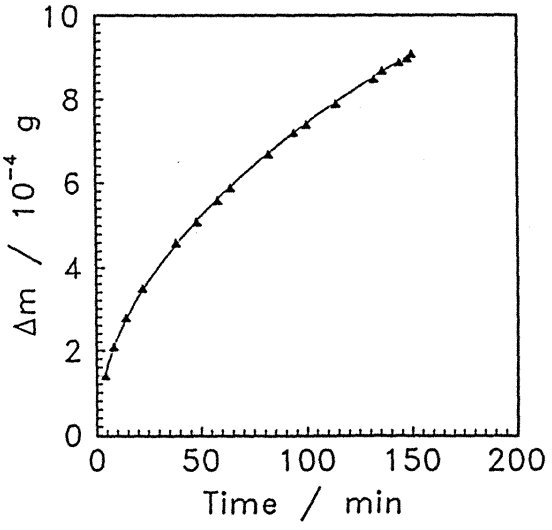

Figure 1 - Mass increase of copper as a function of time (reaction temperature = 712 °C)

Values of rate constants determined by this procedure were plotted in an Arrhenius graph (Figure 3), ln(k) x 1/T, in order to allow the Arrhenius parameters for the system to be calculated.

The variation of Δm as a function of time and Δm^2 as a function of time for all the experiments show curves of the same nature which indicates that the system obeys the same stoichiometry in the temperature range of the present study. The initial assumption that only one copper oxide (Cu_2O) is formed is then confirmed.

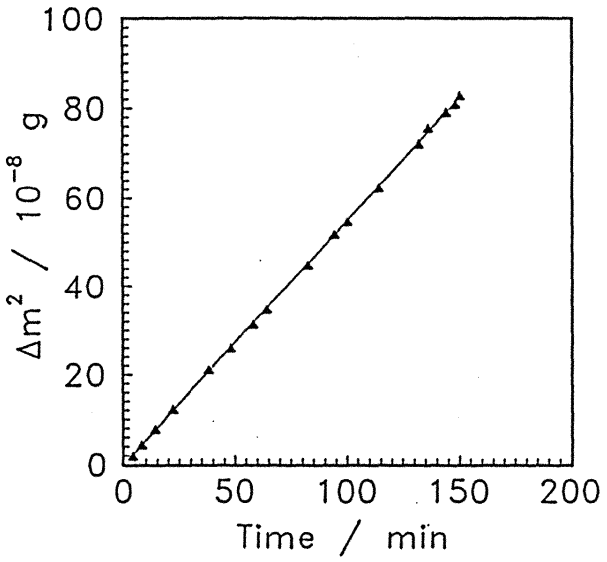

Figure 2 - Square of the mass increase of copper as a function of time (reaction temperature = 712 °C)

The mass change of the samples as a function of time shows a marked increase at beginning of the reaction which corresponds to the formation of the oxide layer. After 15 minutes the system starts to shown a regular increase of Δm, which means that the oxide layer has been formed and the kinetic is diffusion controlled.

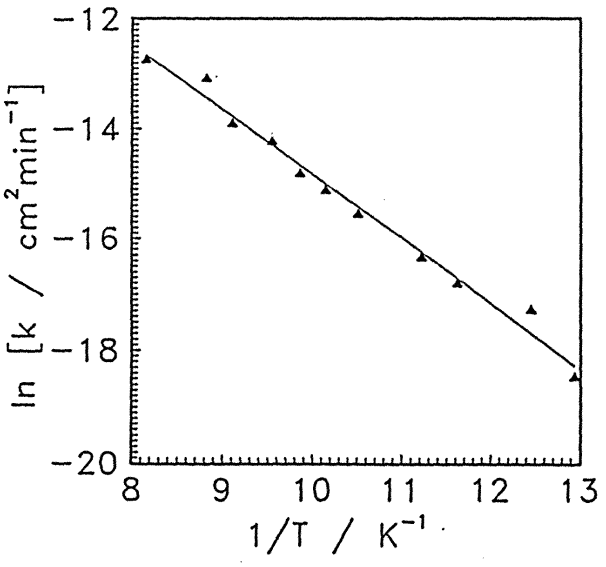

Figure 3 - Arrhenius plot for the oxidation of copper by air

The rate constants are expressed as cm^2min^{-1} showing that the reaction rate depends on the area available for reaction. The control of the sample area, which must remain constant during reaction, is necessary for the correct determination of the rate constants.

The graph presented in Figure 3 allows the determination of a frequency factor of 4.7×10^{-2} cm^2min^{-1} and an Arrhenius activation energy of 23.3 ± 0.9 $kcal.mol^{-1}$ which gives for the rate constant an equation of the form:

$$k = 4.7 \times 10^{-2} \exp[-23.3\ (kcal.mol^{-1})/RT]\ cm^2min^{-1}$$

The fact that the system follows the parabolic law indicates kinetics which is controlled by the diffusion of oxygen through the oxide layer formed on the copper surface.

REFERENCES

1 - Y. Ebisuzaki and W.B. Sanborn, *J.Chem.Ed.*, **62**,341,(1985).
2 - O. Kubaschewski and B.E. Hopkins, *"Oxidation of Metals and Alloys"*, Butterworths, London, 1962.
3 - K. Hauffe, *"Oxidation of Metals"*, Plenun, N.Y., 1965.
4 - G. Garnaud, *J.Thermal Analysis,* **8**,279,(1975).
5 - J. Oudar, *"L'Oxidation des Métaux"*, par J. Benard, Tome 2, Gauthier-Villars, Paris, 1964.
6 - S.F. Hulbert, *J.Brit.Ceram.Soc.*, **6**,11,(1969).
7 - J.B. Holt, I.B. Cretler and M.E. Waldsworth, *J.Amer.Ceram.Soc.*, **45**,133,(1962).
8 - G. Valensi, *Compt.Rend.*, **201**,602,(1935).
9 - S. Benson, *"The Foundations of Chemical Kinetics"*, McGraw-Hill, N.Y., 1960.

SOUTHERN BRAZILIAN JOURNAL OF CHEMISTRY
Vol. 2, No.2, 1994

USE OF SURFACTANTS ADDED TO REFRACTORY SLURRY IN PRECISION FOUNDRY AND INVESTMENT CASTINGS WITH ALUMINUM

Arno Müller, Jorge Luiz S. Barcelos and Lavinel G. Ionescu*
PPGEMM - Programa de Mestrado e Doutorado em
Engenharia Metalúrgica e dos Materiais
Escola de Engenharia, Universidade Federal do Rio Grande do Sul
Porto Alegre, RS BRASIL 90000-200

ABSTRACT

The investment casting process, involving wax models invested with clays to give ceramic moulds from which metal castings are made is characterized by the obtainment of parts of high metallurgic quality , especially as far as dimensional aspects, complexity of design and surface finishings are concerned. The high precision parts have a wide application in the electronics,aeronautical, biomedical, textile and food industries. Twenty one different surfactants, added to refractive zirconite slurry, were tested for their efficiency in obtaining wetting and adherence to the surface of the wax and good quality finished aluminum parts. Only five surfactants, including sodium dodecylbenzene sulfonate, sulfonic acid, dioctyl sodium sulfosuccinate and ethoxylated long chain alcohols gave satisfactory results. Analysis of the specimens manufactured from 98% aluminum, poured at 710ºC, by visual observation, rugosity, optical photography and electron microscopy showed that they were of high quality. The present paper describes the results obtained with sulfonic acid C_{8-16} and sodium dodecyl benzene sulfonate and explains the effect of the surfactants by the formation of a monolayer film or hemi-micelles between the wax and the ceramic slurry.

RESUMO

O processo de fundição de precisão é caracterizado pela obtenção de peças de alta qualidade metalúrgica , principalmente sob o aspecto dimensional e acabamento superficial. Ele consiste da preparação de modelos de cera e de moldes cerâmicos e vazamento do metal fundido dentro dos moldes. A aplicação de peças microfundidas de alta precisão abrange muitas áreas , incluindo a indústria aeronáutica, eletrônica, alimentícia, textil e biomédica. Foram testados vinte e um surfatantes usando lama refratária contendo zirconita com respeito a sua eficiência à molhabilidade e aderência à superficie da cera e a obtenção de peças de alumínio de boa qualidade. Somente cinco surfatantes, incluindo ácido sulfônico, dioctil sulfosuccinato de sódio, dodecilbenzeno sulfonato de sódio e alcoóis etoxilados deram resultados satisfatórios. A qualidade alta dos corpos de prova, fabricados de alumínio com pureza de 98% vazado a 710ºC, foi comprovada usando métodos de análise visual, medidas de rugosidade, fotografia ótica e microscopia eletrônica. Este trabalho descreve os resultados obtidos com ácido sulfônico C_{8-16} e dodecil benzeno sulfonato de sódio e explica o efeito dos agentes tenso-ativos através da formação de uma película (monocamada) ou hemimicelas entre a cera e a lama refratária.

KEYWORDS: Investment Casting, Ceramic Slurry, Surfactants, Hemi-Micelles, Sulfonic Acid, Sodium Dodecylbenzene Sulfonate

*Present Address: Instituto de Química, PUCRS-Pontifícia Universidade Católica do Rio Grande do Sul, Porto Alegre, RS, Brasil 90610-001 & Depto. de Química,ULBRA-Universidade Luterana do Brasil,Canoas,RS 92420-280

INTRODUCTION

The investment casting process is characterized by the obtainment of parts of high metallurgic quality, especially as far as dimensional aspects, complexity of design and surface finishing are concerned. The high precision parts have a wide range of applications including the aeronautical, electronics, biomedical, textile and food industries.[1-4] The value of the investment casting lies essentially in its ability to reproduce complexity of design and to achieve the tolerance necessary to eliminate difficult or impossible machining operations.[5-10]

Pure beeswax or common waxes modified with resins and fats have been used since ancient times in Europe, Asia and Africa to make models that were invested with clays to give ceramic moulds from which metal castings, especially bronze, were made. High quality art objects were manufactured in Italy during the 16th century, but the lost-wax process only became of modern industrial importance with the development of dental metallurgy and particulary the advent of the turbine engine in the years preceeding World War II.[5]

The manufacturing of high precision parts involves the following steps:

- Making of the wax model, as true as possible to the original part
- Fabrication of the ceramic mould using refractory zirconite slurry [6-9]
- Removal of the wax and baking of the ceramic mould
- Melting of the metal or alloy and metal casting (pouring of the melt into the mould) and
- Cleaning of the finished parts.

The refractory slurry usually contains zirconite or zirconium silicate ($ZrSiO_4$), traces of iron and titanium oxide and coloidal silica. An experimental problem that often arises is in obtaining adequate wetting and adherence of the clay to the surface of the wax.

Twenty one different surfactants, added to refractive zirconite slurry, were tested for their efficiency in obtaining good wetting and adherence to the surface of the wax and high quality finished aluminum parts. The surfactants tested were the following: sulfonic acid C_{8-16}, ethoxylated decyl alcohol (3 OE), sodium dioctyl sulfosuccinate, ethoxylated lauryl alcohol (4 OE), sodium dodecylbenzene sulfonate, hexadecyl trimethylammonium chloride, lead oleate; 3,7,11,15-tetramethyl-hexaden-1-ol; modified alkylphenyl polyglycol, ethoxylated castor oil (40 OE), ethoxylated lauryl alcohol (10 OE), nonyl-phenyl ether phosphoric acid, ethoxylated oleic acid (5 OE), triethanolamine dodecyl sulfonate, calcium dodecylbenzene sulfonate, dilauryldimethylammonium bromide, didodecyl phosphon-amide, ethoxylated lauryl alcohol (2 OE), organophosphonic acid and a dispersant with non-surfactant resins. Of these, only the first five gave good experimental results.

Analysis of the specimens or test parts manufactured from 98% aluminum, poured at 710ºC, was done by visual observation, rugosity, optical photography and electron microscopy.

The present paper describes the experimental results obtained with sulfonic acid C_{8-16} and sodium dodecylbenzene sulfonate added to refractive zirconite slurry.

MATERIALS AND METHODS

MATERIALS. The surfactants used were obtained from Chem Service Inc., West Chester, Pennsylvania, USA; Aldrich Chemical Company, Milwaukee, Wisconsin, USA; Henkel Produtos Químicos, Porto Alegre, RS, Brasil or Sarmisegetusa Research Group, Santa Fe, New Mexico, USA. They were used without further purification.

The wax employed is of common use in metal foundries in Brazil and consists of 23,00% paraffin; 53,00% tar; 10,67% Carnaúba wax (palm leaf wax); 12,00% mineral wax and 1,33% EVA (ethylene vinyl acetate).

The material used for the preparation of the refractory slurry or clay, called Zirconite ALM (empirical formula $ZrSiO_4$), was obtained from Nuclemon,São Paulo, Brazil. It has a melting point of 1540-1680ºC and consists of approximately 65% zirconia (ZrO_2); 33% silica (SiO_2); 0,05% ferric oxide (Fe_2O_3) and 0,10% titania (TiO_2).

The aluminum employed was industrial grade aluminum rods (98% purity).

MICELLE FORMATION. The critical micellar concentration (CMC) of the surfactants in water was determined at 25º, 32º and 40ºC by surface tensiometry using a Fisher Model 21 Semi-Automatic Tensiometer. The thermodynamic parameters for micellization, including the free energy, ΔG°_{m}, enthalpy, ΔH°_{m} and entropy of micellization, ΔS°_{m}, were calculated using standard equations.[10-12]

TEST FOR WETTING. The wetting ability of the surfactants was tested by adding approximately 0,03% by volume of the surfactant to the ceramic slurry of density 2,81 g/cm^3, previously prepared. The mixture was stirred for 30 minutes and the wetting of the wax was tested visually. The concentration that gave total wetting was compared to the critical micellar concentration (CMC) in water.

PREPARATION AND PROPERTIES OF REFRACTORY SLURRIES. The refractory slurries or clays used in investment casting are usually classified into primary and secondary. The primary slurry contains particles of smaller size and is the subject of the present study. The secondary slurry contains particles of larger size (200 Mesh) and a lower density. They are both prepared in similar manners. The primary slurries or clays were prepared under controlled conditions (22 to 24ºC and 50% relative humidity) from 4 kg of zirconium silicate (270 Mesh) in 1 liter of ligand (colloidal silica) with mechanical stirring (30 rpm). Subsequently, the

refractory slurries were allowed to rest for 24 hours in closed containers in order to prevent evaporation.

The present paper describes the refractory slurries 0 (no surfactant), 1 (containing 0,01% by volume of sulfonic acid C_{8-16}) and 4 (containing 0,03% by volume of sodium dodecylbenzene sulfonate. The aging process of the refractory slurries was studied over a period of five days by measuring the following properties:

- Viscosity (using a Zahn cup Nº 5 at 22ºC)
- Density (using a 10 ml volumetric flask and an analytical balance
- pH (using indicator paper)
- Capacity of Coverage (determination of quantity of dry clay that adhered to a glass plate of known area immersed in the slurry.

WAX MODELS. The models used had U shape and dimensions of 20 x 20 x100 mm. The wax employed has been described above.

CERAMIC MOULDS. The ceramic moulds were prepared by two alternate immersions of the wax model in the primary slurry and refractory stucco (foundry zirconite, 100 Mesh), followed by four layers of secondary slurry and showering with larger particles containing silicon and aluminum oxides with diameters of 0,5 to 2 mm.The time needed for drying after each immersion bath varied from 2 hours for the first two layers up to 5 hours between the fifth and the sixth layer. The drying was allowed to take place naturally at 22ºC and a relative humidity of 50% . The preparation of the secondary slurry is similar to the primary one, the main difference being the larger granulometry of the zirconite ($ZrSiO_4$), approximately 200 Mesh.

DE-WAXING AND CALCINATION. The removal of the wax (de-waxing) and calcination were done in an autoclave at 900ºc. The procedure usually required 1-2 hours and was usually performed after the covering with the last layer.

MANUFACTURE AND ANALYSIS OF THE ALUMINUM PARTS. Molten aluminum of 98% purity was poured into the ceramic moulds at 710ºC soon after their removal from the autoclave. As soon as the metal solidified, the mould was broken and removed and the surface of the manufactured part was cleaned.Analysis of the finished aluminum parts was then done by visual observation, measurement of rugosity, optical photography and electron microscopy. The castings test specimens were designated CP-0 (ceramic slurry without surfactant), CP-1 (with sulfonic acid C_{8-16}) and CP-4 (slurry containing sodium dodecylbenzene sulfonate.

RESULTS AND DISCUSSION

The thermodynamic parameters determined for the micellization of sulfonic acid C_{8-16} and sodium dodecylbenzene sulfonate in water at 25ºC are summarized in Table I. The sulfonic acid sample, obtained from Henkel Produtos Químicos,contained alkyl chain lenghts that varied from eight to sixteen carbon atoms.

TABLE I. THERMODYNAMIC PROPERTIES FOR THE FORMATION OF MICELLES OF SULFONIC ACID C_{8-16} (SA) AND SODIUM DODECYLBENZENE SULFONATE (SDBS) IN WATER AT 25ºC.

Surfactant	Critical Micellar Concentration (mole/l)	ΔG°_{m} (kcal/mole)	ΔH°_{m} (kcal/mole)	ΔS°_{m} (eu)
SA	$1,81 \times 10^{-4}$	-5,10	-1,65	+11,6
SDBS	$1,05 \times 10^{-3}$	-4,04	+2,70	-22,6

Both surfactants, from the same supplier, were used without further purification. The experimental results obtained for the critical micellar concentration (CMC) and the standard free energy of micellization (ΔG°_{m}) are typical for surfactnts in aqueous solutions.

Figure 1 illustrates the variation of properties such as flow viscosity, surface coverage and density as a function of concentration of zirconite determined for primary slurry without surfactant at 22ºC. The density and the coating or surface

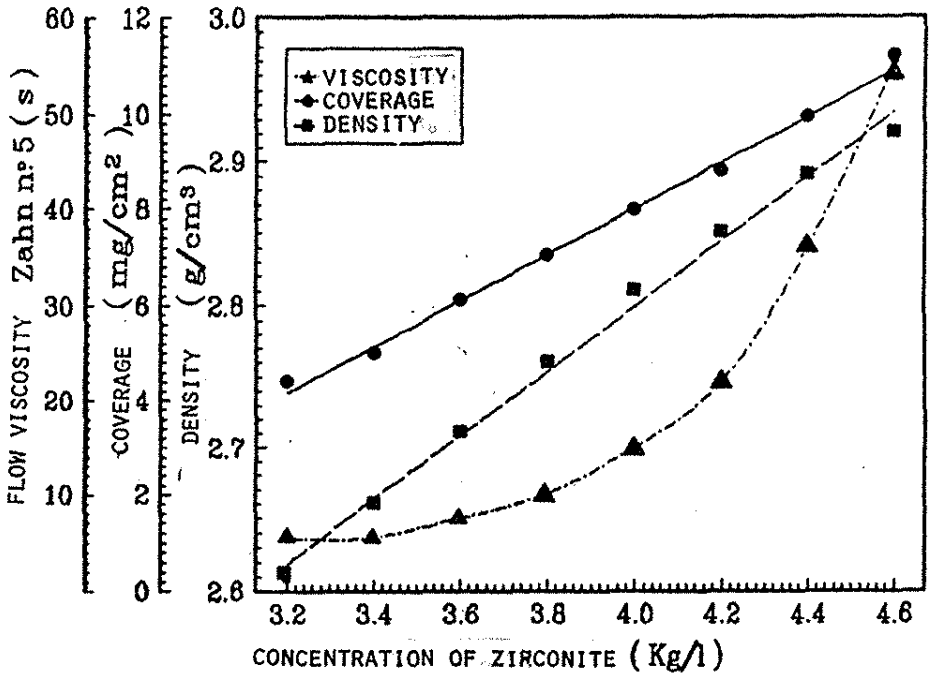

FIGURE 1. VARIATION OF SOME PROPERTIES OF PRIMARY CERAMIC SLURRIES WITHOUT SURFACTANT AS A FUNCTION OF THE CONCENTRATION OF ZIRCONITE AT 22ºC.

coverage varied linearly as a function of the content of zirconite, while the flow vsucosity exhibited an exponential behavior. All the studies described in the present paper were done with slurries of fixed density (2,80 g/cm^3).

Figures 2 and 3 show the variation of the density and flow viscosity of ceramic slurries without surfactant(slurry 0) and in the presence of the two surfactants, sulfonic acid C_{8-16} (SA- 0,01% by volume, slurry 1) and sodium dodecylbenzene sulfonate (SDBS-0,03% by volume, slurry 4) as a function of time.

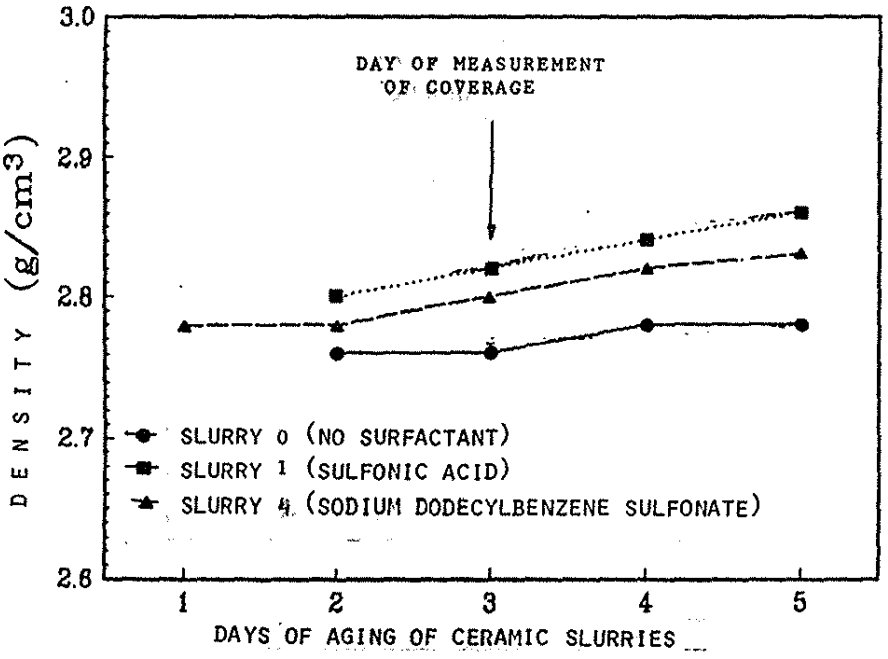

FIGURE 2. EFFECT OF AGING ON THE DENSITY OF CERAMIC SLURRIES IN THE PRESENCE AND ABSENCE OS SURFACTANTS AT 22ºC.

The effect of aging is much more pronounced for the slurries containing surfactants. The surface coverage, determined on the third day by the dipping slide method, showed no significant difference. The corresponding experimental values for the same density (2,80 g/cm^3) were 7,97g/cm^2 (slurry 0); 7,93 g/cm^2 (slurry 1) and 7,60 g/cm^2 (slurry 4), respectively.

Of the twenty one different surfactants added to refractory slurry, only five gave satisfactory wetting and adherence between the clay and the wax model. They were sulfonic acid C_{8-16}, sodium dodecylbenzene sulfonate, sodium dioctyl sulfosuccinate, ethoxylated decyl alcohol (3OE) and ethoxylated lauryl alcohol (4OE). In general, the wetting ability depends to a large extent on the affinity of the hydrophilic parts of the surfactants for the ceramic clay and the chain length of the surfactants.

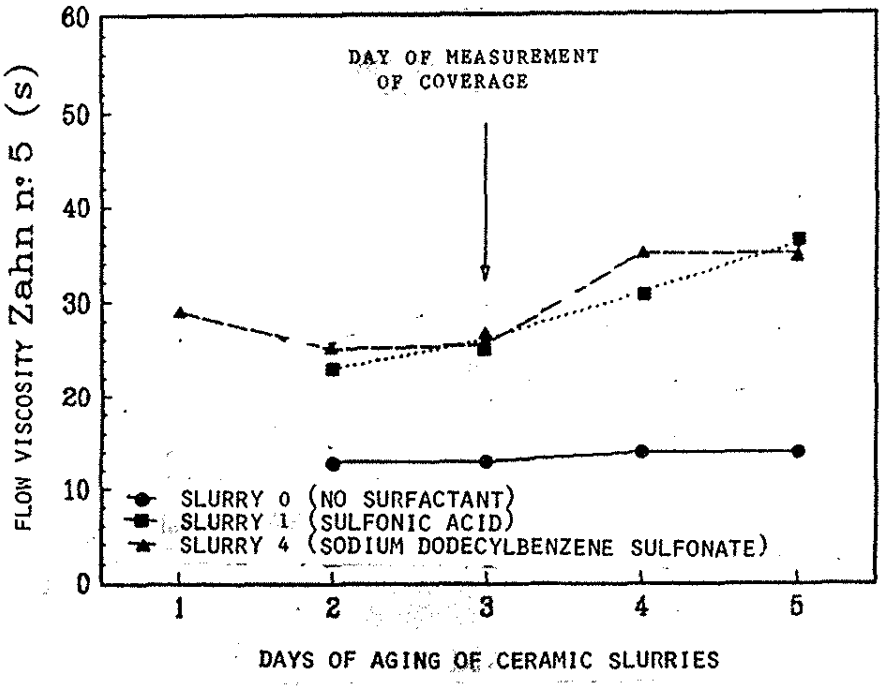

FIGURE 3. EFFECT OF AGING ON THE FLOW VISCOSITY OF CERAMIC SLURRIES IN THE PRESENCE AND ABSENCE OF SURFACTANTS AT 22ºC.

Anionic surfactants such as sulfonic acid C_{8-16} (SA), sodium dodecylbenzene sulfonate (SDBS) and sodium dioctyl sulfosuccinate appear to meet these criteria. For the ethoxylated long chain alcohols, the presence of the oxygen atoms (part of the ethoxy group) and a ceratin critical chain length seem to be important.

The wetting with sodium dodecylbenzene sulfonate occurs at a concentration of 8,73 x 10^{-4}M, that is below the CMC in water. For sulfonic acid C_{8-16} the concentration (3,65 x 10^{-4}M) needed for satisfactory wetting and adherence is above the CMC. For cases of surfactant present in concentrations below the critical micellar concentration (CMC), one model that can be proposed is the formation of a monolayer film between the wax and the ceramic clay. This may be the case of sodium dodecylbenzene sulfonate (SDBS) with the polar head groups in contact with the ceramic slurry and the hydrophobic tails in the proximity of the wax (Figure 4).

For experimental conditions where the concentration of surfactant is slightly above the CMC (as with sulfonic acid-C_{8-16}) the formation of hemi-micelles may be suggested. This is illustrated in Figure 5.

Both kind of aggregates have been described in the literature for various solid-solution interfaces, including silica-water.[13-16]

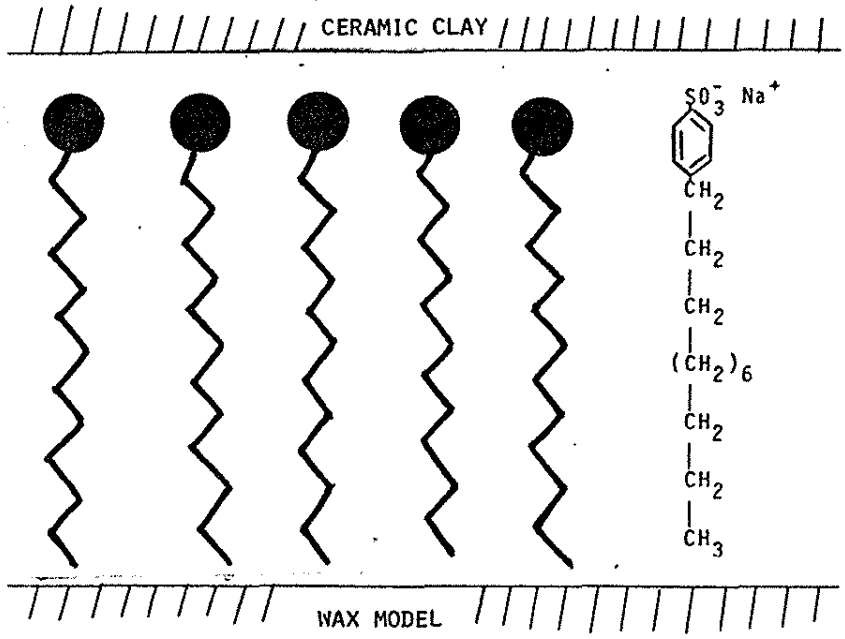

FIGURE 4. DIAGRAM OF THE ORIENTATION OF THE SURFCATANT MONOLAYER FILM BETWEEN THE WAX MODEL AND THE CERAMIC CLAY.

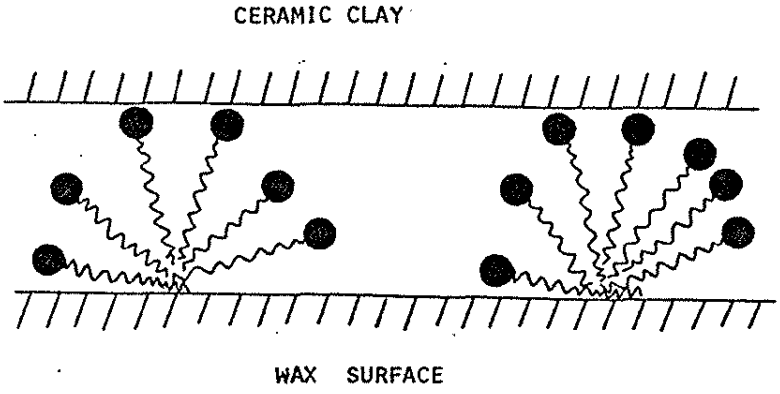

FIGURE 5. DIAGRAM ILLUSTRATING THE FORMATION OF HEMI-MICELLES BETWEEN THE WAX MODEL AND THE CERAMIC SLURRY.

The nature of intermolecular forces and the stability of colloids are rather complex subjects and no attempt will be made to discuss them here. They have been described in detail in the literature.[17,18]

Refractory slurries represent theoretically stable systems since they contain colloidal dispersions with refractory materials and surfactants. Refractory slurries tend to gel when repulsive interactions have been sufficeintly reduced and the Van der Waals attractive forces begin to predominate. London forces are also important in such systems, since apolar molecules may be subject to polarization due to fluctuation of charges in other molecules. At the refractory clay-wax interface London, Van der Waals and Landau forces may be limited due to the presence of surface tension. This appears to be the case for the wetting and adherence of a refractory slurry on the surface of the wax in the presence of surface active agents.

Figure 6 shows optical micrographs (magnification factor 11x) of smooth and rough reference surfaces and also finished aluminum castings specimens obtained with ceramic slurries wihout surfactant (CP-0), containing sulfonic acid C_{8-16} (CP-1) and sodium dodecylbenzene sulfonate (CP-4).

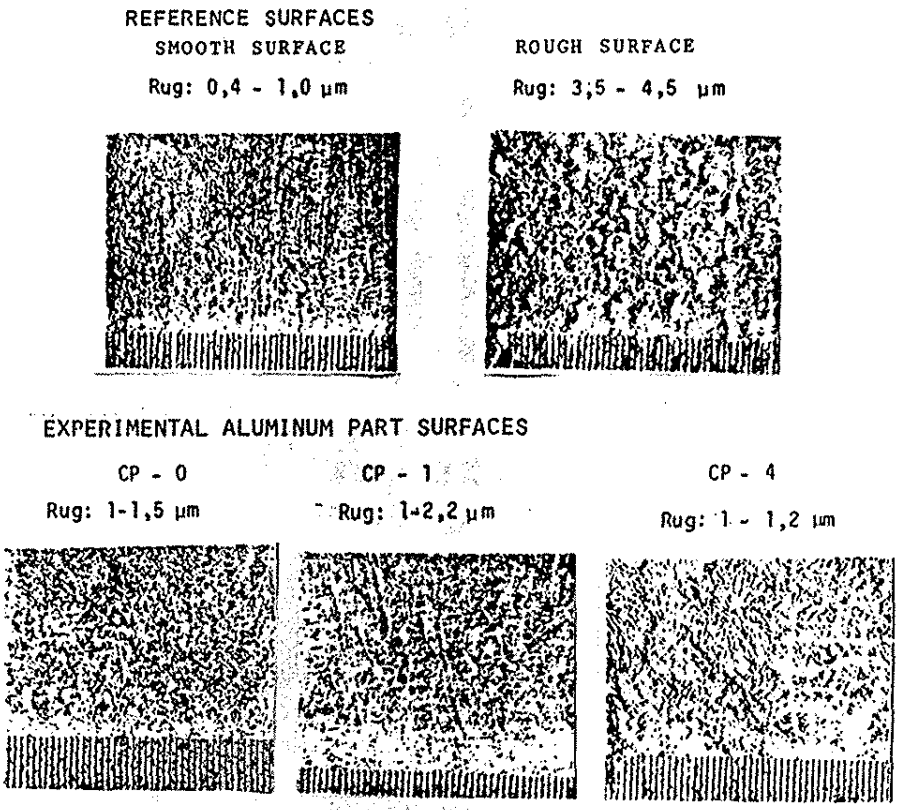

FIGURE 6. OPTICAL MICROGRAPHS OF ALUMINUM CASTINGS SPECIMENS AND THEIR RESPECTIVE RUGOSITY. (CP-0, no surfactant; CP-1, with sulfonic acid C_{8-16}; CP-4, with sodium dodecylbenzene sulfonate).MAGNIFICATION 11X.

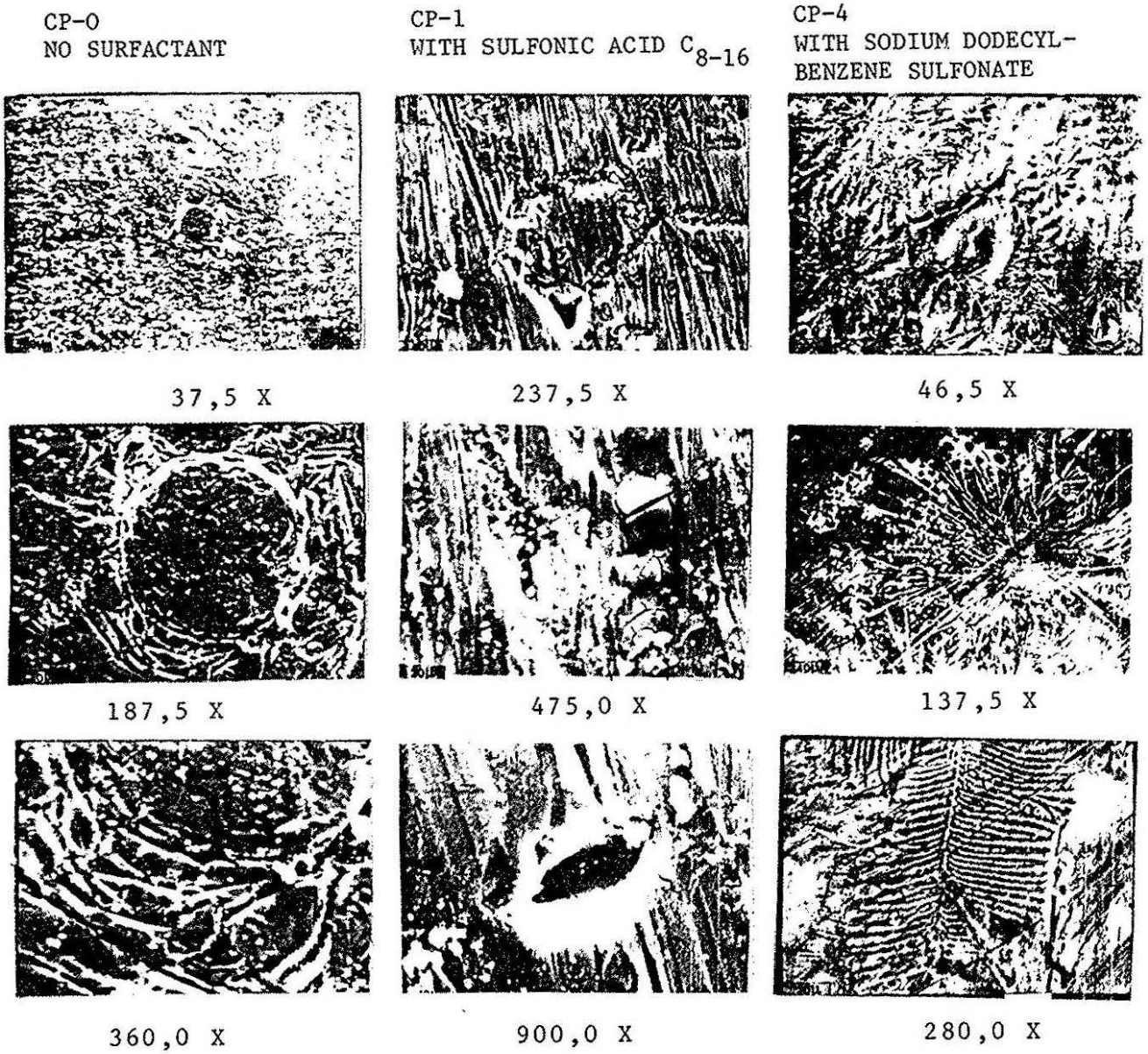

FIGURE 7. SCANNING ELECTRON MICROGRAPHS OF ALUMINUM CASTINGS SPECIMENS.

In general, the optical micrographs show good surface finishing for the aluminum parts.

Figure 7 illustrates some representative scanning electron micrographs of the aluminum castings specimens manufactured in this study. All micrographs show inclusion of refractory material on the surface of the metal, formation of microcavities and an oxide layer. The sequence of micrographs with increasing magnification for CP-0 probably illustrates the formation of a cold drop and a series of ondulations on the surface caused by the variation of temperature during solidification. The sequences for CP-1 and CP-4 show the formation of oxides, among other phenomena.

Rugosity (Ra) may be defined as the average deviation of absolute values of the effective profile ordinates with respect to a median line across a length of sampling.

$$Ra = 1/L \int_0^L |Y| \, dx \quad \text{or} \quad Ra = 1/n \sum^{n} |Y|$$

The determination of rugosity was done with a Mitutoyo Rugosimeter, Model Surftest III. A sensor needle measured the rugosity of the surface in micrometers (μm). It usually scanned a length of 17 mm of test surface at a speed of 2 millimeters per second. The minimum sample length used for measuring the rugosity was 0,80 mm. The average values were obtained by measuring three different castings specimens within each group (CP-0, CP-1 and CP-4).

Figure 8 shows the variation of rugosity in terms of the Brazilian Norm, the average rugosity of the finished parts and the rugosity of the pattern used in this study. The Brazilian Norm (NB 93, 1964) sets the limits for castings between 2,5 and 3,2 μm.

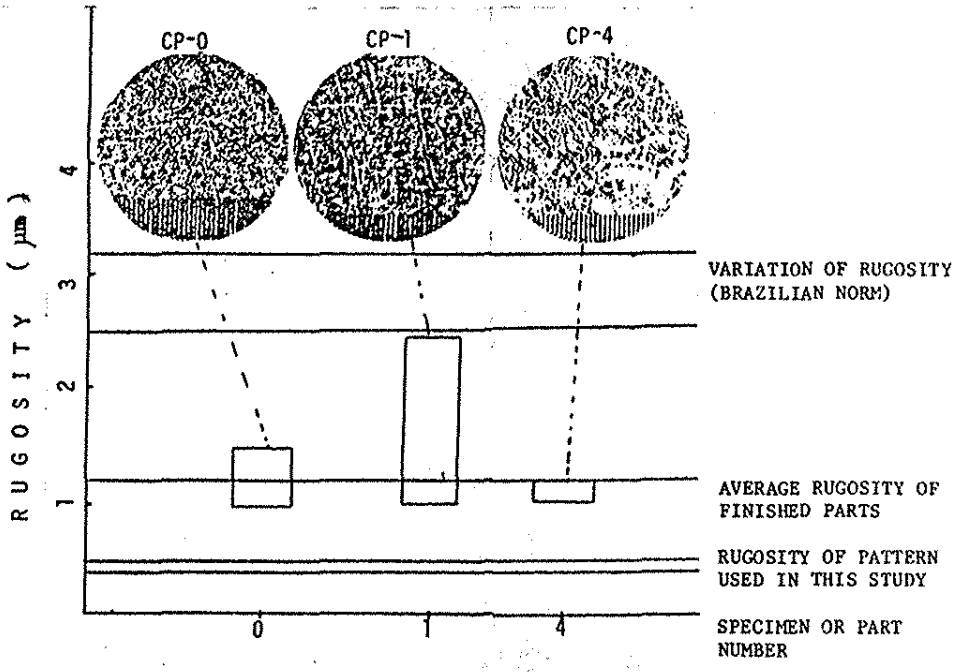

FIGURE 8. VARIATION OF RUGOSITY FOR THE DIFFERENT ALUMINUM CASTINGS.(Optical Micrographs, 11X; CP-0, No Surfactant; CP-1 with Sulfonic Acid C_{8-16}; CP-4 with Sodium Dodecylbenzene Sulfonate).

Test specimen CP-4 had a very low rugosity variation, indicating very satisfactory surface finishing. For CP-1, the rugosity fell within the required norms.

In general, the rugosity of the finished parts is higher than that of the original metal pattern (0,4 -0,5 μm). This increase in the rugosity of the copied or reproduced parts is probably the result of the various steps of the foundry process, involving microdraining of the wax and the effects of temperature, turbulence and erosion. A possible explanation of the evolution of rugosity in the finished metal parts is given in Figure 9.

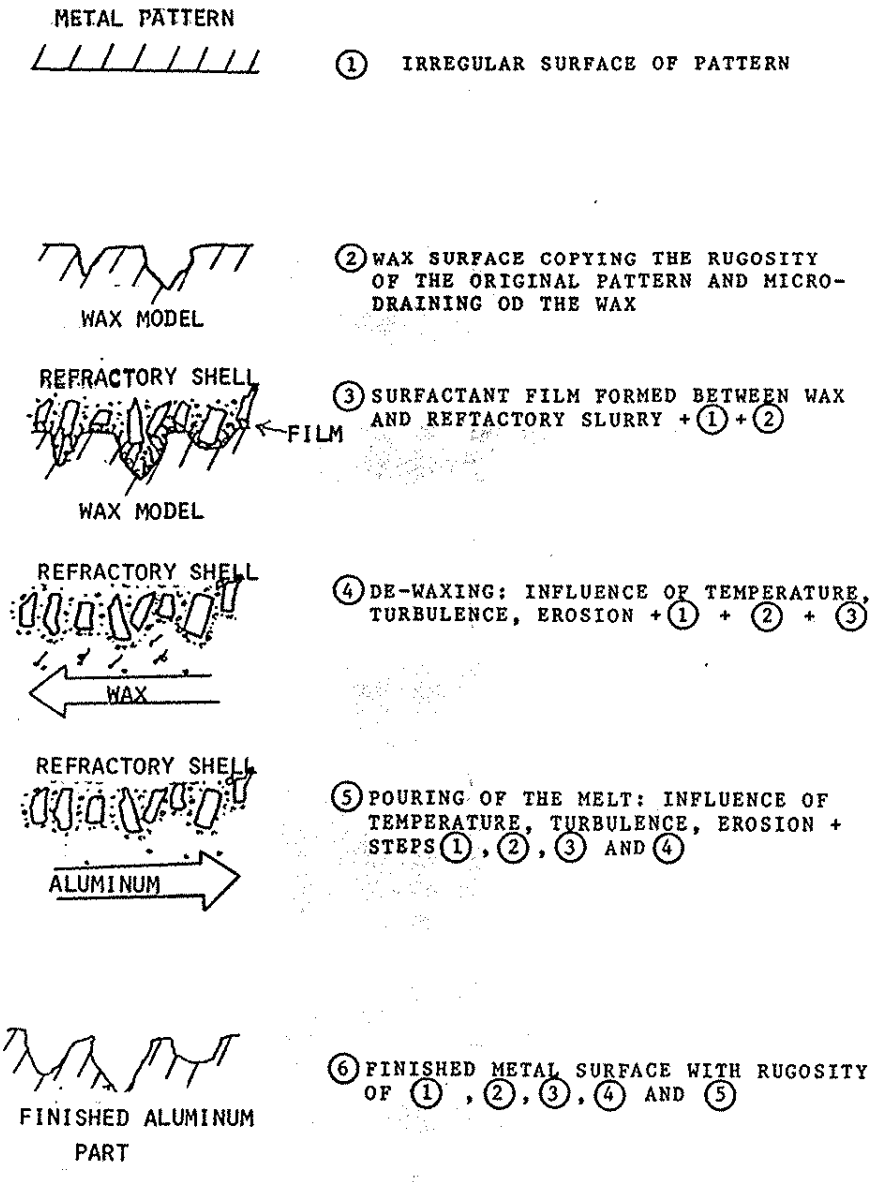

FIGURE 9. POSSIBLE EVOLUTION OF THE RUGOSITY OF THE FINISHED METAL PARTS IN PRECISION FOUNDRY.

Analysis of the experimental results leads to the conclusion that the addition of the surfactants sulfonic acid C_{8-16} and sodium dodecylbenzene sulfonate to refractory zirconite slurry greatly improves the surface quality of the aluminum castings specimens. It appears that in addition to wetting and adherence, the surfactant film or hemi-micelle layer between the soft mold and the wax model also hepls to absorb the shock during the showering of the mold with large zirconite particles, thus preserving the quality and details of the finished surface.

ACKNOWLEDGEMENTS. Financial assistance from CAPES, LAFUN and Sarmisegetusa Research Group, Santa Fe, New Mexico, USA is gratefully acknowledged.

1. H.T. Bidwell, *"Investment Casting"*, The British Investment Casters Technical Association, Sheffield, U.K., 1963.
2. M. Leadbetter, G.L. Knowles, P. Savage and H.T. Bidwell, *Foundry Trade Journal, 29*, 847-860, May 1969.
3. J.L.S. Barcelos, A. Müller and L. G. Ionescu, *"Anais 9º Congresso Brasileiro de Engenharia e Ciência dos Materiais"*, Águas de São Pedro, São Paulo, Brasil, 1990, Vol. 1, pp.80-84.
4. J.L.S. Barcelos, L. G. Ionescu and Arno Müller, *"Anais do 1º Workshop Brasileiro de Fundição de Precisão"*, Porto Alegre, RS, Brasil, 1993, Vol. 2, pp.130-141.
5. J.H.W. Booth, *Foundry Trade Journal, 6*, 707-711, December 1962.
6. D.C. Loriz, *Rev. Metal. CENIM, 16(2)*, 113-116; *16(4)*, 230-236 (1980).
7. P.R. Taylor, *"Problems of Primary Coat Quality Control for Ceramic Shell Moulding"*, Monsanto Europe Technical Centre, Bruxelles, Belgium, 1985.
8. P.R. Taylor and J.M. Libouton, *"Quality Control fo Slurry Materials for Ceramic Shell Moulding"*, Monsanto Europe, S.A., Bruxelles, Belgium, 1978.
9. R. E. Greenwood, *Foundry Trade Journal, 15*, 178-182, March 1984.
10. L. G. Ionescu, T. Tokuhiro and B. J. Czerniawski, *Bull. Chem. Soc. Japan, 52*, 922-924 (1979).
11. L. G. Ionescu and D.S. Fung, *J. Chem. Soc. Faraday Trans. I, 77*, 2907-2912 (1981).
12. L. G. Ionescu, L. S. Romanesco and F. Nome, in *"Surfactants in Solution"*, K. L. Mittal and B. Lindman, Eds., Plenum Press, New York, 1984, pp. 739-803.
13. T. Gu, Y. Gao and Z. Huang, *J. Surface Sci. Technol., 5*, 133-142 (1989).

14. M. K. Chaudhury, T. M. Gentle and E. P. Plueddeman, *J. Adhesion Sci. Technol., 1,* 29-38 (1987).

15. F. M. Fowkes, *J. Adhesion Sci. Technol., 1,* 7-27 (1987).

16. J. M. Garvey and C. I. Griffiths, *"Colloidal Sol Transfer Process for Forming a Coating"*, Unilever, Port Sunlight, U.K., 1987.

17. J. N. Israelachvilli and B. W. Ninham, *J. Colloid Interface Sci., 58,* 14-25 (1977).

18. P. C. Hiemenz, *"Principles of Colloid and Surface Chemistry"*, 2nd edition, revised and expanded, Marcel Dekker, New York, N.Y., USA, 1986.

SOUTHERN BRAZILIAN JOURNAL OF CHEMISTRY
Vol. 2, No.2, 1994

NIOBIUM AS A POTENTIOMETRIC SENSOR IN REDOX TITRATIONS WITH AND WITHOUT PASSIVATION BY AMMONIUM MOLYBDATE.

Claudete J. Valduga, Eunice Valduga, Martha Adaime and Nádia Viaro[1]

Chemistry Department, Federal University of Santa Maria
Santa Maria - RS - Brazil - 97119-900

ABSTRACT

The Pt indicator electrode has been commonly used for redox potentiometric titrations. In this work the Nb indicator electrode is suggested as an alternative for the Pt indicator electrode for the redox potentiometric titrations of the system Fe(II)/$K_2Cr_2O_7$. The utilization of proposed electrode has been studied with and without passivation. The passivation is made by electrode immersion in oxidising anodic inhibitor of NH_4MoO_4. The result was an observed increase of the potentiometric leap from 30 mV to 60 mV, allowing a better visualization of the equivalence point. The same equivalence point was observed with the conventional and proposed electrode. With the Nb electrode an inverse potentiometric leap was also obtained.

RESUMO

O eletrodo indicador de platina tem sido usado nas titulações potenciométricas de oxi-redução convencionalmente. Neste trabalho, o eletrodo indicador de nióbio é considerado como uma alternativa ao eletrodo indicador de platina nas titulações potenciométricas de oxi-redução para o sistema Fe(II)/$K_2Cr_2O_4$. A utilização do eletrodo foi estudada com e sem passivação. A passivação foi feita com a imersão do eletrodo num inibidor oxidante anódico de NH_4MoO_4. Como consequência ocorreu um aumento do salto potenciométrico de 30 mV para 60 mV (ECS), permitindo uma melhor visualização do ponto de equivalência. Foi observado o mesmo ponto de equivalência para o eletrodo proposto em relação ao convencional. Além disso, com o eletrodo de nióbio foi obtido um salto potenciométrico invertido.

Keywords: potentiometric sensor; redox titrations; niobium; passivation; ammonium molybdate

[1] Present Address: UFSM (campus), caixa postal 5051, Santa Maria 97119-911, RS-Brazil.

INTRODUCTION

The indicator electrodes used in potentiometric titrations depend on the type of reaction that is being investigated. In an acid-base titration it may be a hydrogen electrode or any other electrode that responds to hydrogen ions. The equivalence point of the reaction is revealed by a sudden change of potential in the e.m.f. curve vs the volume of the titrant solution.

Many pure metals are resistant to corrosion and have the common characteristic of forming oxides very adherent to the surface that repress the corrosion and are suitable as proton sensors[1].

The metal-oxides.xH_2O indicator electrodes have been used as sensors because of their low price and easy handling.

Some metals, such as Ti, Ni, Ta and alloys such as chromium-cobalt and stainless steel tend to become passive due to the formation of a thin, adherent layer of oxide or another compound that proctects them from oxidation[2].

The sensibility of metal-oxide.xH_2O electrodes in redox titration was studied by Sayed[3]. Redox titrations were made and appreciable potential leaps were observed in the equivalence point.

The Nb is covered by a Nb_2O_5 film that can be dissolved by fusion with hydroxide but is not attacked by the hydrogen ion[4].

Chromium-Nickel alloys, used as potentiometric sensor in redox titrations, show well determined potentiometric leaps, and usually in the same potential range of platinum electrodes. These potentiometric leaps are usually 50% of the value of the leaps obtained when platinum electrode are used[5].

The first studies carried out to verify the response of metallic-oxide films used hastelloy alloys and have shown that the film can respond to protons in solution. Systematic studies in acid-base reactions and the Nernst type behavior extends to the range of pH 1,0 to pH 13,0 [6].

In this work, Nb was used as indicator electrode in redox potentiometric titration for the system Fe(II)/$K_2Cr_2O_7$. The passivation was made to increase the potentiometric leap.

MATERIALS AND METHODS

Potentiometric titrations of 0,01N $FeSO_4.7H_2O$ (in H_2SO_4 solution) with 0,1N $K_2Cr_2O_7$ solution were done, with stirring at room temperature using the calomel electrode as reference and a Nb electrode as indicator, instead of the Pt electrode. The Nb electrode was sanded with granulometry 280, 320, 400 and 600 a paper and then polished with Al_2O_3.

In some cases, the Nb electrodes were treated chemically and the passivation was achieved by immersion in 0,01 N NH_4MoO_4 solution for thirty minutes and for one hour.

The titrations were conducted at 25± 1°C, with a PW 9409 Phillips potentiometer using a Shott Mainz B281 calomel electrode of simple junction, as reference. In order to achieve a better resolution a 274 microburete Methrohm was used. A 702 Fisaton magnetic stirrer, was used to ensure adequate mixing.

RESULTS AND DISCUSSION

Figures 2 and 3 show that the equivalence points in the titrations coincide exactly with that verified when the Pt electrode is used (Figure 1), although the potential leap is reversed and smaller.

The Nb electrode passivated by immersion in oxidizing anodic inhibitor solution of NH_4MoO_4 for thirty minutes and one hour presented a potentiometric leap of about 60 mV, that is twice that observed without passivation in the Fe(II) titration by $K_2Cr_2O_7$ (30 mV). The passivated electrode allows a better detection of the equivalence point.

When the Nb is exposed to the air, it has the characteristic of formation of a film mainly of Nb_2O_5.

The oxidizing anodic inhibitor of NH_4MoO_4, probably makes this layer thicker and the redox potential becomes higher than the original one.

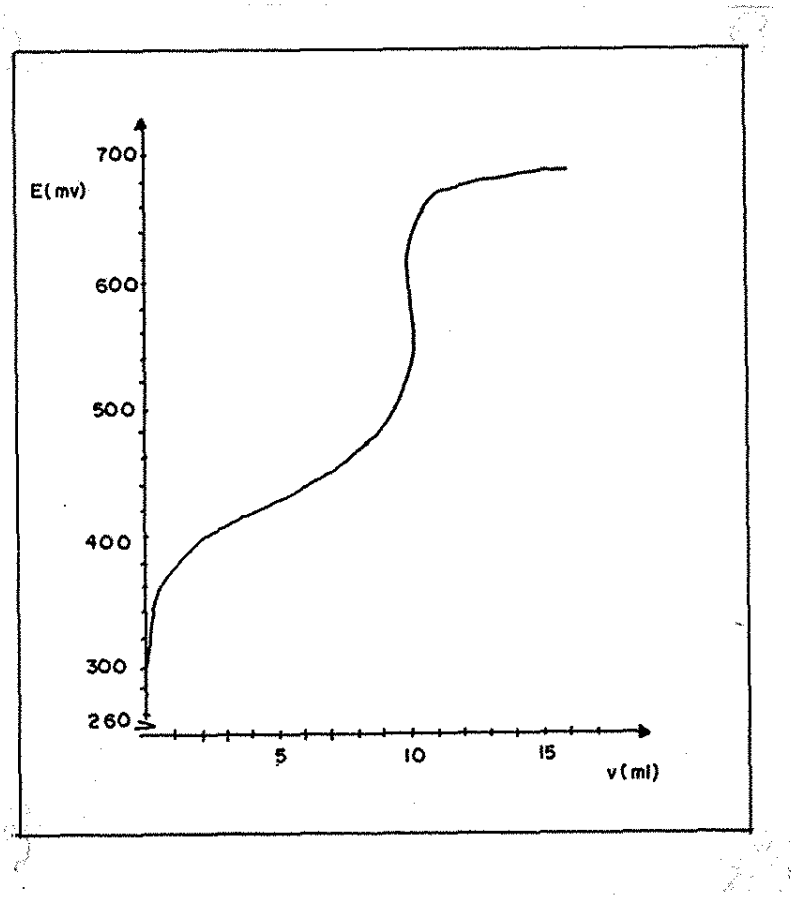

Figure 1. Titration curve using Pt indicator electrode for the system Fe (II)/Cr (VI).

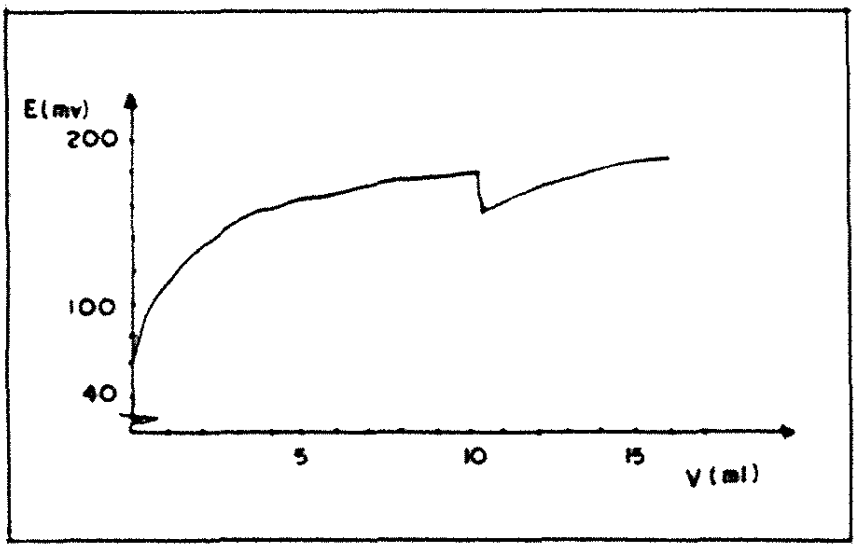

Figure 2. Titration curve using Nb indicator electrode without passivation for the system Fe(II)/Cr (VI).

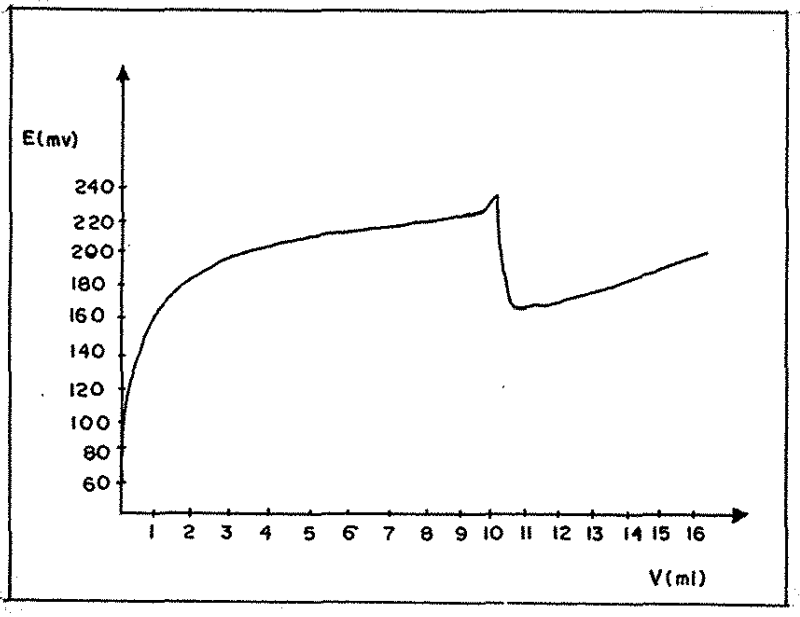

Figure 3. Titration curve using Nb indicator electrode with passivation for the system Fe (II)/Cr (VI).

REFERENCES

1. M. Ashrof-Chorassani and R.D. Braum, *Corrosion - NACE, 43*, 32(1987).

2. J. Breme, *"Titanium and Titanium Alloys the Biomaterial of Preference"* (Plenary Lecture), 6th International Conference on Titanium, Cannes (1988).

3. S.M. Sayed, *J. Chem., 21* , 431 (1978).

4. R. C. Leite, *"Nióbio, uma Conquista Nacional"*, 1ª Edição, Livraria Duas Cidades Ltda, São Paulo, S.P. , 1988

5. A.C. Magalhães, M.D. Capelato, Uso de Ligas Ni-Cr como Sensor Potenciométrico em Titulações Redox, *Química Nova 14* (4), 37 (1991).

6. K. Nomura, Y.Ujhara, *Anal. Chem., 60*, 2564 (1988).

SOUTHERN BRAZILIAN JOURNAL OF CHEMISTRY

Vol. 2, No.2, 1994

THE INFRARED SPECTRA OF METALLOTETRANAPHTYLPORPHYRINS

Rodica Mariana ION, Dumitru LICSANDRU, Florin MOISE*; Cristina MANDRAVEL**;

* - ZECASIN S.A., Splaiul Independentei 202, 79611 Bucharest, Romania ;

** - Bucharest University,bd.Carol 13, Bucharest;

ABSTRACT

The infrared spectra of some metallic complexes of tetranaphtylporphyrins [Me(II) TNP (Me(II) = Mg, Zn, Co, Cu, Cd, Pb, Pd, Ni) and Me(III) TNP X(X2).(Me(III)=Fe,Mn,Co,Al; X=Cl, Imidazole)], have been studied over the range 4000-200 cm^{-1}. The main bands have been assigned in this paper. The correlation between the metal-nitrogen or metal-axial ligand frequencies and the photostability for all these porphyrins hase also been analysed in this paper.

RESUMO

O espectro de alguns complexos metálicos de tetranaftil-porfirinas (Me(II) TNP, (Me(II) = Mg, Zn, Co, Cu, Cd, Pb, Pd, Ni) e Me(III) TNP $X(X_2)$, Me(III) = Fe, Mn, Co, Al; X = Cl, Imidazol) foi estudada na região infravermelha entre 4000 cm^{-1} 200 cm^{-1}. As bandas importamtes foram atribuidas. As correlações entre as frêquencias metal-nitrogênio e metal-ligante axial e a foto-estabilidade de estas porfirinas foram analisadas.

Keywords : Porphyrins, metalloporphyrins, IR spectra, tetranaphtylporphyrins

INTRODUCTION

The metalloporphyrins are one of the most important biological class of compounds [1]. The wide range of biological activity is due, in part, to the nature of the interaction of the central atom with the porphyrin nucleus.

The IR spectroscopy can provide some information about the nature of metal-ligand interactions [2-8].

In this paper, the infrared frequencies for some metallo-tetranaphtylporphyrins, prepared and studied for the first time in the literature, are presented.

It is anticipated that low frequency infrared spectra will provide valuable information about the structure of the complex, the strength of the metal-ligand bonds and the photostability of the metallotetranaphtylporphyrins analysed.

EXPERIMENTAL PROCEDURE

1.Materials

The preparation and the purification of TNP and TNP-Zn(II), have been reported in the literature [9]. The other metallic complexes of TNP, have been prepared for the first time in the literature and have been reported elsewhere [5, 10-12].

2.Spectral Measurements

Infrared spectra were measured on a Specord M 80, Carl Zeiss Jena type spectrophotometer, using either the KBr pellets technique (for the 4000-300 cm^{-1} region) or CCl4 solution technique (for the 4000-200 cm^{-1} region) or the Nujoll pellets technique (for the 400-200 cm^{-1} region).

UV-Vis spectra for the porphyrins were measured on a Specord M 400, Carl Zeiss Jena spectrophotometer, in benzene solutions.

RESULTS AND DISCUSSION

A typical absorption spectrum in the IR region ,e.g.for tetranaphtylporphyrine, (TNP), is given in Figure 1.

As we know, for free base porphyrins,the main frecquency is located in 3400-3600 cm^{-1} region and it is atributed to inner N-H bond vibrations[25].

The main absorption frequencies in the IR domain of free TNP and of its metallic complexes are given in Table 1.

The spectra of free porphyrin bases and metalloporphyrins of the same ligand differ considerably, the latter generally exhibiting less and sharper infrared absorptions due to their higher symmetry [13]. The differences are more pronounced for the vibrations of the porphyrin skeleton than fot the inner vibrations of the peripheral substituents. They are most obvious in the far infrared where the M-N vibrations of metalloporphyrins are located. These cannot be considered to be isolated, since they are coupled with skeletal bending modes (Table 1).

All the TNP complexes show three weak absorptions above 3000 cm^{-1} which can be assigned to the C-H methine stretching vibrations.

Porphyrins exhibit only weak infrared absorptions between 1700 and 1470 cm^{-1} . The low infrared intensity of these vibrations is obviously due to the highly symmetrical macrocycle of metal complex than that of the free ligand, [13-20].

Hydrogenation of the pyrole ring (⇨chlorins) causes the appearance of a strong infrared absorption close to 1600 cm^{-1} (chlorine band). These absorptions arise from the activation of a porphyrin vibration which is forbidden or weak in the infrared under D4h symmetry, [21-28].

Chlorine bands are of particular analytical value. Table 2 summarizes some experimental data.

For many types of metallo-porphyrins, there are metal sensitive bands near 1000

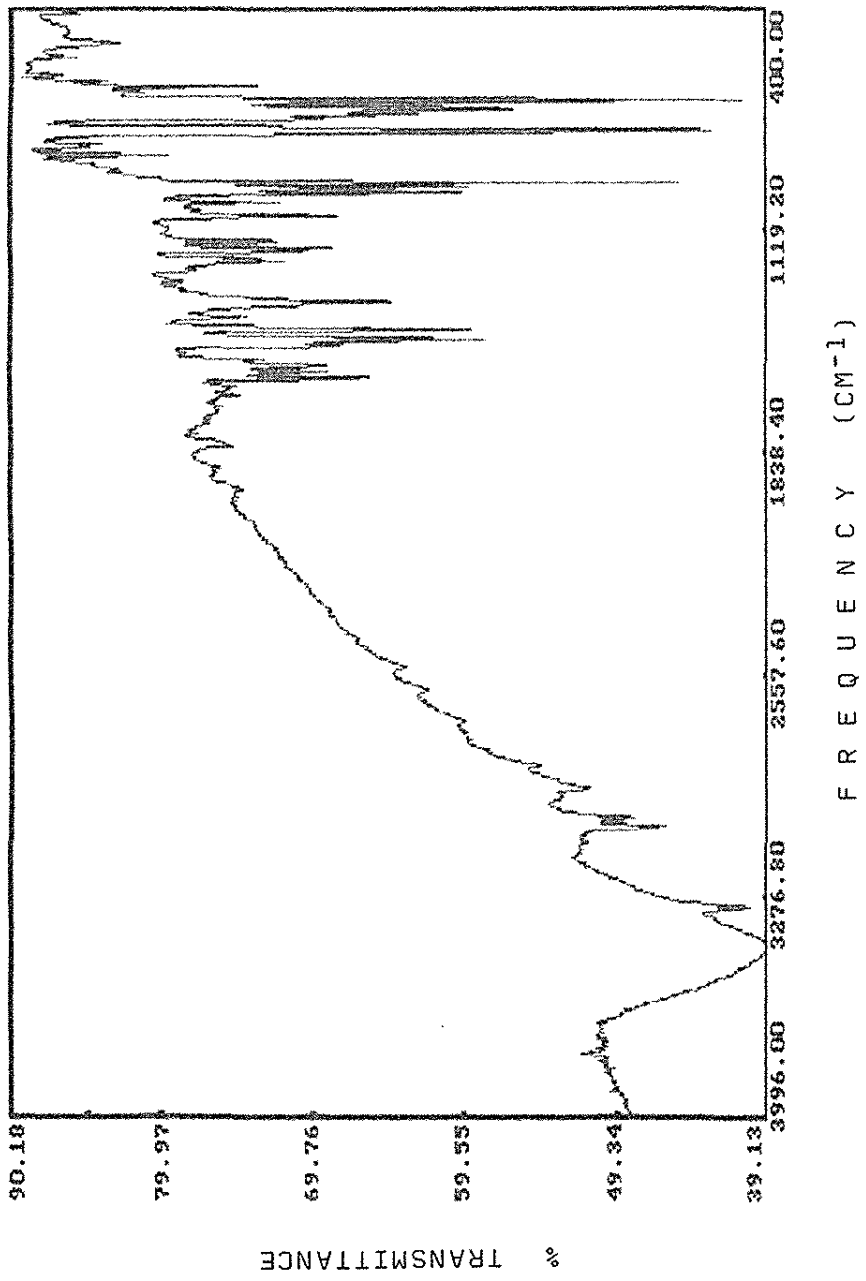

Figure 1. The IR absorption spectrum of TNP

Table 1. Observed frequencies of metallotetranaphtylporphyrins (cm^{-1}):

TNP	Mg	Zn	Pd	Pb	Cd	Co	Cu	Ni	Assignment
3320									ν (N-H)
3110	3120	3185	3160	3130	3130	3140	3150	3160	ν (C-H)methine
3030	3040	3030	3065	3062	3060	3060	3060	3062	ν (C-H)phenyl
3060	2975	2940	3015	3000	3020	2095	3010	2965	
2930	2940	2925	2935	2930	2930	2922	2925	2930	
2850	2860	2860	2860	2860	2860	2860	2850	2855	
1600	1605	1635	1675	1610	1600	1697	1670	1600	ν (C=C)
1580	1525	1575	1545	1555	1575	1550	1545	1580	ν (C=N)
-	1490	1490	1463	1485	1465	1475	1466	1470	δ (C-H)
-	1447	1450	1445	1455	1445	1430	1425	1435	
-	1160	1150	1160	1160	1155	1160	1160	1165	ring deformation
1075	1070	1068	1065	1067	1070	1070	1070	1075	
985	975	980	990	970	973	980	982	987	ν (C-H)methine
-	975	965	955	940	950	930	950	955	
840	835	830	838	835	830	834	833	837	ring deformation
765	760	780	775	770	752	750	771	772	π(ring)
730	725	710	713	712	715	716	718	716	
-	336	334	348	338	340	351	336	355	ν M-N + Ligand
-	214	223	275	287	210	264	234	275	νM-N

Table 2. The Chlorine bands are as following:

Porphyrin	Frequency[cm^{-1}]
TNP-H_2	1600
TNP-Zn	1635
TNP-Pd	1675
TNP-Ni	1675
TNP-Cu	1670
TNP-Cd	1600
TNP-Mg	1605
TNP-Pb	1610
TNP-Co	1687
TNP-MnCl	1660
TNP-FeCl	1652
TNP-CoCl	1650
TNP-AlCl	1649

cm^{-1} [29-33].

TNP complexes show two bands at about 960 and 980 cm^{-1}, which are dependent on the nature of the metal (Table 1).

We assign these two bands to the rocking vibrations of the CH group. The 960 and 980 cm^{-1} bands shift to higher frequencies in the order, (Table 3) :

$$Pd \sim Ni > Co > Cu > Zn > Pb > Mg > Cd$$

The Me-N stretching vibrations are observed among 200 and 300 cm^{-1}. These vibrations may additionally contribute to a smaller extend of vibrations among 300 and 400 cm^{-1} (see Table 4).

Table 3. The Metal bands in the IR spectra :

Metal	Frequency [cm^{-1}]	
Mg	948	975
Zn	950	980
Cu	952	982
Co	953	985
Ni	955	987
Pd	955	990
Pb	940	976
Cd	946	973
Mn	952	987
Fe	920	978
Co	930	980
Al	930	978

Axially substituted metalloporphyrins have been investigated by IR spectroscopy regarding both characteristics.

Definitely assignable inner-ligand vibrations and metal-ligand vibrations typical examples are quoted in Table 5.

All the specific IR frequencies for metallotetranaphtylporphyrins studied, varies in the same way :

$$Pd \sim Ni > Co > Cu > Zn > Mg > Cd ,$$

contrary as vary the photodegradation rate of these porphyrins, and also, the photosensitizer effect of these porphyrins [34].

Table 4. The Metal-Nitrogen vibrations:

Porphyrin	Frequency [cm^{-1}]
TNP-Zn	223
TNP-Mg	214
TNP-Cu	234
TNP-Co	264
TNP-Cd	210
TNP-Pd	275
TNP-Pb	287
TNP-Ni	275

Table 5. The frequencies of the metal- axial ligand bonding:

Porphyrin	Frequency [cm^{-1}]	
TNP-FeCl	280, 290, 305, 330	ν Fe-Cl
TNP-MnCl	310- 330	ν Mn-Cl
TNP-CoCl	300, 364, 402	ν Co-Cl
TNP-AlCl	370, 400	ν Al-C
TNP-$FeIm_2$	335, 370	ν Fe-N
TNP-$MnIm_2$	340, 390	ν Mn-N
TNP-$CoIm_2$	375, 400	ν Co-N
TNP-$AlIm_2$	360. 400	ν Al-N

Conclusions

The specific absorbance frequencies for metallotetranaphtylporphyrins studied, both in the UV-Vis (α, β and Soret bands) and in the low frequency IR spectra (metal-nitrogen and metal-axial ligand bonding) provide valuable information about the strength of the metal-ligand bonds and the photostability of the metallotetranaphtylporphyrins. All this frequencies varyy in the same way, contrary as vary the photodegradation rate and the photosensitizer effect of these copmpounds.

REFERENCES

1. J. E. Falk, *"Porphyrins and Metalloporphyrins"*, Elsevier, Amsterdam, (1964);

2. L. J. Boucher and J. J. Katz: *J. Am. Chem. Soc., 89*, 1340, (1967);

3. L. J. Boucher, H. H. Stain and J. J. Katz: *J. Am. Chem. Soc., 88*, 1341, (1966);

4. H. Ogashi, N. Masai, Z. Yoshida, J. Takemoto and K. Nakamoto: *Bull.Chem. Soc. Jap., 44*, 49, (1971);

5. R. M. Ion, L. Teodorescu, C. Mandravel, E. Volanski and M. Hillebrand: *Rev. Chim., 2*, 129, (1990);

6. C. Mandravel, R. M. Ion and A. M. Alstanei: American-Romanian Congress - USA, (1991);

7. C. Mandravel, A. M. Alstanei and R. M. Ion: *Anal. Univ. Buc., 1*, 61, (1991);

8. C. Mandravel, A. M. Alstanei and R. M. Ion: European Conference on Molecular Spectroscopy, Viena, (1992);

9. L. Guilleux, P. Kransz, L. Nadjo, R. Uzan and C.Giannottii: *J. Chem. Soc. Perkin Trans.II, 3*, 204, (1975);

10. L. Teodorescu, R. M. Ion, D. Badica, H. Culetu: *Rev. Chim., 38*, 129, (1988);

11. R. M. Ion, D. Mardare and S. Coca: *Progr. Catal., 1*, 54, (1993);

12. R. M. Ion : unpublished data;

13. C. Mandravel, R. M. Ion: American-Romanian Academy Congress-USA, (1992);

14. S. Coca, R. M. Ion and F. Moise: *J. Molec. Catal., 1*, in press, (1994);

15. S. Coca, L. Teodorescu, R. M. Ion, L. Popescu and F. Moise: JOM-Hungary, (1993);

16. H. Burger, K. Burczyk, J. M. Buchler, J. C. Fuhrlop, F. Hofler and B. Schrader: *Inorg. Nucl. Chem. Lett., 6*, 171, (1970);

17. K. N. Solovyov, N. M. Ksenofontova, S. F. Shkirman, T. H. Kachura: *Spectrosc. Lett., 6*, 455, (1973);

18. H. Burger, K. Burczyk and J. C. Fuhrlop: *Tetrahedron, 27*, 3257, (1971);

19. H. Ogashi, Y. Saito, and K. Nakamoto: *J. Chem. Phys., 57*, 4, 94, (1972);

20. H. Ogashi, E. Watanabe, Z.Yoshida, J. Kincaid and K. Nakamoto: *J. Am. Chem. Soc., 95*, 2845, (1973);

21. T. Kobayashi: *Spectrochim. Acta, 26A*, 1313, (1970);

22. H.Ogashi and Z.Yoshida: *Bull.Chem. Soc. Jap., 44*, 1722, (1971);

23. R. H. Felton, N. T. Yu, D. C. O'Shea and J. A. Shelmitt: *J. Am. Chem. Soc., 96*, 3675, (1974);

24. L. A. Nafie, M. Pezolet and W. L. Peticolas: *Chem. Phys. Lett., 20*, 563, (1973);

25. S. F. Mason: *J. Chem. Soc.*, 976, (1958);

26. N. Sadavisan and E. B. Fleischer: *J. Inorg. Nucl. Chem., 30*, 591, (1968);

27. L. J. Boucher and J. J. Katz: *J. Am. Chem. Soc., 89*, 4703, (1967);

28. J. W. Buchler and L. Puppe: *Ann. Chem., 740*, 142, (1970);

29. H. H. Inhoffen, J. W. Buchler and R. Thomas: *Tetr. Lett.*, 1145, (1969);

30. H. H. Inhoffen, J. W. Buchler and R. Thomas: *Tetr. Lett.*, 1141, (1969);

31. J. W. Buchler and K. Rohback: *J. Organometal. Chem., 65*, 223, (1974);

32. I. A. Cohen and B. C. Chaco: *Inorg. Chem., 13*, 488, (1974);

33. L. J. Boucher: *J. Am. Chem. Soc., 92*, 2725, (1970);

34. R. M. Ion and L. Ceafalau: *Rev. Chim.*, accepted for publication.

SOUTHERN BRAZILIAN JOURNAL OF CHEMISTRY
Vol. 2, No.2, 1994.

HYDROPHOBIC EFFECTS IN WATER AND WATER/UREA SOLUTIONS

A COMPARISON

E.A.Lissi and E.B.Abuin

Departamento de Ciencias Químicas - Facultad de Química y Biología - Universidad de Santiago de Chile, Casilla 307, Santiago-2, Chile

ABSTRACT

The partition of several n-alkanols, from methanol to n-nonanol, between n-hexane and water and between n-hexane and water containing 20 % (w/v) urea has been measured at temperantures ranging from 0 °C to 60 °C. The standard free energy of transfer from water to the urea containing solution decreases with the length of the alkyl chain, being positive for the small alcohols and negative for the higher alkanols. The same tendency is observed upon all the temperature range considered. On the other hand, the standard entropy of transfer from water to the urea containing solution increases with the length of the alkyl chain of the alkanol. These results are compatible with a simple description of the urea effect in terms of increasing the entropy of dissolution of the hydrophobic alkyl chain in the aqueous solution.

RESUMO

As constantes de partição de álcoóis variando de metanol a n-nonanol foram medidas para água e n-hexano e n-hexano e água contendo 20% (peso/volume) de uréia a temperaturas entre 0 ºC e 60 ºC. A energia livre padrão de transferência de água para solução contendo uréia diminui em função do comprimento da cadeia alquila, sendo positiva para álcoois curtos e negativa para álcoóis de cadeia comprida. Por outro lado, a entropia padrão de transferência de água para a solução contendo uréia aumenta em função do comprimento da cadeia do álcool. Os resultados experimentais são compatíveis com a simples descrição do efeito da uréia em termos do aumento da entropia de dissolução da cadeia alquila na solução aquosa.

INTRODUCTION

The properties of aqueous solutions of urea are interesting and intriguing. The solubility of urea in water is extremely high (> than 20 M at room temperature [1]) and solubilization takes place following almost ideal behaviour.[2] Addition of urea to water increases the solubility of nonpolar solutes with relatively large size but decreases (or barely affect) the solubility of the small size members of this type of solutes at room temperature ; the size discriminating effect of urea on solubility of nonpolar solutes is more important at low temperatues.[3] Urea in aqueous solution is a strong protein denaturant [4] , it inhibits the micellization of surfactants and alter micellar characteristics [5-15]. All these properties of aqueous urea solutions have been the subject of numerous studies performed with the aim to clarify the mechanism of urea action. From these studies, two plausible mechanisms have been proposed [3,16] : (1) An indirect mechanism in which urea acts only at the level of the solvent, altering the structure of water in a way that facilitates the dissolution of hydrophobic species (i.e., by invoking the capacity of urea to act as a "water structure breaker", so allowing the free energy required for cavity formation to decrease) and, (2) A direct mechanism in which urea participates in the solvation of hydrophobic species by replacing some water molecules in the hydration shell of the solute. Mechanism (1) has received the majority of the attention in the literature , an many experimental studies seem to support it. [17,18] However, recent experiments seem to contradict it.[19] Furthermore, computer-simulation studies indicate that urea hardly affects the structure of water , going against mechanism (1) and that a few molecules of water around a hydrophobic moiety are replaced by urea, consistent with mechanism (2).[20] In recent years, mechanism (2) is increasingly employed and several studies seem to support the hypothesis of a direct mechanism of urea action. [10,11,14]

Due to the potential applicability of either mechanism of urea action, the literature data on the effects of urea in micellar solutions are conflicting. Miyagishi et al.[7] performed an study on the alterations in properties of micelles induced by perturbation in the external environment and used urea as an additive assumed to be able to penetrate the micelles. Similarly, urea was assumed to be a nonpenetrating agent in a study performed by Gonzalez at al. [6] on the effect of additives upon the solubility of naphthalene derivatives in micellar solutions . Alternatively, recent studies are in line with the participation of a direct mechanism of urea action in several properties of micelles. [10,11,14,15] Furthermore, the effect of urea upon the critical micelle concentration of surfactants seems to be non understable in terms of either mechanism of urea action upon the solubility of the hydrocarbon parts of the amphiphiles / strong effects of the surfactant head groups must be exerted and / or, more likely , the effect of urea upon the cmc of surfactants also reflects a change in the chemical potential of the surfactant in the micelle . If this were the case, the question arises on whether urea replaces water at the micelle surface (mechanism (2) or the alterations of the chemical potential of the surfactant in the micelle are simply due to a facilitated solvation of the first methylene groups near the head groups (mechanism 1). As an example, urea barely modifies the critical micelle concentration (cmc) of sodium dodecylsulphate,[5,8] while it considerably increases the cmc of dodecyltrimethylammonium bromide [8,12] and cetyltrimethylammonium bromide. [6] Ideally, studies on the thermodynamics (free energy, entropy and enthalphy) of transference of surfactants from water to urea solutions performed at surfactant concentrations well below the critical micelle concentration in water would help to clarify some of these aspects. Unfortunately, these type of studies are scarce. [21]

Primary alkanols afford an homologous series of amphiphilic molecules with identical

head groups in which the size of hydrophobic moiety can be widely varied by simply changing the hydrocarbon length, its concentration in dilute solutions is easy to measure and have been employed in several studies on hydrophobic interactions. [22] We have selected this series of compounds to perform an study on the thermodynamic parameters involved in the transference of methylene groups from water to aqueous urea solutions. The results are here reported.

MATERIALS AND METHODS

The partition of the alkanols between water and n-hexane was evaluated by the shake flask method. The alkanol was dissolved in water (or water containing 20 % w/v urea) at concentrations far below saturation and, after addition of n-hexane, the flasks were shaken by several minutes at the desired temperature. The solutions were kept two hours in closed tubes in a thermostatized bath and samples from both phases were analyzed by gas chromatography. The alkanols were Aldrich products of the highest purity avalilable and were employed without purification. Since the concentration of the alkanol in both phases was evaluated chromatographically after equilibration, the posible presence of impurities does not interfere with the results.

RESULTS AND DISCUSSION

At the low alkanol concentrations employed in the present work, the thermodynamic partition constant can be directly obtained from the ratio of the concentrations in the organic and aqueous phase:

$$K = [ROH]_{hex}/[ROH]_{water} \qquad (1)$$

The values obtained at 0 , 25 and 40 °C when water or water plus urea were employed as aqueous phase, are compilled in Table 1. These data allow an evaluation of the free energy change associated to the transfer of the alkanol from water to water/urea solutions ($\Delta(\Delta G^o)$). The values obtained at 0 °C and 25 °C are shown in Fig. 1 . Although they are rather small and affected by high relative errors, they indicate that the transfer becomes more favoured when the length of the alkyl chain increases. The same tendency is observed for the data at 40 °C previously reported by Abu- Hamdiyyah et al. [9], which have also been included in Fig. 1. These results imply that addition of urea to water decreases the magnitude of the hydrophobic effect. Similar conclusions can be derived from the data obtained at the other temperatures, which show that the effect of the alkyl chain length upon ΔG^o becomes larger at lower temperatures.

Table 1. Partition Constants at different temperatures

Alkanol	0 °C		25 °C		60 °C	
	water	water/urea	water	water/urea	water	water/urea
Methanol	0.0012	0.0035	0.0029	0.0046	0.0052	0.0081
Ethanol	0.0020	0.0030	0.0053	0.0070	0.0160	0.0250
Propanol	0.0110	0.0150	0.025	0.032	0.1	0.1
Hexanol	0.98	1.13	3.35	2.45	9.5	6.4
Octanol	21.6	19	67.1	59	155	83
Nonanol	76	20	145	100	345	240

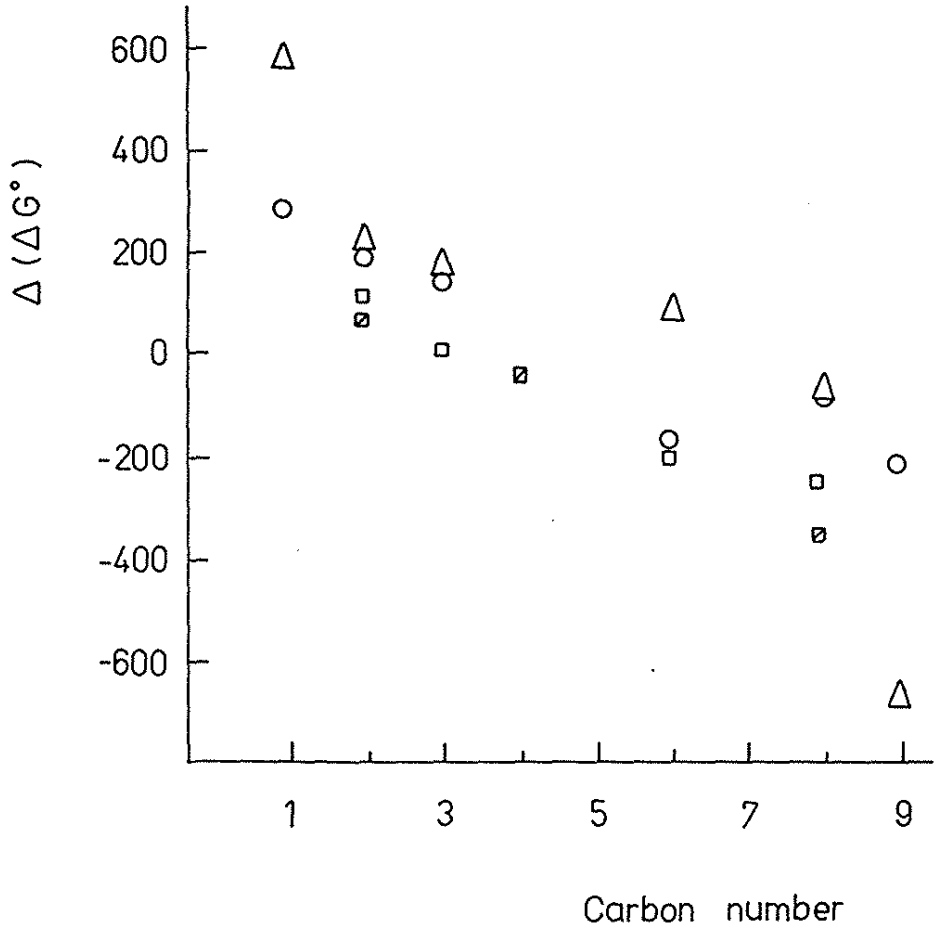

Figure 1. Values of the standard free energies of transfer (in cal/mol) from water to water/urea solutions plotted as a function of the number of carbon atoms in the alkanols. (△) Data obtained at 0 °C ; (○) Data obtained at 25 °C ; (□) Data obtained at 40 °C ; (▨) Data reported at 40 °C in Ref. 9 .

The changes in enthalpy and entropy associated to the transfer processes can be obtained from the change with temperature of the ln K. Typical values obtained are given in Fig. 2. The curvature of the plot indicate that the enthalpy changes, $\Delta H°$, cannot be considered as constant and makes difficult the calculation of the values of the thermodynamic quantities. In order to obtain an estimation of them, the data were fitted to a parabola and the slope at 25 °C analytically derived. The values obtained for the transfer from n-hexane to aqueous solutions are shown in Fig. 3. From these values and the free energy changes, the entropy changes ,$\Delta S°$ can be derived. The values obtained are shown in Fig. 3. Although these values are affected by rather large uncertainties, they show that passage from the organic solvent to the aqueous phase implies a significant decrease in both, enthalpy and entropy. In particular, it is noticeable the steady increase in $\Delta S°$ with the size of the alkyl chain. Similar trends are observed when the transfer from the organic solvent to the urea/water solution is considered. The effect of urea can be best analyzed by considering the transfer from the aqueous solution to the urea/water solution. The values of $\Delta H°$ and $T\Delta S°$ associated to the transfer of the alkanols from water to urea/water solutions are given in Fig. 4. The data given in this figure show compensatory effects in $\Delta H°$ and $T\Delta S°$ which can be partly due to the rather large experimental errors involved in their determination. However, the results indicate that, particularly for the larger alkyl chains where the hydrophobic effect must be maximal, the transfer from water to urea/water solutions take place with both an increase in $\Delta H°$ and $T\Delta S°$, a result compatible with a reduced hydrophobic effect in the presence of urea. This is fully compatible with the data of Fig. 1 which indicate that transfer of the alkanol to the urea/water solution becomes more favoured when the length of the

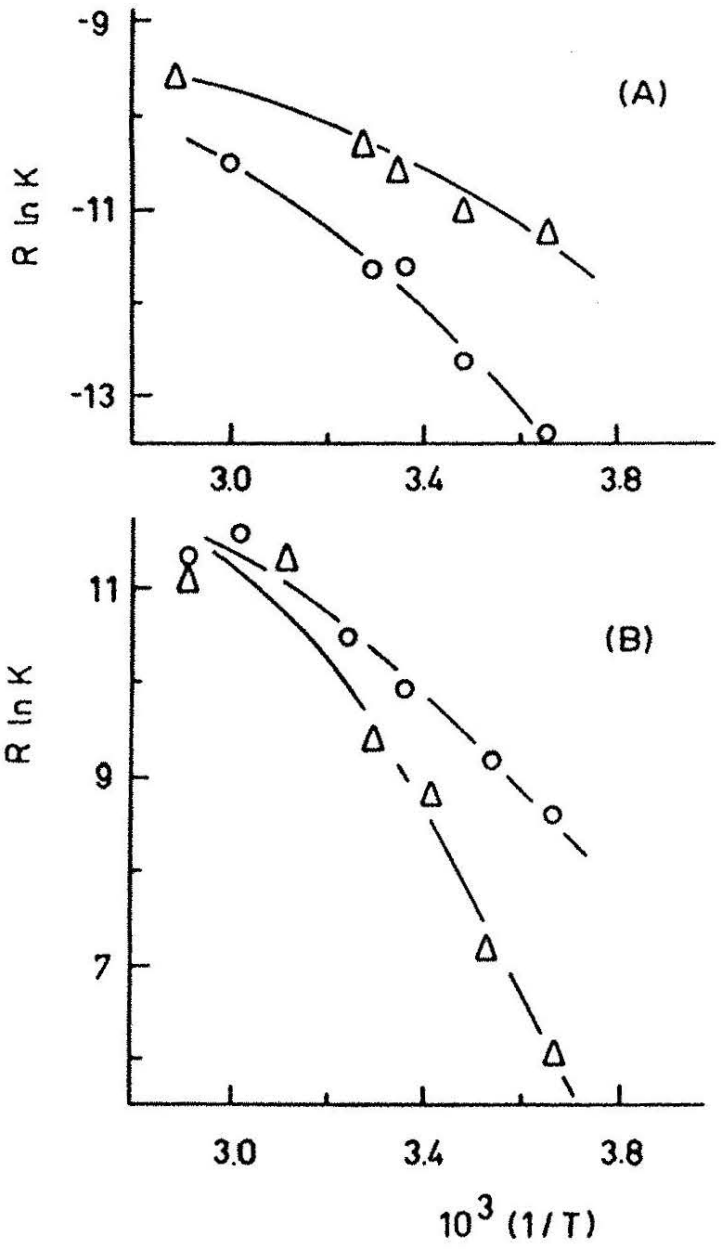

Figure 2. Dependence of the n-hexane/water (○) and n-hexane/water plus urea (△) partition constants with temperature. Data plotted as R ln K (in cal/mol) against the inverse of the temperature (Kelvin)
(A) Data obtained for methanol
(B) Data obtained for 1-nonanol.

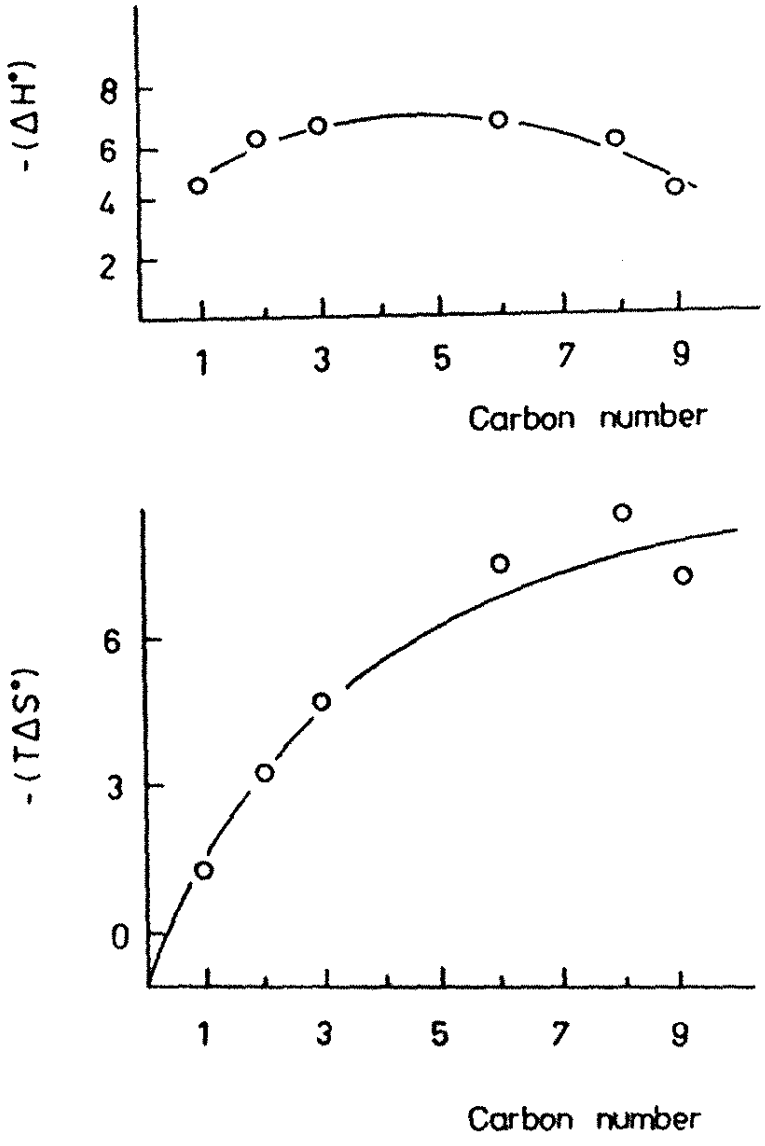

Figure 3. Dependence of the enthalpy and standard entropy of transfer (in kcal/mol) from n-hexane to water with the number of carbon atoms of the alkanol. Values reported were obtained at 25 °C.

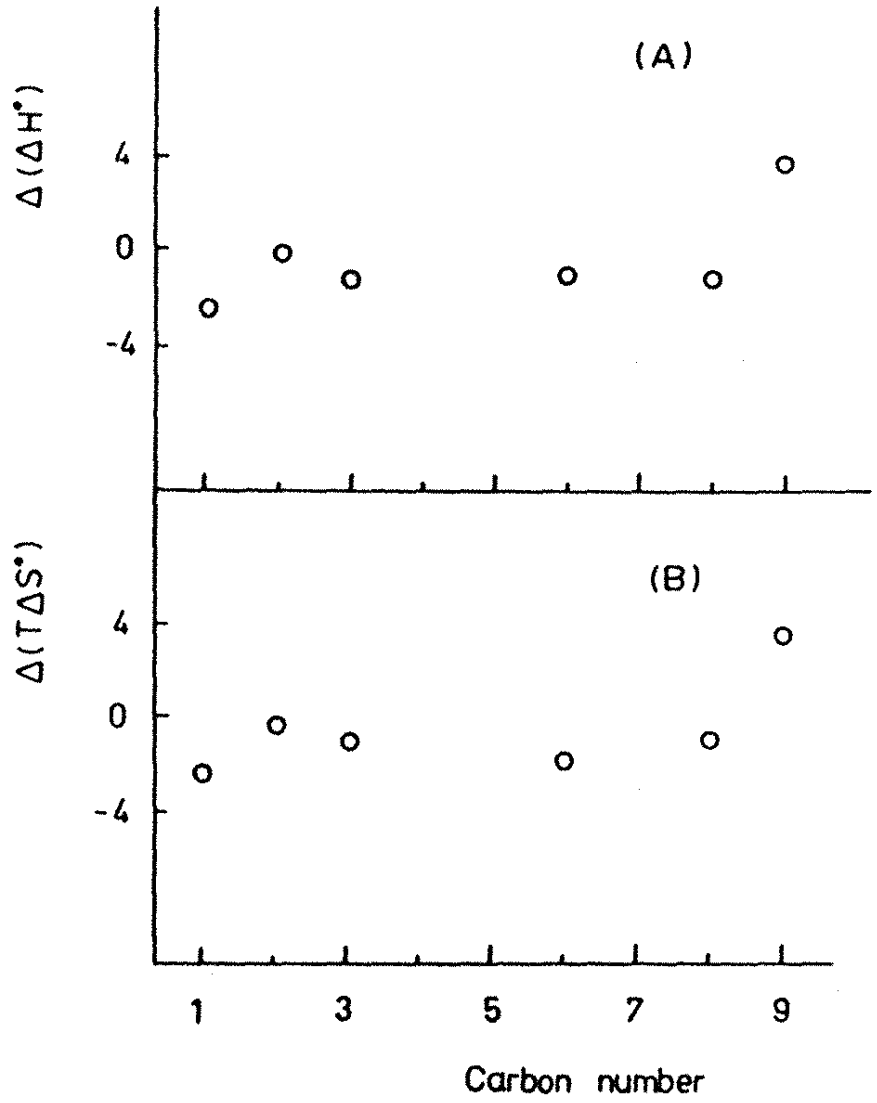

Figure 4. Dependence of the standard enthalpy and standard entropy changes for the transference from water to water/urea solutions with the number of carbon atoms of the alkanol. Values reported were evaluated at 25 °C.

alkyl chain increases. Although these results do not allow to establish the origin of these effects (either reducing the structure of water and/or a direct interaction of urea with the alkyl chain), they clearly indicate that the decreased free energy of the alkyl chain in the urea/water solutions, relative to that in aqueous solution, is mostly due to a larger partial entropy of the solute in the presence of the additive.

ACKNOWLEDGMENTS. Thanks are given to DICYT (Universidad de Santiago de Chile) for financial support.

REFERENCES

1. H.D. Ellerton and P. Dunlop, J.Phys.Chem.,70, 1831 (1966)
2. R.H. Stokes, Aust. J. Chem.,20, 2087 (1967)
3. D.B. Wetlaufer, S.K. Malik, L. Stoller and R.L. Coffin, J.Amer.Chem.Soc.,86, 508 (1964)
4. J.F. Brandts and L. Hunt, J.Amer.Chem.Soc.,89, 4826 (1967)
5. M. J. Schick, J. Phys. Chem., 68, 3585 (1964)
6. M. Gonzalez, J. Vera, E.B. Abuin and E. A. Lissi, J. Colloid Interface Sci., 98, 152 (1984)
7. S. Miyagishi, T. Asakawa and M. Nishida, J. Colloid Interface Sci., 115, 199 (1987)
8. P. Baglioni, E. Rivara-Minten, L. Dei and E. Ferroni, J. Phys. Chem., 94, 8218 (1990)
9. M. Abu-Hamdiyyah and K. Kumari, J. Phys. Chem., 94, 6445 (1990)
10. P. Baglioni, E. Ferroni and K. Kevan, J. Phys. Chem., 94, 4296 (1990)
11. G. Briganti, S. Puvvada and D. Blankschtein, J. Phys. Chem., 95, 8989 (1991)

12. S. Causi, R. De Lissi, S. Milioto and N. Tirone, J. Phys. Chem., 95, 5664 (1991)

13. E. Caponetti, S. Causi, R. De Lisi, M. A. Floriano, S. Milioto and R. Triolo, J. Phys. Chem., 96, 4950 (1992)

14. K. Bhattacharyya and M. Chowdhury, Chem. Rev., 93, 507 (1993)

15. C. Carnero Ruiz and F. García Sánchez, J. Colloid Interface Sci., 165, 110 (1994)

16. O. Enea and C. J. Jolicoeur, J. Phys. Chem., 86, 3370 (1982)

17. G.C. Kresheck and H. A. Scheraga, J. Phys. Chem., 69, 1704 (1965)

18. M. Manabe, M. Koda and K. Shirahama, J. Colloid Interface Sci., 77, 189 (1980)

19. R. Breslow and T. Guo, Proc. Nat. Acad. Sci., U.S.A., 87, 167 (1990)

20. (a) R.A. Kuharsky and P. Rossky, J. Amer. Chem. Soc., 106, 5786 and 5794 (1984) (b) H. Tanaka, H. Tohura, K. Nakanishi and N. J. Watanabe, J. Chem., Phys., 80, 5170 (1984)

21. N.R. Choudhury and J. C. Ahluwalia, J. Chem. Soc. Farad. Trans. I, 77, 3119 (1981)

22. Y. Ulloa, M. A. Rubio, E. A. Lissi and A. Aspee, Bol. Soc. Chil. Quím., 39, 129 (1994) and references cited therein.

SOUTHERN BRAZILIAN JOURNAL OF CHEMISTRY
Vol. 2, No.2, 1994

An Attempt to Develop a New Fire-Resistant Hydraulic Fluid Based on Water-in-Oil Microemulsions

N. Garti, A. Aserin and S. Ezrahi

Casali Institute of Applied Chemistry
The Hebrew University of Jerusalem
91904 Jerusalem, Israel

ABSTRACT

The strategy for the development of microemulsion-based fire-resistant hydraulic fluids has been expounded. Phase diagrams were constructed for mixtures of water, oil and nonionic surfactants with and without cosurfactants. From these phase diagrams the boundaries of the monophasic area were outlined. After the major components had thus been determined, several preliminary formulations were developed by incorporating suitable additives into the oleic ingredient of the hydraulic fluid. These carefully chosen additives improve considerably the performance of the hydraulic fluid. The resulting microemulsion-based compositions complied with most of the requirements set for fire-resistant hydraulic fluids.

Model systems pertinent to such formulations were utilized in order to investigate structural factors, which induce enhanced water solubilization. The role played by alcohols in this context was elucidated in terms of an empirical equation. Sophisticated scattering and NMR methods have demonstrated the variations in the microstructure of a high water content model system. Sub-zero differential scanning calorimetry (DSC) techniques have revealed the existence of two types of water (free and bound) and determined their relative concentrations.

RESUMO

A técnica de desenvolvimento de flúidos hidráulicos não-inflamáveis foi descrita. Foram construidos diagramas de fase para misturas de água, óleo e surfatantes com e sem cosurfatantes e a região monofásica foi bem definida. Subsequentemente, foram preparadas formulações preliminares incorporando aditivos adequados na fase oleosa do flúido hidráulico. As composições, baseadas em microemulsões, satisfazeram a maioria dos prerequisitos de flúidos hidráulicos não-inflamáveis. As interações no meio e particularmente a função dos álcoois e da água foi estudada usando técnicas de espalhamento de raios-X à ângulo baixo (SAXS), calorimetria diferencial de varredura (DSC) e ressonância magnética nuclear (RMN). Foi demonstrada a existência de dois tipos de água (livre e ligada) e foi determinada a concentração relativa.

INTRODUCTION

In principle, almost every liquid may function as a hydraulic fluid. However, because of its obvious economic and environmental advantages water was normally used for transmission of power[1]. The advent of high-performance pumps has introduced the use of mineral oils. These hydraulic fluids have been improved by refining the mineral oil and incorporating adequate additives. The Achilles heel of mineral oil-based hydraulic fluid is its high flammability, which may, in some important applications, almost nullify its numerous advantages. Such hydraulic fluids have already caused many disasters in both civilian and military applications. The risk of fire will be more pronounced in future applications since much higher pressures are planned to be applied[2]. The historical evolution of hydraulic fluids and the present situation are described in the following scheme:

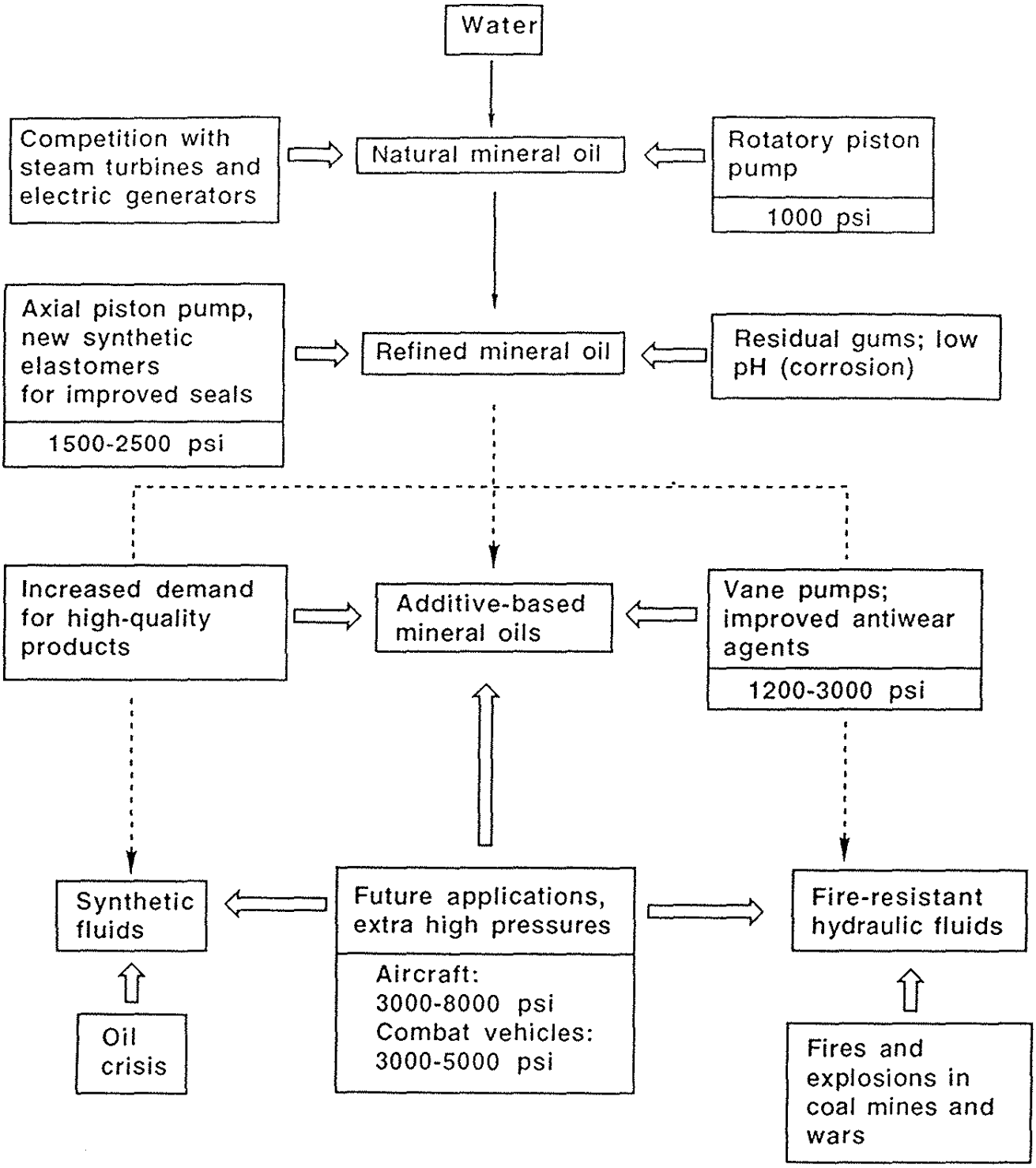

Fig. 1: The historical evolution of hydraulic fluids.

Most suggested fire-resistant hydraulic fluids may be classified[3] in one of the four groups: HFA, HFB, HFC and HFD (see Table 1).

TABLE 1: Classification of fire-resistant hydraulic fluid.

Classification	Description
HFA	High water-based fluids which are further divided into:
HFA-E	Oil-in-water emulsions or aqueous solutions containing max. 20 mass % of combustible materials.
HFA-S	Solutions of chemicals in water containing min. 80 mass % water.
HFB	Water-in-oil emulsions containing max. 60 mass % of combustible materials. Water content normally 40-45 mass %.
HFC	Aqueous solutions with viscosity-increasing (polymeric) additives or water-glycol solutions. Usually contained min. 35 mass % water.
HFD	Fire-resistant nonaqueous fluids such as phosphate esters (most common), halogen-containing compounds, etc.

Each type has its pros and cons. The main disadvantage of the four types will now be described in a nutshell. HFA suffers from almost all the drawbacks of water, such as rust, poor lubricity and wear resistance[4], limited range of operating temperatures[5] and microbial infestation[6]. HFB fares no better, as like any other emulsion, it is inherently unstable[1]. HFC suffers from poor lubricity[7] and incompatibility with some metals and sealants[8]. HFD is expensive[8], too heavy for certain applications and suffers from incompatibility with construction materials and additives[2].

In our case, the hydraulic fluid could not have had density higher than 0.95-1.00 g/cc as this fluid was designed to operate in a given system. Our research strategy was based on the following principles:

Of all the possibilities suggested for fire-resistant hydraulic fluids, most promising seems to be a combination of the excellent hydraulic qualities (especially lubricity) of mineral oil with the fire-resistance and environmental advantages of water. This rules out the HFC and HFD types.

There should be an optimal balance between the fire-resistance (maximum water content) and the hydraulic qualities (maximum mineral oil content) of the hydraulic fluid. Excess of either water or oil will be detrimental to the product. This principle rules out the HFA type.

The remaining type, HFB, suffers from instability, and our solution to this is to use microemulsions instead of emulsions. The idea of using microemulsions as hydraulic fluids is quite recent and does not appear often in the relevant technical literature (scientific articles and patents). A microemulsion is a clear and thermodynamically stable mixture of water, oil and suitable amphiphiles (substances that due to their unique molecular structure can hold water and oil together). Microemulsions are much easier to prepare than ordinary emulsions, as they form spontaneously[9]. They are stable under a wide range of operating conditions[10] and in storage, have high solubilization capacity for both oil and water[11], and provide better protection than simple emulsions against corrosion and wear[12]. They are also easier to filter[13] and are less volatile. Thus, microemulsions may be a most promising solution to the problem of fire-resistant hydraulic fluids. In the future, we will be able to replace the mineral oils by more sophisiticated and efficient synthetic fluids and hopefully to microemulsify them.

EXPERIMENTAL PROCEDURE

Materials

In all formulations the oleic phase was based on a paraffinic mineral oil (produced by Paz Oil Co., Ltd., Israel) consisting of ca. 70% paraffinic oil and 30% naphtenic and aromatic fractions. The surfactants used were polyoxyethylene (2) oleylalcohol (known also as $C_{18:1}(EO)_2$ or Brij 92), polyoxyethylene (20)-oleylalcohol (knowl also as $C_{18:1}(EO)_{20}$ or Brij 98), both purchased from ICI Specialty Chemicals, Germany, and 2-ethylhexylsulfosuccinate sodium salt (known also as AOT) from American Cyanamid Company, USA. 1-pentanol (Aldrich Chemical Co., Inc., USA) was used in some experiments as a cosurfactant. Distilled water was used as the aqueous phase. Alkylbenzotriazole, ethoxylated alkanolamide, tetraethylene glycol, zinc dialkyldithiophosphate (ZDDP), a nitroalkylmorpholine derivative and 1-phenyl dodecane, all obtained from Paz Oil Co., Ltd., Israel, were used as additives in various formulations as will be described in the text. For the model systems, n-dodecane (sometimes also n-decane, n-tetradecane and n-hexadecane) from Aldrich Chemical Company, Inc., USA (purity ca. 99%) was used as the oleic phase. The surfactants used were polyoxyethylene (10) oleylalcohol (known also as $C_{18:1}(EO)_{10}$ or Brij 97), polyoxyethylene (10) stearylalcohol (known also as $C_{18}(EO)_{10}$ or Brij 76) of ICI Specialty Chemicals, Germany, and highly purified octaethylene glycol mono-n-dodecylether [$C_{12}(EO)_8$] from Nikko Chemicals Co., Japan; 1-pentanol was one of the main cosurfactants, but sometimes other n-aliphatic alcohols (such as 1-butanol, 1-hexanol, etc.) were also used. All of them were purchased from Aldrich Chemical Company, Inc., USA. Water for the model systems was double distilled.

Determination of the phase diagrams

The phase behavior of the three-component systems was depicted on ternary phase diagrams. These diagrams are outlined on triangles. Each corner of

such a triangle represents 100% of the component whose name appears near that corner. The behavior of four-component systems is described on a pseudo-ternary phase diagram in which the weight ratio of two components was fixed. Usually, the alcohol:oil weight ratio was held constant at 1:1. The construction of the phase diagram was conducted in a thermostatic bath at a given temperature in the following way. Mixtures of surfactant, alcohol (cosurfactant) and oil were prepared in culture tubes sealed with viton-lined screw caps at predetrmined weight ratios of (alcohol + oil) to surfactant of 9:1, 8:2, . . . 1:9, 0.5:9.5 (10 samples in all). To these mixtures small weighed amounts of water were added dropwise at first and then larger aliquots such that the weight fraction of each water increment was at least 0.02. These aqueous mixtures are samples along water dilution lines drawn to the water apex from the opposite side of the triangle. In all the samples tested, evaporative loss was negligible. Nearly all samples were equilibrated during a time interval which varied from a few minutes to 24 hours. The tubes were then inspected visually. Optical birefringence (observed between crossed polarizers) and apparent increased viscosity indicated the presence of a liquid crystalline phase. Identification of the liquid crystals was done by small angle X-ray scattering (SAXS). Appearance of turbidity was considered as an indication for phase separation. In some doubtful cases, the samples were let to settle and give clear phases. The phase behavior of such samples was determined only after sharp interfaces have become visible. The completion of this process was hastened by centrifuging the samples. Every sample which remained transparent and homogeneous after vigorous vortexing was considered as belonging to a monophasic area in the phase diagram. In this way we were able to outline the phase diagram of the system.

RESULTS AND DISCUSSION

$C_{18:1}(EO)_2$ and $C_{18:1}(EO)_{20}$ systems

Figure 2 is a tricomponent phase diagram of $C_{18:1}(EO)_2$/mineral oil/water at two different temperatures The surfactant is too hydrophobic (HLB 4.9) to solubilize appreciable amount of water, even in the presence of high concentrations of surfactant. The L_2 phase represents reverse micelles swollen by the water solubilized in their core. Quasielastic light scattering (QLS) measurements seem to show that the aggregates are few and very small. The area of the L_2 phase is narrow and practically unaffected by the temperature. This is understandable as the temperature effect on the very short EO chains is quite limited.

Figure 3 is the phase diagram of the system $C_{18:1}(EO)_{20}$/mineral oil/water at two different temperatures. This surfactant is hydrophilic (HLB 15.3), has only minor solubility in oil but increased solubility in water. However, geometrical considerations suggest that L_2 will still be rather small though the amount of solubilized water (ca. 10 wt%) is larger than that in the case of the $C_{18:1}(EO)_2$ system. QLS measurements indicate the presence of small aggregates in the L_2 region. In addition, a large area of liquid crystalline phase is seen (region E in Fig. 3). Optical microscopy and SAXS measurements have proved the hexagonal nature of this phase. This is in good agreement with statements[14] that nonionic surfactants containing long hydrophilic chains tend to strongly hydrate the water and therefore transform into a hexagonal structure. The variation of temperature from 25°C to 45°C did not significantly affect the phase diagram.

Figure 4 is the phase diagram of the system $C_{18:1}(EO)_2$ + $C_{18:1}(EO)_{20}$ at 0.42:0.58 (wt/wt), respectively/mineral oil/water (HLB 10.9). This ratio between the surfactants was selected because it represents the required HLB of the paraffinic oil used in these experiments. The required HLB is the optimal HLB for the preparation of O/W macroemulsions in which the oil phase was a similar paraffinic oil.

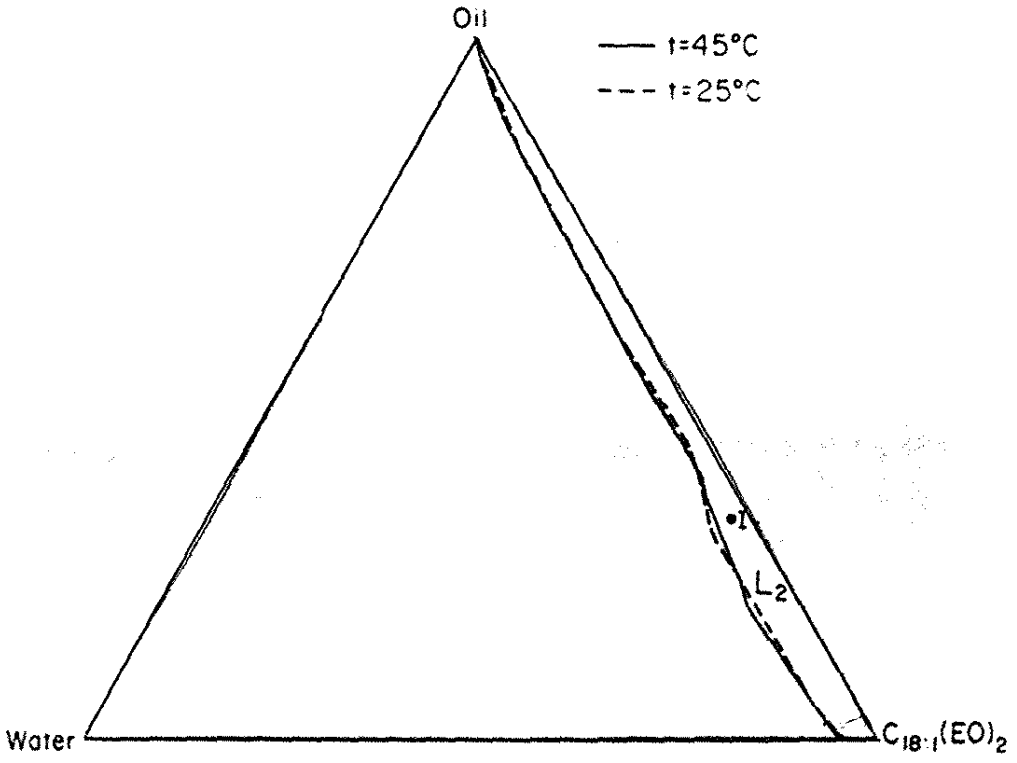

Fig. 2: Phase diagram of the system $C_{18:1}(EO)_2$/mineral oil/water.

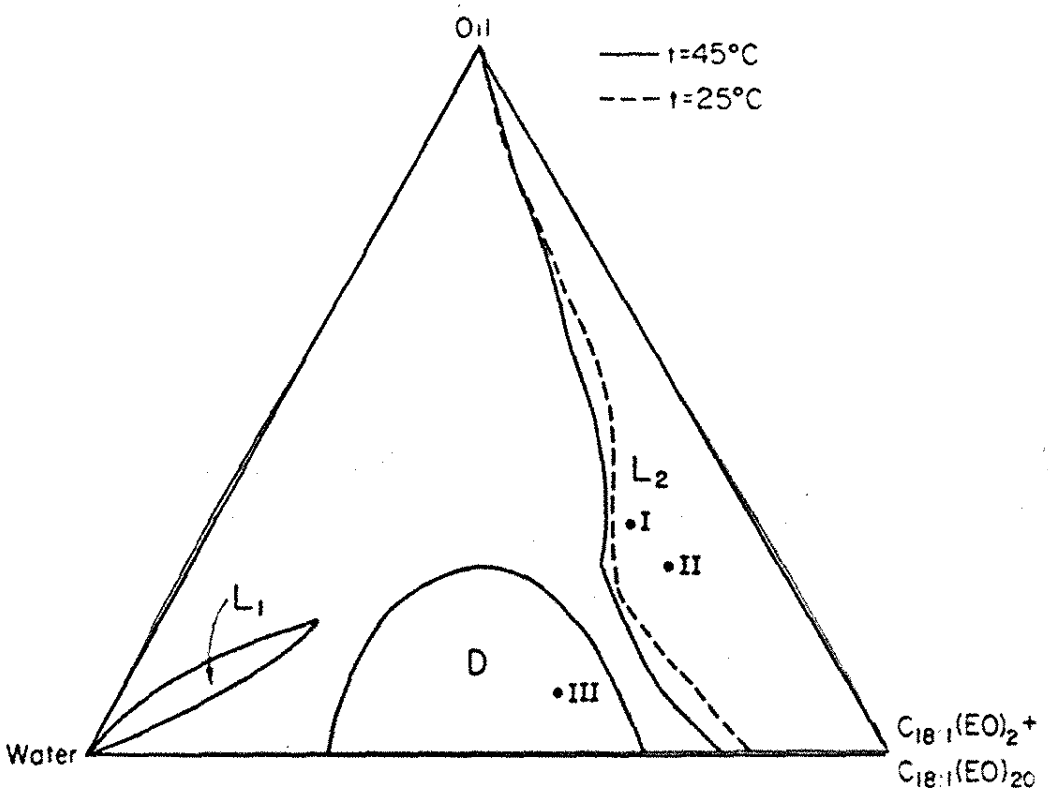

Fig. 3 Phase diagram of the system $C_{18:1}(EO)_{20}$/mineral oil/water.

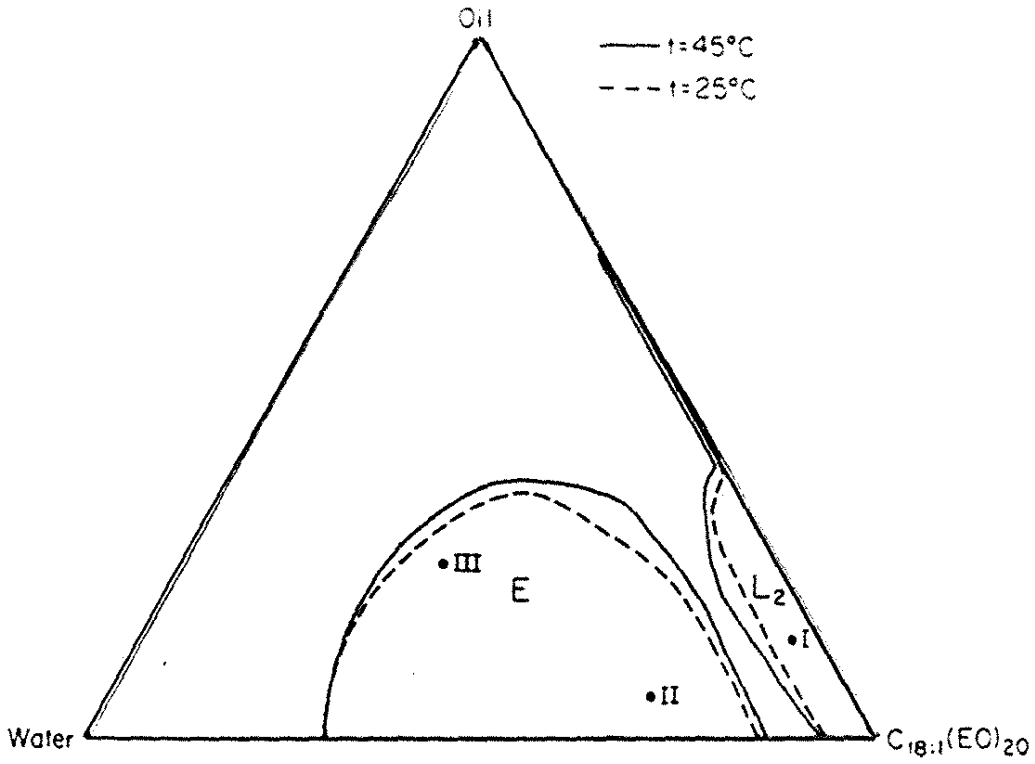

Fig. 4: Phase diagram of the system $C_{18:1}(EO)_2+C_{18:1}(EO)_{20}$ [0.42:0.58 (wt/wt)]/mineral oil/water.

The synergism between the two surfactants is expressed in the amount of solubilized water, which is larger than in the case of $C_{18:1}(EO)_2$ and $C_{18:1}(EO)_{20}$ operating separately. The L_2 phase is relatively larger and 22 wt% water may be solubilized. In addition, a small L_1 phase is detected. The L_1 phase consists of swollen regular micelles in which small amounts of oil have been solubilized. Between the L_1 and L_2 regions of the phase diagram, a liquid crystalline phase is also well defined. This mesophase was identified as lamellar. Table 2 compares the results of these three systems.

TABLE 2: Factors for quantitative evaluation of the surfactants relative efficiency for solubilizing water. system: Mineral oil/surfactant/water.

	$C_{18:1}(EO)_2$		$C_{18:1}(EO)_{20}$		$C_{18:1}(EO)_2$/ $C_{18:1}(EO)_{20}$ (0.42/0.58)	
TEMPERATURE (°C)	25	45	25	45	25	45
Water solubilization (max. wt%)	6.3	7.3	6.3	8.7	22.1	25.4
Surfactant content at max. water solubilization (wt%)	68.9	80.1	72.9	79.0	60.9	67.1
Water/surfactant weight ratio at max. solubilization	0.09	0.09	0.09	0.11	0.36	0.35
L_2 area fraction (%)	5.3	6.1	2.7	6.9	17.0	21.8

Stability of additives-containing microemulsions

Preparing a stable microemulsion that functions as a hydraulic fluid is not a simple task. It is accomplished by judiciously assimilating suitable additives in the oil, or sometimes also in the aqueous phase. The selection of an inappropriate additive may, however, cause the breakdown of the microemulsion, especially in the case of water-rich formulations or when the microemulsion is subjected to relatively high and low temperatures. The

resulting two phases have a detrimental effect on the hydraulic system: the oil is highly flammable and the water, while able to douse any fire in the oil, may lead to severe corrosion and wear problems. Thus, although the preparation of a microemulsion per-se is not necessarily difficult, the adaptation of a microemulsion for a specific application, such as the preparation of a fire-resistant hydraulic fluid, is far from being straightforward. We will illustrate our way of attacking this problem on three selected compositions shown in Table 3. For proprietary reasons we obviously cannot demonstrate here our more advanced formulations.

TABLE 3: Compositions of three selected formulations derived from phase diagram presented in Fig. 4.

Formulation	Composition in wt%			
	Water	Oil	$C_{18:1}(EO)_2$	$C_{18:1}(EO)_{20}$
1	8.8	49.8	17.4	24.0
2	13.8	25.7	25.4	35.0
3	83.7	5.2	4.7	6.4

Formulations 1 and 2 correspond to the L_2 region and formulation 3 corresponds to the L_1 region of the phase diagram. In each formulation six additives were incorporated during the preparation step. The list of these additives, together with their function and their recommended concentration range, is shown in Table 4.

TABLE 4: Selected additives for improving physical, chemical, rheological and tribological properties of hydraulic fluids.

	Additive name	Functional application	Recommended concentration range (wt%)
1	Alkylbenzotriazole	Copper passivator	0.1-1.0
2	Ethoxylated ethanolamide	Corrosion inhibitor	0.1-1.0
3	Tetraethylene glycol	Anti-foam and pour-point depressant	0.1-1.0
4	ZDDP*	Antiwear agent	0.1-1.0
5	Nitroalkylmorpholine derivative**	Biocide	0.001-2.0
6	1-Phenyldodecane	Anti-swelling agent	0.001-0.2

*Zinc dialkyldithiophosphate.
**This additive consists of a mixture of 4-(2-nitrobutyl)morpholine and 4,4'-(2-ethyl-2-nitrotrimethylene)dimorpholine.

The additives were consecutively added, each at its minimum level, without destabilizing the microemulsion. We have also determined the additive dissolution capacity of our system. This parameter is defined as the maximum concentration of each additive that could be introduced into the microemulsion without destabilizing it, measured in the absence of other additives. Thus, it enables us to estimate the mutual compatibility of the additives as well as the stability of the system additives + microemulsion (see Table 5).

TABLE 5: Microemulsion dissolution capacity for each additive incorporated individually in the three selected formulations.

Additive name	Maximum capacity (wt%)		
	Formulation 1	Formulation 2	Formulation 3
Alkylbenzotriazole	26.0	27.1	0.1
Ethoxylated alkanol-amide	27.0	26.7	0
Tetraethylene glycol	27.0	7.8	0.3
ZDDP	26.0	26.3	0
Nitroalkylmorpholine derivative	25.7	27.2	0.5
1-Phenyldodecane	27.0	27.5	0

It is clearly seen that the dissolution capacity of Formulation 3 for all the additives tested is low, while Formulations 1 and 2 may be infused with the same additives at levels well above their minimum required concentration. Formulation 2 was selected for performance evaluation since it seemed to be more stable in the long range stability tests than Formulation 1, which has quite similar dissolution capacity for these additives. The final composition of Formulation 2 is given in Table 6.

TABLE 6: Final composition of microemulsion prepared for performance testing.

Component	wt%
Mineral oil	24.6
$C_{18:1}(EO)_2$	24.0
$C_{18:1}(EO)_{20}$	33.3
Water	13.3
Additives:	
ZDDP	2.5
Ethoxylated alkanolamide	0.5
Alkylbenzotriazole	0.5
Tetraethylene glycol	0.1
Nitroalkylmorpholine derivative	1.0
1-Phenyldodecane	0.2

Hydraulic fluids have to undergo a long series of chemical, physical, rheological and tribological tests, according to stringent specifications. Preliminary tests done on Formulation 2 have shown it to be stable for more than two years. It has good anti-wear protection (four-ball test) and it complies with the foaming characteristics required by Military Specification MIL-H-46170 B (1982). However, the most obvious flaw in this preliminary formulation is its low water content.

Improvement of water solubilization by addition of alcohol

In order to enhance water solubilization in the L_2 phase, the oil component in the phase diagram was replaced by 1:1 (wt/wt) mixture of the same oil with pentanol. Fig. 5 shows clearly that the addition of pentanol improved the water solubilization of the system. A similar but more pronounced effect was demonstrated (see Fig. 6) for the system $C_{18:1}(EO)_{10}$/dodecane/pentanol/water, where the weight ratio dodecane:pentanol was held constant at 1:1. This has led

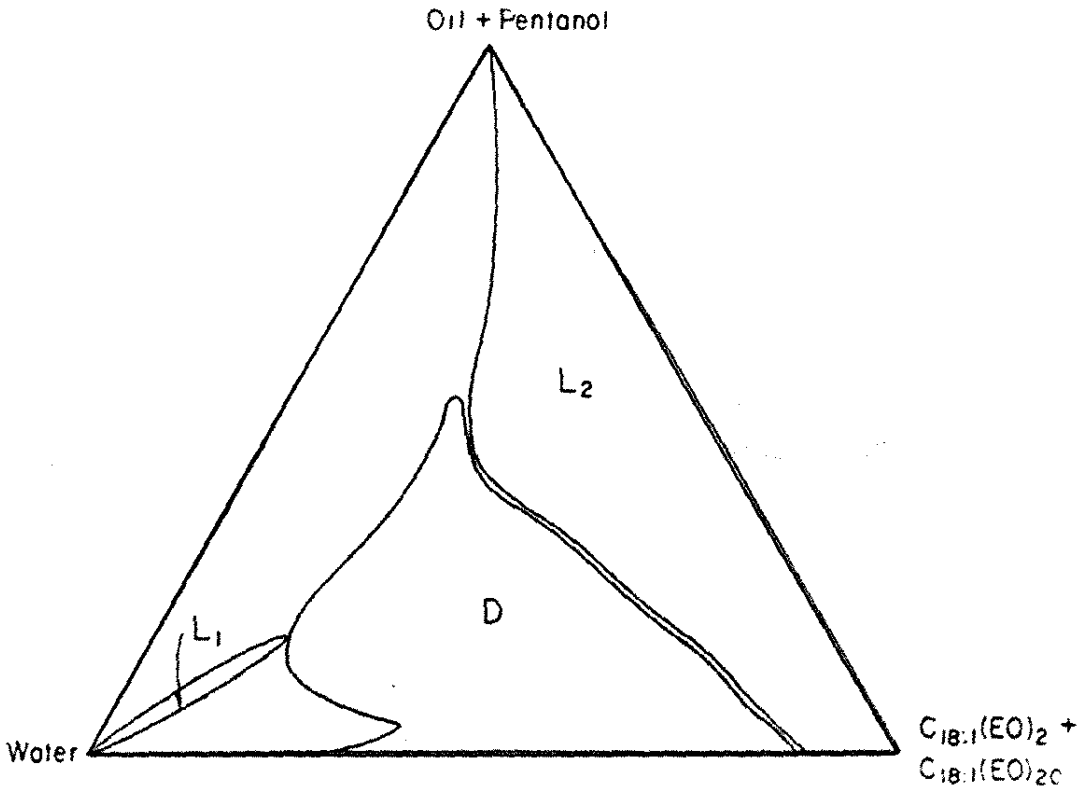

Fig. 5: Phase diagram of the system $C_{18:1}(EO)_2$+$C_{18:1}(EO)_{20}$ [0.42:0.58 (wt/wt)]/mineral oil + pentanol [1:1 (wt/wt)]/water.

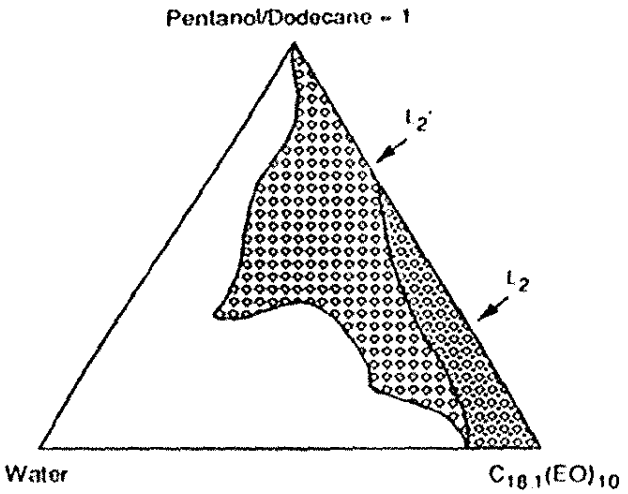

Fig. 6: Phase diagram of the system $C_{18:1}(EO)_{10}$/dodecane/pentanol/water; weight ratio dodecane:pentanol is 1:1.

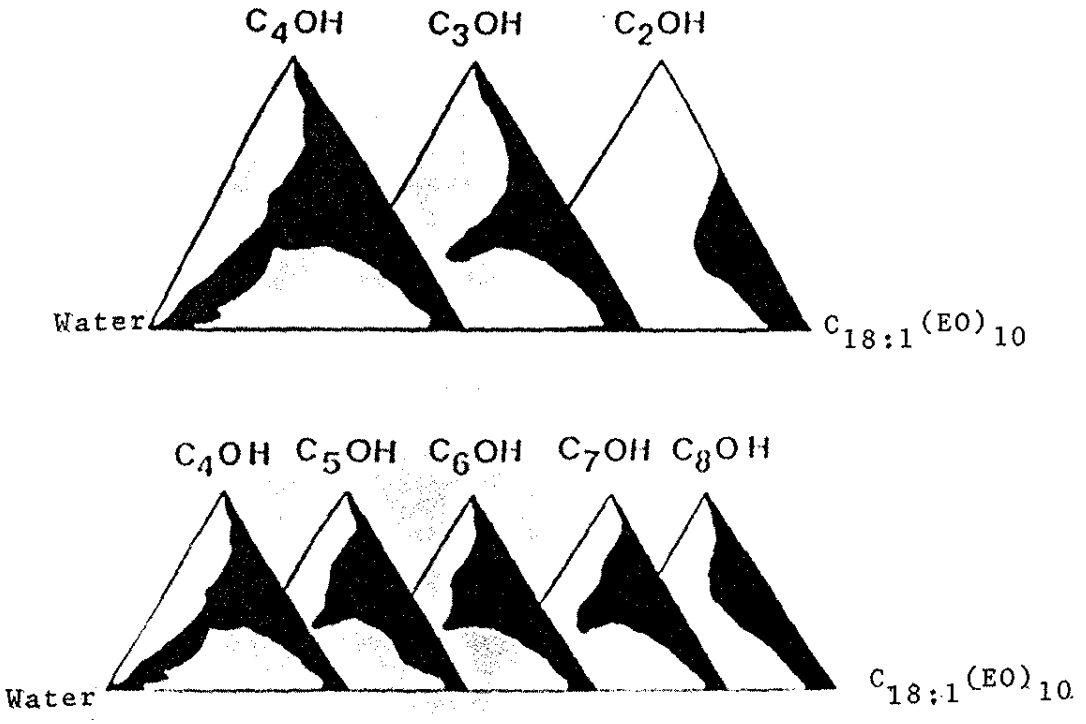

Fig. 7: Variation of water solubilization with the alcohol chain length (N_A) for the system $C_{18:1}(EO)_{10}$/dodecane/n-aliphatic alcohol/water.

us to systematically investigate the effect of a series of n-aliphatic alcohols on water solubilization. Naturally, in the presence of all the additives needed for adequate functioning of hydraulic fluid, such a systematic study is not feasible and a model system with rather similar major constituents is used here instead. The multi-component mineral oil was replaced by the pure hydrocarbon n-dodecane and the nonionic surfactant $C_{18:1}(EO)_{10}$ was substituted for the less effective binary mixture of the surfactants $C_{18:1}(EO)_2$+$C_{18:1}(EO)_{20}$. Thus, the model system tested was $C_{18:1}(EO)_{10}$/dodecane/n-aliphatic alcohol/water. The weight ratio dodecane:alcohol was fixed at 1:1. The results are shown in Fig. 7. It is evident that the water solubilization capacity is sensitive to the alcohol chain length (N_A) and moreover, passes through a maximum at a certain N_A. For anionic microemulsions it was shown[16] that the maximum amount of water, which may be solubilized, is reached when the oil chain length, N_O, plus that of the cosurfactant, N_A, is equal to the surfactant chain length, N_S, i.e. $N_O + N_A = N_S$. This BSO (Bansal, Shah, O'Connell) equation was examined by us for the first time in relation to nonionic surfactants. Our analysis, which elucidates the conditions for which this equation is obeyed, may assist in optimization of nonionic microemulsion systems (Garti, N., Aserin, A., Ezrahi, S. and Wachtel, E., accepted).

Investigation of the microstructure of a model system

The improvement of the preliminary microemulsion-based formulations of fire-resistant hydraulic fluid is a complicated task. It may be benefited by the intensive study of the variations in the microstructure of a similar model system. The system chosen is composed of $C_{12}(EO)_8$/dodecane/pentanol/water [dodecane:pentanol=1:1 (wt/wt)]. These variations may *prima facie* have only a theoretical significance, as they are not visualized on a macroscopic scale. However, we may take advantage of them for our purpose. Our model system contains more than 85 wt% water, but it is obvious that the amount of water,

which may be solubilized in the inner phase of the microemulsion, is limited. Thus, an inversion from a water-in-oil (W/O) to an oil-in-water (O/W) microemulsion has necessarily occurred. When water constitutes the outer phase of the microemulsion, the system is prone to the drawbacks typical of water, such as rust, poor lubricity, pump cavitation, microbial intrusion, etc. Evidently, it is necessary to locate the region of this inversion in the phase diagram. Another significant point is the distinction between bound and free water. The free water is similar in their properties to bulk water, while the bound water (which is associated with surfactant molecules) has quite different properties. From an operational point of view it is important that bound water evaporates slower than free water[17].

The inversion region was determined by nuclear magnetic resonance (NMR) methods (D. Waysbort et al., submitted) and differential scanning calorimetry (DSC) techniques (N. Garti et al., in preparation). DSC was also used to evaluate the distribution of free and bound water in the model system. On the basis of our experimental data the monophasic area in the phase diagram may roughly be divided into three regions: the water poor- and water rich- regions and an intermediate region connecting them. The shape and size of the surfactant aggregates, which prevail in these regions, have been determined using scattering methods and direct imaging by transmission electron microscopy (N. Garti et al., in preparation).

CONCLUSIONS

- The conception of preparing fire-resistant hydraulic fluids on the basis of nonionic microemulsions has been proved.
- Such microemulsions were obtained by preparing phase diagrams of the major components (water, oil, surfactants and cosurfactants). Inspection of the single-phase region of the phase diagrams has led us to the selection of adequate compositions into which effective additives were incorporated.

These preliminary formulations were examined by standard test methods and the results seem to be very promising.

The most pronounced drawback of the preliminary formulations was their rather low water content. It has been shown that pentanol (as well as other alcohols and other types of cosurfactants, which cannot obviously be described here) increases water solubilization in these systems.

The BSO equation, which has formerly been applied to anionic microemulsions was shown by us to be also valid for nonionic systems.

The investigation of a suitable model system may yield useful information about the desired formulations too. The microstructure of such a model system has profoundly been investigated, using advanced spectroscopic calorimetric and microscopic techniques. The results of this investigation have shown the variation of the structure with the water concentration, and located the region in which the inversion from water-in-oil to oil-in-water microemulsion had occurred.

REFERENCES

1. Garti, N., Feldenkriez, R., Aserin, A., Ezrahi, S., and Shapira, D., *Lubrication Engineering* 49, 401, 1993.

2. Van Brocklin, C., *Army Research, Development & Acquisition Bulletin* 34, 9/10, 1990.

3. Möller, U.J., in "Ullmann's Encyclopedia of Industrial Chemistry" (B. Elvers, S. Hawkins, M. Ravenscroft and G. Schulz, Eds.) Vol. A13, p. 165. VCH, 1989.

4. Little, R., Pande, S., Romans, J., and Matuszko, J.S., *Fire Resistance J.* 17, 57, 1991.

5. Kovacs, A., "Strategies in Lubricant Research and Development". Hungarian Hydrocarbon Institute, n.d.

6. Wilson, B., *Industrial Lubrication and Tribology* 20, 1/2, 1992.

7. Millett, W.H., *Iron and Steel Engineer* 54, 36, 1977.

8. Paige, N.M., *Transactions Institute Marine Engineering (TM)* 98, 9, 1986.

9. Friberg, S.E., *Colloids Surf.* 4, 201, 1982.

10. Bourrel, M., and Schechter, R.S. in "Microemulsions and Related Systems. Formulation, Solvency and Physical Properties" (M. Bourrel and R.S. Schechter, Eds.) Surface Science Series, Vol. 30, p. 1. Marcel Dekker, Inc., New York, 1988.

11. Shinoda, K., and Lindman, B., *Langmuir* 3, 135, 1987.

12. Janko, K., *J. Synthetic Lubrication* 4, 99, 1987.

13. Webb, T.H., Chan, K., and Vest, H.F., *Eur. Pat. Appl.* 0069540, 1.7.1982.

14. Ekwall, P., in "Advances in Liquid Crystals" (G.H. Brown, Ed.) Vol. 1, p. 1. Academic Press, New York, 1975.

15. Shinoda, K., and Kunieda, H., in "Microemulsions - Theory and Practice" (M.L. Prince, Ed.), p. 64. Academic Press, New York, 1977.

16. Bansal, V.K., Shah, D.O., and O'Connell, J.P., *J. Colloid Interface Sci.* 75, 462, 1980.

17. Pathananthan, K., and Johari, G.P.,*J. Chem. Soc. Faraday Trans.* 90, 1143, 1994.

SOUTHERN BRAZILIAN JOURNAL OF CHEMISTRY
Vol. 2, No.2, 1994

FLOW INJECTION ANALYSIS FOR METHANOL WITH ALCOHOL OXIDASE AND CHEMILUMINESCENT DETECTION

Andrei F. Dăneț[a#], *Mihaela Oancea*[b], *Silviu Jipa*[c] *and Tanța Setnescu*[c]

[a] Department of Analytical Chemistry, University of Bucharest, 13, Bd. Republicii, 70031-Bucharest, Romania
[b] Department of Biotechnology, ICECHIM, Bucharest, Romania
[c] Institute of Research for Electrotechnical Industry, Bucharest, Romania

ABSTRACT. A highly sensitive flow injection system was developed for the methanol determination. The system is based on the oxidation of methanol in the presence of alcohol oxidase to yield formaldehyde and hydrogen peroxide. The concentration of the hydrogen peroxide produced was determined by luminol chemiluminescence. A four-line flow injection assembly was used. The sample was injected into a flow of phosphate buffer at *p*H 9 that merged with a flow containing alcohol oxidase. The enzymatic reaction takes place in a coiled tube, 2 meters long and 0.8 mm i.d. Just in front of the chemiluminescence cell, the flow containing the sample merged with a flow of luminol (1.5 *m*M) and potassium ferricyanide (20 *m*M). The injected volume was 50 μL and the total flow rate 1.6 $mL\,min^{-1}$ The determination range was $5x10^{-4}$ - $1x10^{-2}$ %(v/v) methanol. The throughput was 40 samples per hour. From 20 tested substances, only *L*-cysteine generated a signal comparable with that of methanol. The others, at concentrations equal to those of methanol, either gave no signal at all (*n*-butanol, *cyclo*-hexanol, glycine, *L*-threonine, *L*-proline, copper sulphate) or gave signals much smaller than that of methanol.

RESUMO. Foi desenvolvido um método altamente sensível para para a análise de metanol na presença de álcool oxidase levando à formação de formaldeído e peróxido de hidrogênio. A concentração de peróxido de hidrogênio foi determinada usando a quimiluminescência do luminol.

KEYWORDS: methanol, flow injection analysis, chemiluminescence, alcohol oxidase.

To whom all correspondence should be addressed.

INTRODUCTION

It is well known that central nervous system disorders, particularly optic disorders, may occur from ingestion or inhalation of methanol, hence the development of simple and sensitive methods for the detection of methanol is important. Also, there is a lack of simple, specific methods for the rapid on-line monitoring of methanol in technological processes. Gas chromatography has been widely used for this purpose, but it requires a long time (at least 30 min) for each sample.

Biological methods using microorganisms or enzymes have also been reported.[1-6] A microbiological sensor consisting of an oxygen electrode covered with a membrane with immobilized microorganisms has been prepared[1]. However, this sensor may be difficult to handle, because the metabolic conditions of the immobilized microorganisms could be easily modified. In enzyme sensors for alcohols, alcohol oxidase (*EC* 1.1.3.13) (AOD) or alcohol dehydrogenase (*EC* 1.1.1.1) (ADH) have generally been used.[2-6] For methanol detection, AOD was used because ADH does not react very well with methanol. The specifications of enzymes given by manufacturers indicate that the response of AOD is about ten times higher for methanol than that for ethanol.

In a recently published paper,[7] however, a possibility was suggested for increasing considerably the sensitivity of the determination of methanol in the presence of ethanol by using a multienzymatic system which includes AOD.

Chemiluminescence (CL) has been widely used analytically because of its high sensitivity, wide dynamic range and simple instrumentation.[8,9] This detection technique presents some advantages

compared with other detection systems, such as amperometric methods,[10,11] for the determination of hydrogen peroxide. The difficulty of reproducing the physical and chemical conditions in CL can be eliminated by using a flow injection analysis (FIA) system.[12,13]

The purpose of our study was to develop a sensitive and automated FIA method for the rapid determination of methanol in fermentation broths, using on-line enzymatic conversion to H_2O_2 and CL detection of the H_2O_2 formed. We prefered to use a solution of alcohol oxidase instead of an immobilized enzyme, because, according to literature data, the activity of immobilized AOD decreases appreciably over time and, in the accidental presence of some poisons, the microreactor may be completely damaged.

EXPERIMENTAL PROCEDURE

Materials and Equipment

- Alcohol oxidase (*EC* 1.1.3.13), catalase-free, with an activity of 6.11 U/mL (1 U = 1 μM H_2O_2/min). It was extracted and then purified from methylotrophic yeast (*Hansenula polymorpha*) in the Biotechnological Department of the Institute of Chemical and Biochemical Energetics of Bucharest.

- 1.5 *m*M solution of luminol (5-amino-2,3-dihydro-1,4-phthalazine-dione) in 0.1 *m*M sodium carbonate.

- 20 *m*M solution of potassium ferricyanide in water.

- 1 *m*M solution of disodium phosphate, containing 1 *m*M of EDTA, having *p*H 9, used as a carrier stream into which the analyzed sample is injected.

- Methanol, absolute, from which water solutions with concentrations in the range $5x10^{-4}$ - 10^{-2} % (v/v) were prepared.

- Alcohols: ethanol, *n*-propanol, isopropanol , *n*-butanol, cyclohexanol, allyl and benzyl alcohols.

- Amino acids: glycine, *L*-threonine, *L*-tyrosine, *D, L*-serine, *L*-proline and *L*-cysteine.

- Glucose, copper acetate, zinc sulfate, manganese acetate, lead acetate, copper sulfate.

All reagents were of analytical grade. Doubly distilled water was used for preparing the solutions.

Figure 1 presents the flow injection analysis line. The carrier flows, those of the enzyme solution and of the reagents, were obtained by means of a 4-channel peristaltic pump (from IAUC - Bucharest), provided with 1.02 mm i.d Tygon tubes. A second, one-channel, peristaltic pump was used for filling up the injection loop with the sample solution and a 6-channel valve (Rheodyne-type, Modell 5051), was used for injection.

All tubes used for the FIA assembly presented in Figure 1 were of Teflon, with an i.d. of 0.8 mm. The carrier flow, into which the sample was injected, merges with the enzyme flow 40 cm down-stream from the injection valve. The enzymatic reaction with H_2O_2 generation takes place in the reaction loop L_1. The luminol and ferricyanide flows merge and mix in mixing loop L_2. The resulting flow merges afterwards with the flow in which the enzymatic reaction has taken place, just in front of the detector cell. In order to detect the chemiluminescence radiation, a coil-shaped cell, about 50 cm long, was built from a 0.8 mm i.d. Teflon tube. The flow cell was mounted directly in front of the photomultiplier tube (type FEU-19M, Russia) and was covered with an aluminium reflecting foil in order to improve the detection of the emitted light. The signals were measured with a

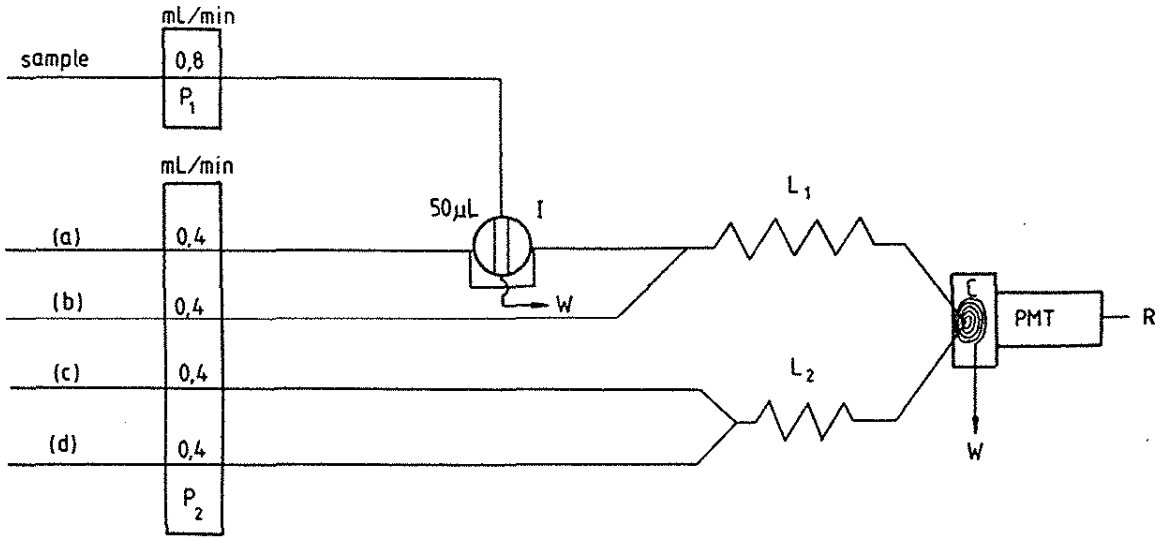

Fig. 1. Optimized flow injection manifold for methanol determination with chemiluminescent detection. P_1 and P_2 - peristaltic pumps; I -injection valve; L_1 *and* L_2 - mixing loops of 200 and 60 cm lengths, respectively; C - flow cell; *PMT*- photomultiplier tube; R - recorder; W - waste; (*a*) carrier; (*b*) - enzyme solution; (*c*) - 1.5 *m*M luminol solution; (*d*) - potassium ferricyanide solution.

y-t recorder (type Endim 621.02, Germany). All measurements were carried out at 19 ± 1 °C.

Recommended Procedure

The mixing loops L_1 and L_2 of the FIA manifold with optimized parameters are 200 cm and 60 cm long, respectively. One works with equal flow rates of the enzyme solution, of the reagents and of the carrier flow, i.e. 0.4 mL min^{-1}. The volume of the injected sample is 50 μL. The enzyme solution used has an activity of 0.12 U mL^{-1} (after a 1/50 dilution of the initial enzymatic solution). The compositions of the luminol solution and of the carrier flow, as well as that of the potassium ferricyanide solution, are those specified earlier (see the Materials and Equipment Section). The voltage applied to the PMT is 820 V. The measurement of the chemiluminescent signal was made in all cases by measuring the height of the recorded FIA peaks.

RESULTS AND DISCUSSION

The influence of the enzyme activity on the height of the signals recorded after injecting a 10^{-2} % (v/v) solution of methanol is shown in Figure 2. The experiments were carried out by observing the directions given in the Recommended Procedure Section. One can see from the figure that for enzyme activities higher than 0.12 U mL^{-1}, the recorded peak heights are practically equal, and for this reason subsequent experiments were carried out with enzyme solutions having an activity of 0.12 U mL^{-1} (which corresponds to a 1/50 dilution of the original enzyme solution in doubly-distilled water).

The parameters of the FIA system were optimized by modifying the flow rate, the volume of the injected sample, and the length of the

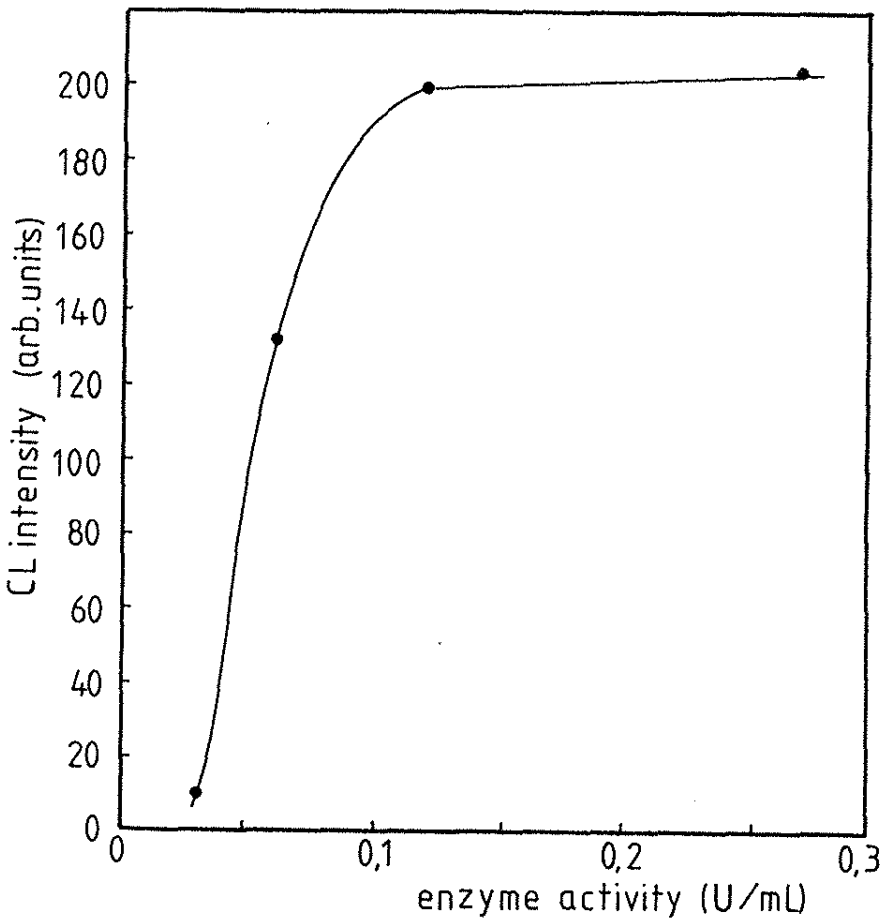

Fig. 2. The influence of the enzyme activity on the FIA output. $c_{methanol} = 10^{-2}$ % (v/v).

reaction loop L_1. The flow rate influences the intensity of the CL radiation by way of both the enzymatic and chemiluminescent reactions, since both these reactions have slow reaction rates. Samples of 5×10^{-3} % methanol solution were injected in portions of 50 μL, the total flow rate being varied between 1.6 and 10 mL min^{-1} (Fig. 3). The

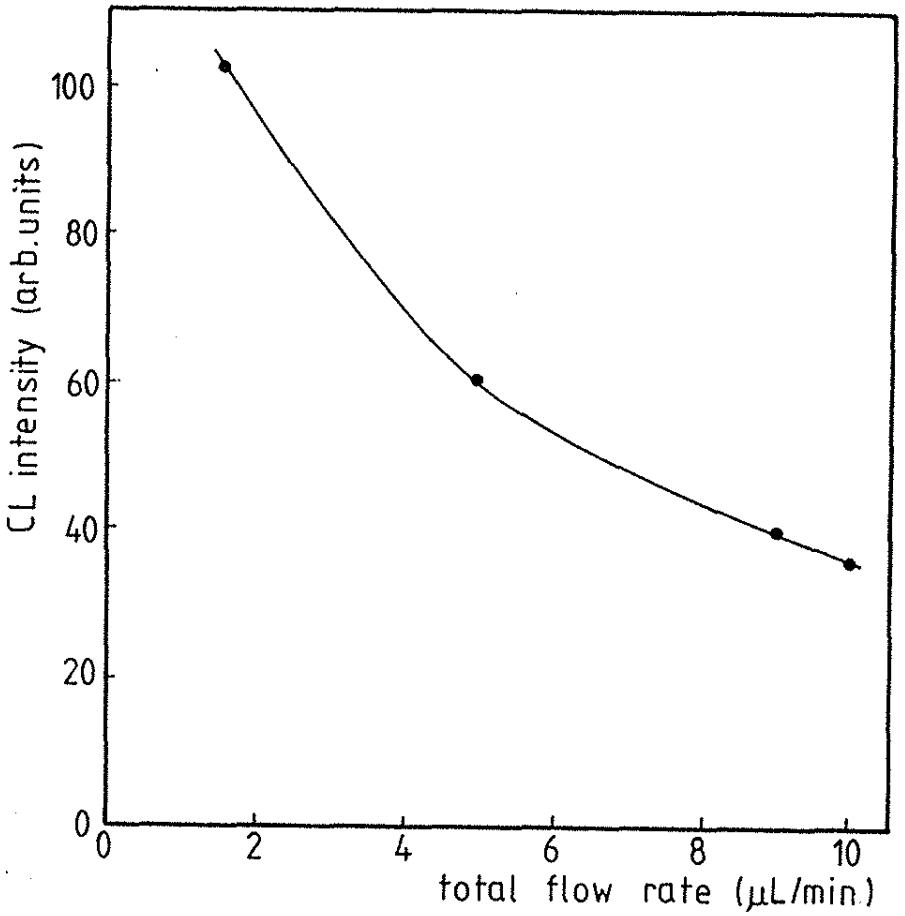

Fig. 3. The influence of the total flow rate on the FIA output. $c_{methanol}$ = $5x10^{-3}$ % (v/v).

flow rates in the four channels of the FIA installation were identical. When the flow rate was high, the peak height decreased appreciably, due to the short time available for the enzymatic reaction and also to the decrease of the time interval in which the CL radiation is measured. The experiments were therefore continued using a total flow rate of 1.6 mL min^{-1}, a flow rate which was considered optimal because the intensity of the CL radiation is then at its maximum value, the reagent

consumption is low and at the same time the duration of a single determination is reasonably short.

Calibration curves were drawn for various volumes of injected sample: 50, 100, 150, 200, and 250 μL. It was noticed that for small volumes of injected sample a linear dependence of the signal on the methanol concentration is obtained over a wider range. The value of 50 μL was thus selected as optimal.

In order to increase the reaction time, beside decreasing the flow rate, we increased the length of reaction loop L_1. Initially, the length had been set at 100 cm. If the length of the L_1 loop is doubled, one gets signals two times higher. The base line was very stable under these conditions. If very low methanol concentrations are sought, the length may be further increased or, alternatively, one can work in a stopped-flow manner.

The effect of the potassium ferricyanide concentration on the height of the recorded signals is illustrated in Figure 4. The intensity of the CL radiation increases linearly with the concentration of potassium ferricyanide, up to 10 *m*M, whereas at higher values, up to 20 *m*M, it remains constant. Therefore, an optimal concentration of 20 *m*M was chosen. The other parameters used have been mentioned in the Recommended Procedure Section.

The influence of the luminol concentration on the the height of the recorded signals is presented in Figure 5. For a luminol concentration higher than 1.5 *m*M, the intensity of the CL radiation no longer increases and for this reason the subsequent determinations were carried out by using the luminol solution at the above mentioned concentration. We should mention that it is necessary to work with

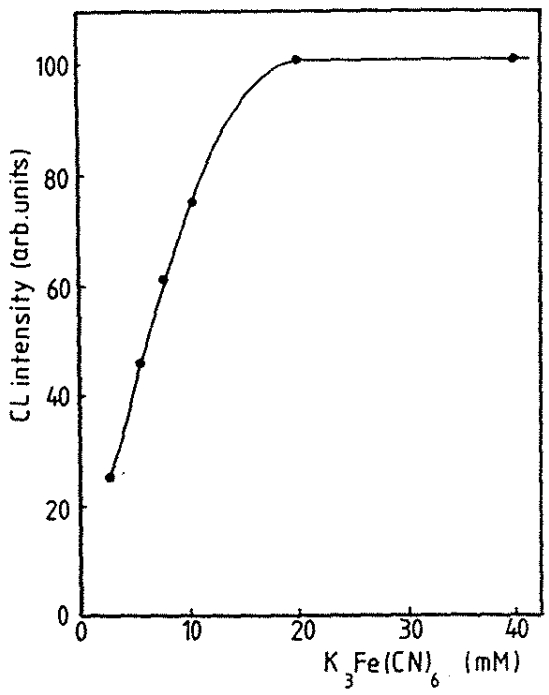

Fig. 4. The influence of the concentration of potassium ferricyanide on the FIA output. $c_{methanol}$ = 5x10^{-3} % (v/v).

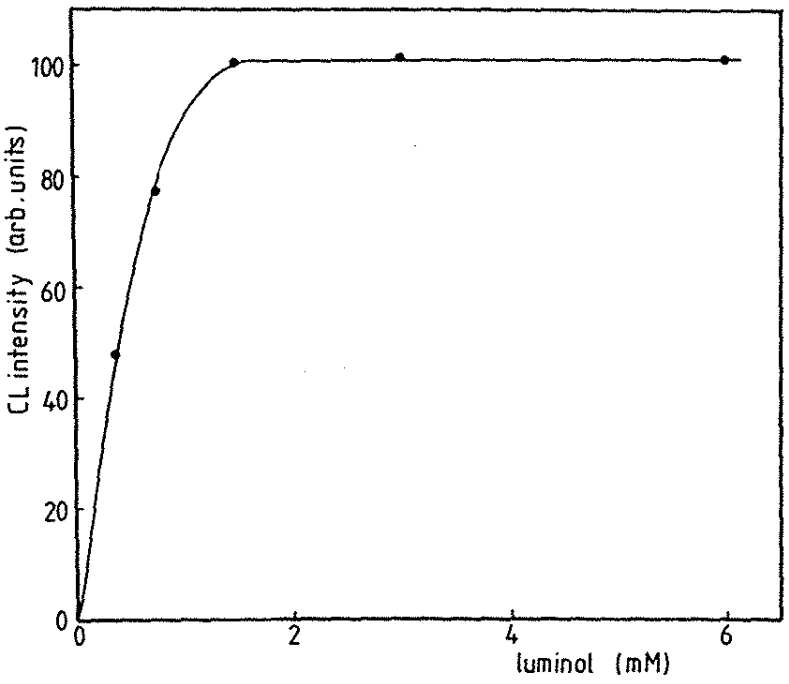

Fig. 5. The influence of the luminol concentration on the FIA output. $c_{methanol}$ = 5x10^{-3} % (v/v).

freshly prepared luminol solutions. Luminol solutions kept in the refrigerator preserve their activity over several days, but after some time, e.g., after 10 days, the height of the recorded signals for the same methanol sample decreased by half compared to the signal obtained with a fresh luminol solution.

System Performance

The calibration straight line obtained during the analysis of methanol-containing samples, in the $5x10^{-4}$- 10^{-2} % (v/v) concentration range, is shown in Figure 6. The experiments were carried out according to the directions described in the Recommended Procedure Section.

The equation of the calibration line was

$$y = 20{,}100c + 1.36$$

and the correlation coefficient 0.9998. The reproducibility of the method was checked by injecting 10 methanol samples of $5x10^{-3}$ % concentration. The relative standard deviation was 0.35%. The proposed

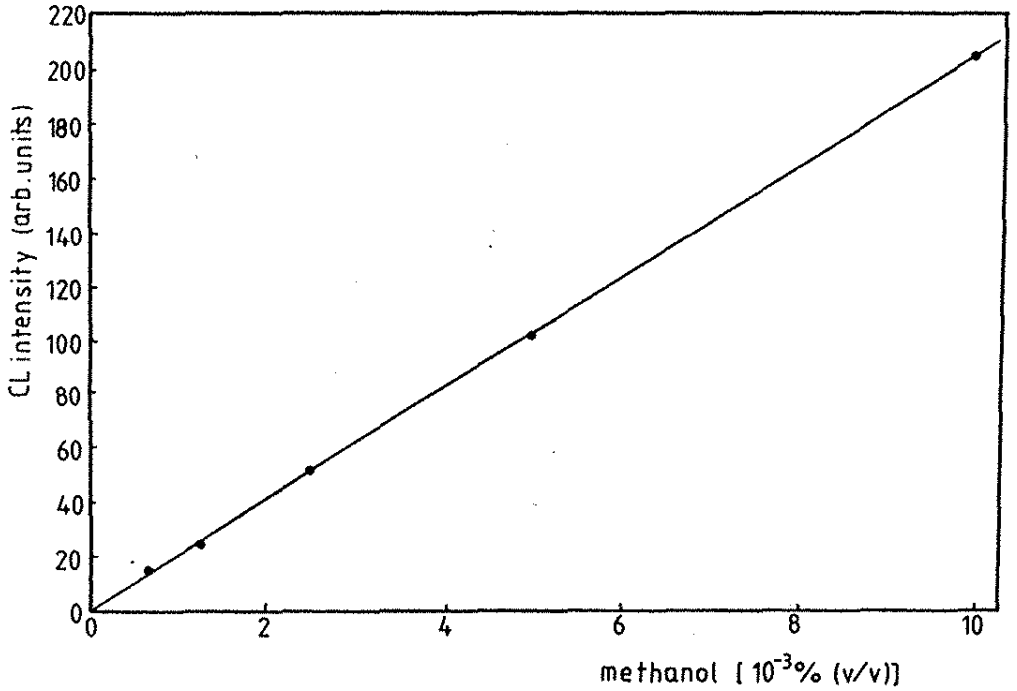

Fig. 6. Calibration curve for methanol, obtained by using the flow injection system.

analysis method allows for a throughput of about 40 samples per hour.

The Relative Activity of the Enzyme

Alcohol oxidase is specific for alcohols, but it is very selective for the length of the chain.[15] Due to differences existing between the specific activities for various alcohols, the amount of H_2O_2 produced by a given quantity of substance will depend on the nature of the alcohol.

The relative activity of the enzyme towards various alcohols, determined under the working conditions described above (injecting 50 μL samples) is shown in Table I. Solutions of various alcohols in doubly-distilled water, at concentrations of 10^{-2} % (v/v), were used. Methanol was taken as reference, considering that the enzyme has a specific activity of about of 100 % upon it.

Interferences

Starting from the idea of using the proposed method for monitoring the methanol concentration in the culture medium of a bioreactor, we have attempted to detect some possible interferences which may occur in a complex reaction medium.

The influence of some amino acids on the methanol determination was therefore investigated. Various amino acids were injected in concentrations of 10^{-2} % (m/v). The previously described procedure was strictly followed. A 10^{-2} % methanol solution was taken as reference. From the tested amino acids (glycine, threonine, tyrosine, serine, proline, cysteine), only cysteine gave a signal which indicated an interference of 54.1 % under the assumed conditions. It was noted that cysteine interferes due to a chemiluminescent reaction that takes place after its merging with the luminol and potassium ferricyanide flows.

Table I

The relative specific activity of AOD for various alcohols

Substrate (10^{-2} %, v/v)	Relative specific activity (%)
Methyl alcohol	100
Ethyl alcohol	36.6
n-Propyl alcohol	7
iso-Propyl alcohol	23.5
Allyl alcohol	22.6
n-Butyl alcohol	0
Benzyl alcohol	18
cyclo-Hexanol	0

Table II

The interference of some metal ions in the determination of methanol

Interferent ($5x10^{-3}$ M)	Percent modification of the signal, compared to a sample which does not contain interfering ions
Copper acetate	+22.3
Zinc sulfate	+28.7
Manganese acetate	+25
Lead acetate	+17.5
Copper sulfate	0

The alcohol oxidase has no influence upon this reaction. The interference of cysteine can be completely avoided by prior complexing with Cu^{2+} ions.

The influence of urea and glucose has also been checked, at concentrations of 10^{-2} % (m/v). Urea gave no signal at all, whereas glucose gave a signal which represented only 2.4 % of the height corresponding to samples of methanol with the same concentration.

The interference of some ionic metals is presented in Table II. Samples consisting of methanol samples ($2.5x10^{-3}$ %), containing metal ions in concentrations of $5x10^{-3}$ M, were injected. The $2.5x10^{-3}$ % methanol solution was taken as reference, and any modification of the height of the signals was related to it. All other measurements were carried out according to those specified in the Recommended Procedure Section.

Taking account of the fact that the concentrations of metal ions in culture media is lower than the tried concentrations (i.e. $5x10^{-3}$ M), and that, generally, for carrying out the analysis a dilution of about 1/100 of the samples is necessary, the interference of the metal ions mentioned in Table II, in the case of culture media, is practically negligible.

Application of the Proposed Analysis Method to the Determination of Methanol in Culture Media

The culture samples were collected from a bioreactor designed to produce the *Hansenula polymorpha* yeast; they were centrifugalized in order to separate the cells. The obtained supernatants were diluted in a ratio of 1/100 with doubly-distilled water, then were analyzed according to the indications given in the Recommended Procedure Section.

Samples resulting from culture media collected at different

biosynthesis time were analyzed. The range of methanol concentrations was 0.36 - 1.0 % (v/v). A relative standard error of 0.52 % was calculated by using t-test (n=10) for a concentration of methanol in culture medium of 0.56 % (v/v) and for a level of confidence of 90 %.

CONCLUSIONS

The described chemiluminescence/FIA enzymatic detection method for methanol determination is characterized by short analysis times and good reproducibility and sensitivity. The catalysts and luminol were injected simultaneously into two separate streams and then allowed to merge in a strictly reproducible manner before being mixed with the H_2O_2 produced in the enzymatic reaction. The proposed method is much faster then other methods of analysis for methanol in fermentation broths (e.g. gas chromatography). Adaptation of this system for monitoring other biotechnological processes based on the utilization of methanol seems promising.

REFERENCES

1. M. Hikuma, T. Kuba and T. Yasuda, *Biotech. and Bioeng., 21,* 1945-1950 (1979).
2. G. G. Guibault, B. Danielson, C. F Mandenius and C. Mosbach, *Anal. Chem.,* 55, 1582-1589 (1983).
3. J. A. Klavons and R. D. Bennet, *J. Agric. Food Chem., 34,* 597-602 (1986).
4. A. Maquieria, M. D. Luque de Castro and M. Valcarcel, *Microchem. J., 26,* 309-404 (1987).
5. V. J. Smith, R. A. Green and T. R. Hopkins, *J. Assoc. Off. Anal. Chem.,* 72, 30-35 (1989).
6. Y. Kitagawa, K. Kitabatake, I. Kubo, E. Tamiya and I. Karube, *Anal. Chim. Acta, 218,* 61-68 (1989).

7. Y. Sekine, M. Suzuki, T. Takeushi, E. Tamyia amd I. Karube, *Anal. Chim. Acta, 280,* 179-184 (1993).

8. K. Nakashima and K. Imai, *"Chemiluminescence"*, in: S. L.G. Schulman, Ed., *"Molecular Luminescence Spectroscopy"*, Part 3, Wiley, New York, (1993), Vol. 77.

9. M.A. DeLuca and W.D. McElroy, Eds., *"Bioluminescence and* Chemiluminescence", Academic Press, New York (1981).

10. K. Matsumoto, H. Matsubara, M.Hamada, H. Ukeda and Y. Osajima, *J. Biotech., 14,* 115-126 (1990).

11. J. Abdul Hamid, G.J. Moody and J.D.R. Thomas, *Analyst, 114,* 1587-1592 (1989).

12. B. A. Petersson, E. H. Hansen and J. Ruzicka, *Anal. Lett., 19,* 649-665 (1986).

13. P. J. Worsfold, J. Farrelly and M. S. Mathoru, *Anal. Chim. Acta, 164,* 103-109 (1984).

14. M. Garn, M. Gisin, Ch. Thommen and P. Cevey, *Biotech. and Bioeng., 34,* 423-428 (1989).

15. T. R. Hopkins and F. Muller, Eds., *"Microbial Growth on C_1 Compounds"*, Martinus Nijhoff Publishers, Dordrecht (1987), pp. 150-162.

SOUTHERN BRAZILIAN JOURNAL OF CHEMISTRY

Vol. 2, No.2, 1994

REDOX REACTIONS INVOLVING N-ALKYL-DIHYDRONICOTINAMIDES

Nadir Ana Wiederkehr
Departamento de Física, Setor de Físico-Química
Universidade Federal de Santa Maria
97.119-900 - Santa Maria, RS, Brazil

ABSTRACT

Electron transfer reactions involving a series of N-alkyl-dihydronicotinamides (R-NAH) as donors were studied in homogenous solvents and in micellar media. In particular the redox chemistry and kinetics of the reduction of methylene blue and cytochrome-C, by varying the alkyl chain length (R= C_4, C_8, C_{12}) were investigated. The schemes proposed for functionalized surfactants of nicotinamide suggest photochemical conversion based on light-induced electron-transfer reactions.

Keywords: Dihydronicotinamide derivatives, functionalized surfactants, photo-redox mechanisms.

RESUMO

Reações de transferência de elétrons utilizando sistemas modelo, tais como a redução do azul de metileno (AM) e citocromo-C (CC) por N-alquil-dihidronicotinamidas (R-NAH) foram estudados em solventes homogeneos e meios micelares. Os mecanismos redox e a cinética química, determinada em função do comprimento da cadeia carbonada (R= C_4, C_8, C_{12}), permitem concluir que os sistemas investigados apresentam características de reações de transferência de elétrons por indução foto-química.

INTRODUCTION

Nicotinamide adenine dinucleotide (NAD+) is an important cofactor taking part in numerous cellular processes, particularly in the intermediary metabolism and energy conversion processes (e.g., electron transport and oxidative phosphorylation). It has been firmly established that the nicotinamide chromophore is the portion that undergoes reversible redox reactions during the numerous processes involving NAD+ or NADP+. The reduction of NAD+ to NADH (particularly to the 1:4-isomer) is a complex, stereospecific process involving transfer of two electrons and a proton reaction [1,2]:

$$\text{NAD+} + \text{H+} + 2e^- \rightarrow \text{NADH} \qquad \text{(I)}$$

Assisted by enzymes, the reduction occurs very efficiently as a one-step process 2. The reduced form, NADH is a good electron donor and undergoes thermal and light induced electron transfer reactions. Various systems studied include, for exemple:

(a) reductive irreversible quenching of metalloporphyrins 3,4 (Equation II), where S = Zn(II) or Sn(IV)-tetramethylpyridylporphyrin, as follows:

$$NADH + S^* \rightarrow SH^- + NAD^+ \qquad (II)$$

(b) The irreversible photoreduction of viologens by photoexcited NADH 5, (Equation III), as follows:

$$NADH^* + 2MV^{2+} \rightarrow NAD^+ + 2MV^+ + H^+ \qquad (III)$$

(c) As a "sacrificial" reductant of photooxidized sensitizer dyes or for thermal reduction of organic dyes 6, (Equation IV), as follows:

$$NADH + S^+ \rightarrow S + NAD^+ + H^+ \qquad (IV)$$

where S is ruthenium bypiridyl [$Ru(bpy)_3^{+2}$], chlorophyl or methylene blue. The mechanism of action of NADH continues to be controversial 7 wheter the reaction involves a direct hydride (H^-) transfer or a sequential transfer of an electron, a proton and an electron, (e^-, H^+, e^-) 7.

As regards to redox potentials, representative E_0' values in water, relative to NHE at pH 7.0 are as follows: E_0' (NADH/NAD+) = -0.315 V; E_0'(Benzyl-NAH/Benzyl-NA+) = -0.361 V and E_0'(C_3-NAH/C_3-NA+) = -0.387 V. The one electron oxidation potential of NADH closely related 1,4-dihydronicotinamides has been established to be ≈ -1.30 V vs. NHE by indirect methods 8. This implies that only very powerful oxidants can oxidize NADH by one electron pathway. Accordingly, thermal oxidation of NADH and analogs have been found to occur by hydride exchange, thereby avoiding the high energy intermediates by a stepwise pathway.

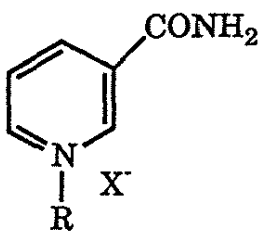

1-N-alkyl-nicotinamide surfactant (RNA^+X^-)

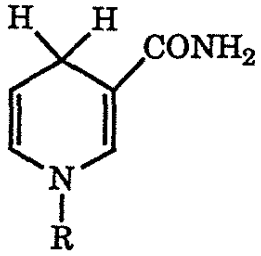

1-N-alkyl-1,4-dihydro nicotinamide (R-NAH)

MATERIALS AND METHODS

N-alkyl-1,4-dihydronicotinamides were prepared from the corresponding n-alkyl-nicotinamides by chemical reduction using sodium dithionite as a reductant, following the procedures described in the literature [9, 11, 12]. Sodium lauryl sulfate (SLS) (Fluka) was used after single recrystallization. Phosphate buffer solution of pH= 7.41 from Fluka, containing 0.0087 M KH_2PO_4 and 0.03 M of Na_2HPO_4 was used as supplied. Methylene blue (MB) (Fluka) was recrystallized once from ethanol/water mixture. Cytochrome-C (Sigma-Chemical Company) was used as supplied.

Kinetic studies of reduction of methylene blue (MB) and cytochrome-C (CC) by N-alkyl-1,4-dihydronicotinamides were performed by monitoring the UV-Visible spectra, recorded on a 8000 Diode Array Spectrophotometer (Hewlett-Packard). Known amounts of C_8-NAH and C_{12}-NAH were solubilized in methanol or micellar solutions of sodium lauryl sulfate (SLS). These were then mixed with different concentrations of MB or CC in a buffer solution. C_4-NAH (being water soluble) was studied in an aqueous buffer solution. Dihydronicotinamide solutions were freshly prepared and used the same week. A cuvette containing 1.8 ml of a MB or CC buffer solution was placed in a 1-cm cell holder and a solution of R-NAH was injected into the sample solution. Degassing of solutions was made by helium bubbling, during 15 minutes. Solution were illuminated under continuous stirring using a 450 nm Xe arc lamp, light filtered using a solution filter that passes light in the wavelength range of 300-400 nm , a 10 cm solution filter containing 2:1 mixture of $CoSO_4$ (0.30 M) and $CuSO_4$ (0.20 M) [13].

RESULTS AND DISCUSSION

Some current work has been devoted to systematic studies of some of the above basic chemistry of the nicotinamide chromophore using a series of functionalized surfactants, (viz., long chain derivatives of nicotinamide / dihydronicotinamide) as model compounds [9, 10]. As mentioned, functionalized surfactants allow model system studies to be carried out both in homogenous solvents and in organized assemblies.

An important finding has been the ability to tune the solubility of the neutral molecule R-NAH by varying the chain length. The shorter chain derivatives of dihydronicotinamides (R-NAH, $R \leq C_6$), are fairly water soluble. The longer chain derivatives are totally insoluble in water and hence can serve as excellent hydrophobic donors for studies in reversed micellar systems.

In this work, as a model system, the reduction of two water-soluble substrates *methylene blue* (abbreviated hereafter as MB) and *cytochrome-C* (abbreviated hereafter as CC) by a series of 1,4-dihydronicotinamide surfactants has been studied (Equations V and VI):

$$RNAH + MB \rightarrow RNA^+ + MB\text{-}H \quad (V)$$

$$RNAH + 2Fe^{+3}(CC) \rightarrow RNA^+ + 2Fe^{+2}(CC) + H^+ \quad (VI)$$

It is known that methylene blue (MB) can be reduced to leucomethylene blue (MB-H) ($E_0' = 0.011$ V vs. NHE) [11]. The reduction generally proceeds as a two-electron process, although at low pH, semiquinone formation has been reported [14]. The potentiality of 1,4-dihydronicotinamides to reduce MB+ was noted by Karrer and his coworkers in the late 1930's [15]. Since then only a few studies have been reported that deal with the reactivity of MB+ towards 1,4-dihydropyridines, which are those of Engbersen and Verhoeven and their coworkers [16, 17]., with important kinetic studies in homogeneous solutions. If molecular oxygen is present in the system involving MB, the leuco-MB produced in Equation V is rapidly re-oxidized to MB (Equation VII) , see Figure 1:

$$\text{MB-H} + O_2 \rightarrow \text{MB} + O_2^- + \text{H+} \qquad \text{(VII)}$$

In homogenous solution, the reaction described by Eq. (VII) is 100 times faster than the rate of R-NAH oxidation (Eq. VI). Under such conditions, *Scheme 1* represents a sensitized reaction and MB serves as a reversible electron relay.

Scheme 1 :

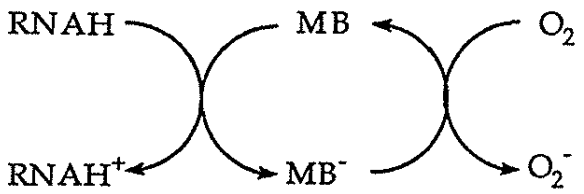

Cytochrome-C (CC) is an electron-transferring heme-protein (mol.wt.: 13000), involved in the respiratory chain. Its chromophore unit, Fe-protoporphyrin undergoes reversible Fe(II) - Fe(III) valence changes (E_0') = 0.254 V). In the reduced form, the heme group has its characteristic absorption bands α, β and Soret located at 550, 521 and 415 nm respectively ($\varepsilon_{550nm} = 2.95 \times 10^4$ M-1.s-1) [1-c, 1-d]. The reduced form of the CC is not readily reoxidized by molecular oxygen, except in the presence of enzymes such as oxidase, peroxidase or catalase. Thus reduction of cytochrome-C via Scheme 2 is essentially irreversible.

Scheme 2 :

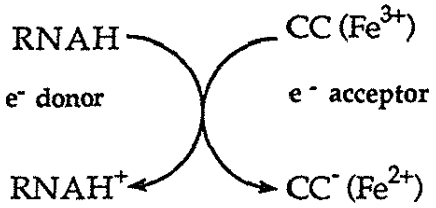

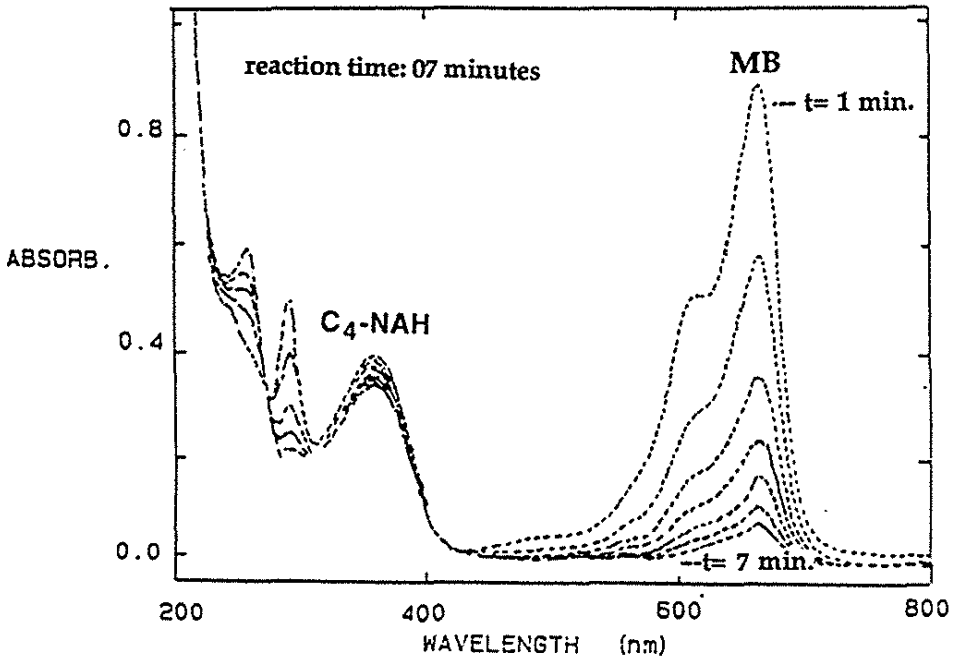

FIGURE 1. SPECTRAL CHANGES OBSERVED DURING THE REDUCTION OF METHYLENE BLUE BY C_4-NAH IN AQUEOUS DEAERATED - (He DEGASSING) BUFFER SOLUTIONS. CONDITIONS: [C_4-NAH] = 14.43 x 10-5 M AND [MB] = 1.12 x 10-5 M. Δt FOR EACH REACTION = 1 MINUTE. 1/10 V/V PHOSPHATE/PHOSPHATE BUFFER, pH = 7.41 AND T = 22 ° C.

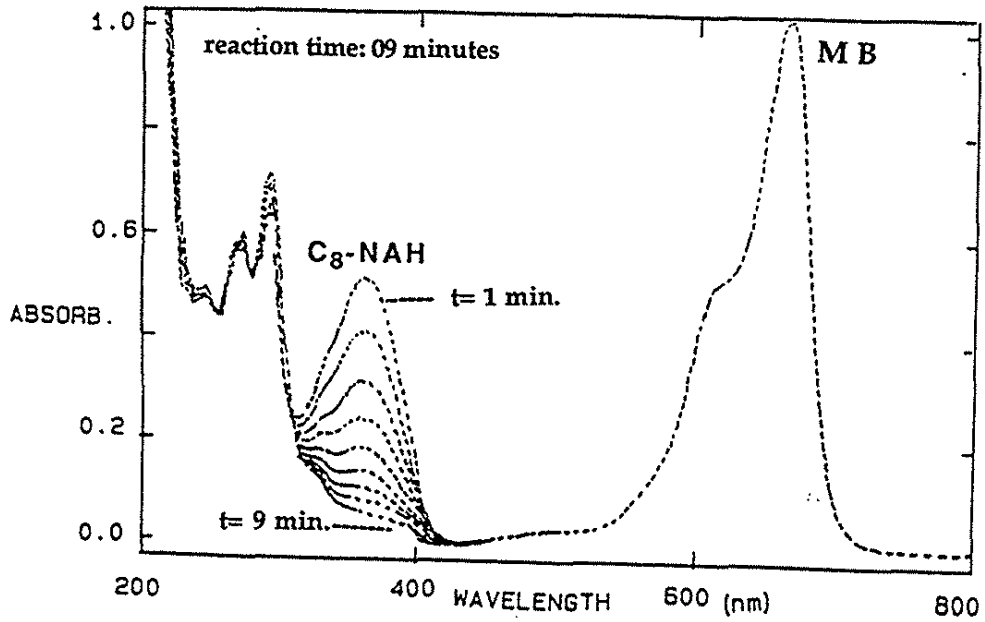

FIGURE 2. SPECTRAL CHANGES OBSERVED DURING THE REDUCTION OF METHYLENE BLUE BY C_8-NAH IN METHANOL. CONDITIONS: [C_8-NAH] = 8.13 x 10-5 M AND [MB] = 1.12 x 10-5 M. Δt FOR EACH REACTION = 1 MINUTE. 1/10 V/V - METHANOL/AQ. PHOSPHATE BUFFER, pH = 7.41 AND T = 22 ° C.

Variations in the alkyl chain length of R-NAH allowed the reduction reactions to be followed under a variety of conditions: C_4 derivative in aqueous medium (being very soluble in water); C_8, C_{12} derivatives either in solvents as methanol or solubilized molecules in host micelles of SLS (sodium lauryl sulfate), concentration of the donor and acceptor(s), temperature, molecular oxygen and reaction medium (homogenous solvent vs. micelles). The organized assembly consists of a neutral hydrophobic donor (R-NAH) solubilized in the anionic micelles with cationic acceptor (MB+ or CC) adsorbed on the surface.

The redox reactions involving dihydronicotinamides are conveniently monitored via their absorption spectral changes. In the oxidized form the nicotinamides do not have any absorption in the visible light region. In the reduced form (1:4-isomer), there is an intense absorption band at ≈ 355 nm. In our studies, reduction processes under scheme 1 and 2 have been studied under pseudo first-order conditions, i.e., {[R-NAH] >> [MB] or [CC]} [18].

Figure 1 presents typical absorption spectral changes observed during the thermal reduction of MB by C_4-NAH under homogenous solvent conditions (aqueous aerated solutions). Figure 2 and 3 present similar spectra in methanol as solvent for the C_8 and C_{12} derivatives respectively. In all cases at time(t) =0 , the absorption spectrum of the reaction mixture is composed of absorption of the two reactants (R-NAH at 360 nm and MB at 660 nm). Subsequent to the mixing of R-NAH and MB, the absorption maximum corresponding to R-NAH at 360 nm decreases with smaller absorption changes occurring at the MB maximum.

Kinetics of oxidation of R-NAH has been followed by monitoring the disappearance of the 360 nm band. Figure 4 shows representative first-order kinetic plots for the disappearance of R-NAH as a function of time.In all cases the disappearance of R-NAH follows first order kinetics as expected. Table I presents a collection of derived rate constants data for MB-reduction reaction measured under various conditions. Figure 5 and 6 shows the variation of the observed rate constant K_{obs}, with the concentrations of MB+ for both C_8 and C_{12}-NAH. The second order rate constants (k_2) derived from such plots are summarized in Table II.

The hydrophobic long chain derivative of dihydronicotinamide (C_{12} derivative for example) can be readily solubilized in anionic micelles of sodium lauryl sulfate. With the cationic acceptor adsorbed on the surface, the reduction process takes place as an intramicellar process. Table II also contains kinetic data for methylene blue reduction carried out in the presence of anionic micelles SLS. Complex formation between the electron donor and acceptor methylene blue has been reported earlier [16]. Under our experimental conditions we could not detect any such complexation spectroscopically.

Figure 7 and 8 presents some representative absorption spectral changes observed during the reduction of cytochrome-C (CC) by C_8 and C_{12} derivatives solubilized in host micelles of SLS (10^{-2} M). At t = 0 the absorption spectrum is composed of absorption maxima characteristic of the two components, R-NAH at 360 nm and CC at 530 nm (their typical spectrum). Subsequent to the mixing, kinetics of R-NAH oxidation was followed by monitoring the disappeareance of the 360 nm band, after correcting for the absorption of CC. The disappearance of R-NAH follows first order kinetics in non-irradiated systems.

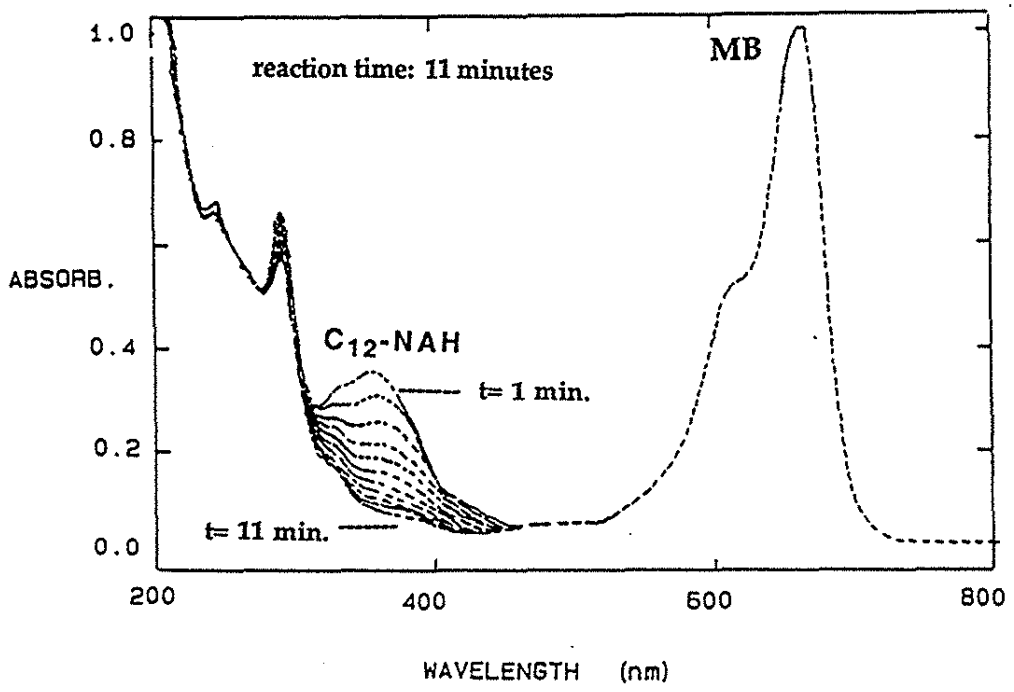

FIGURE 3. SPECTRAL CHANGES OBSERVED DURING THE REDUCTION OF METHYLENE BLUE BY C_{12}-NAH IN METHANOL. CONDITIONS: [C_{12}-NAH] = 8.91 x 10-5 M AND [MB] = 1.12 x 10-5 M. Δt FOR EACH SPECTRUM = 1 MINUTE. 1/10 V/V - METHANOL/ PHOSPHATE BUFFER, pH = 7.41 AND T = 22 °C.

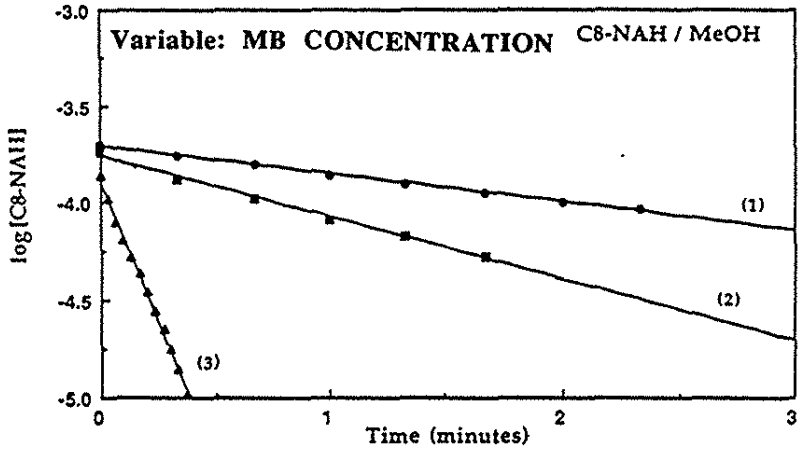

FIGURE 4. PLOT OF LOG OF [C_8-NAH] (in M) vs. TIME (in MINUTES). REACTION OF C_8-NAH (ε = 6350) MONITORED AT λ = 360 nm WITH MB. (CURVE 1 = 5 x 10-5 M, K_{obs} = 0.3342 min-1; CURVE 2 = 2 x 10-4 M, K_{obs} = 0.7283 min-1; CURVE 3 = 5 x 10-4 M, $K_{obs.}$ = 6.7457 min-1)

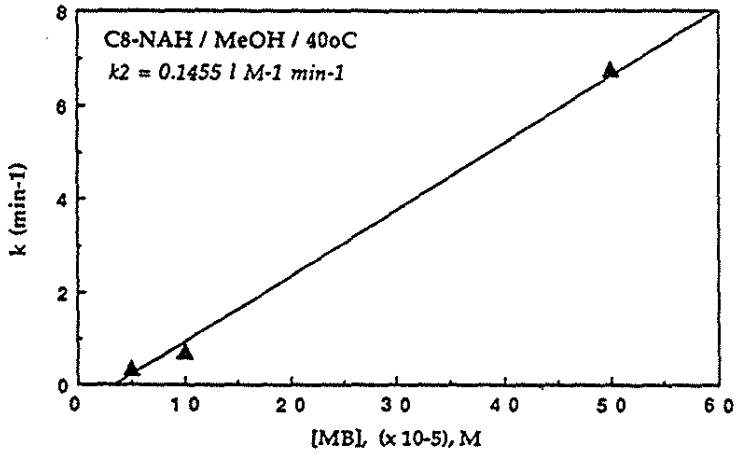

FIGURE 5. VARIATION OF THE OBSERVED RATE CONSTANTS FOR C_8-NAH REACTION WITH [MB] IN METHANOL OVER THE CONCENTRATION RANGE 5 x 10-5 M TO 50 x 10-5 M AT 40 °C.

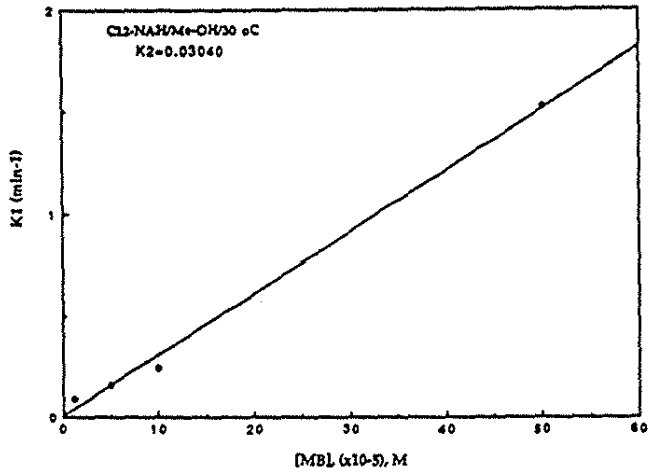

FIGURE 6. VARIATION OF THE OBSERVED RATE CONSTANTS FOR C_{12}-NAH REACTION WITH [MB] IN METHANOL OVER THE CONCENTRATION RANGE OF 0.5 TO 50 x 10-5 M AT 30 oC.

TABLE I : FIRST ORDER RATE CONSTANTS (K_1) FOR THE REDUCTION OF METHYLENE BLUE (MB) BY VARIOUS N-ALKYL DIHYDRONICOTINAMIDES UNDER VARIOUS CONDITIONS

Experiment	RNAH M ($x10^{-5}$)	M.Blue M($x10^{-5}$)	Temp. ^{o} C	Experimental Conditions#	k (min^{-1})
C_4-NAH					
1	14,43	1,12	22	1	0,0898
2	6,48	1,12	22	3a	0,0614
3	12,9	1,12	22	3a	0,1095
C_8-NAH					
4	7,52	1,12	10	2	0,0497
5	8,84	1,12	15	2	0,0648
6	8,13	1,12	22	2	0,1303
7	6,2	1,00	22	2,5	0,6565
8	20.5	50,0	30	2	5,7890
9	20.3	1,15	38	2	0,1429
10	20.63	5,0	40	2	0,3342
11	20.8	10,0	40	2	0,7283
12	24.7	50,0	40	2	6,7457
13	20.0	1,19	45	2	0,1701
14	5,15	1,12	22	3a	0,1647
15	14.0	5,0	35	3c	0,1738
16	17.2	5,0	35	3b	0,1892
17	9.7	5,0	35	3a	0,5029
18	8,66	1,12	22	2	0,0560

Experimental Conditions: (1) - Buffer: 0,03 M Na_2HPO_4; 0,0087 M KH_2PO_4;

(2) MeOH ; (3) a)SLS- 10^{-2} M; b) 5x 10^{-2} M ; - c) 10^{-1} M

(4) Irradiation: 300 to 400 nm (filter solution: 2 $CoSO_4$ + 1 $CuSO_4$), Xe arc lamp - 140 mW/ cm^2; (5)Degassing:. 15minutes with.He.or.N_2

TABLE I. FIRST ORDER RATE CONSTANTS (K_1) FOR THE REDUCTION OF METHYLENE BLUE (MB) BY VARIOUS N-ALKYL DIHYDRONICOTINAMIDES UNDER VARIOUS CONDITIONS

Experiment	RNAH M(x 10-5)	M.Blue M (x 10-5)	Temp. o C	Conditions#	k (min -1)
C_{12}-NAH					
19	8,91	1,12	22	2	0,0715
20	32.5	50,0	22	2	1,0579
21	12,73	1,12	22	2,4	0,2253
22	20.5	0,5	30	2	0,04187
23	7,43	1,12	30	2	0,1223
24	22.75	5,0	30	2	0,1600
25	26.5	10,0	30	2	0,2445
26	31.25	50,0	30	2	1,5241
27	21.25	10,0	40	2	0,4246
28	23.25	50,0	40	2	3,0989
29	9,77	1,12	22	3a	0,0926
30	17.45	5,0	35	3c	0,1271
31	15.02	5,0	35	3b	0,2065
32	12.60	5,0	35	3a	0,4260

#**Experimental Conditions:** (1)aqueous buffer of 0.03 M Na_2HPO_4; 0.0087 M KH_2PO_4; (2) MeOH ; (3) a) SDS- 10^{-2} M; b) 5x 10^{-2} M ; c) 10^{-1} M; (4) Irradiation: 300 to 400 nm using filter solution of $CoSO_4$ +$CuSO_4$ (2:1), Xe arc lamp - 140 mW/ cm^2; (5) Degassing: 15minutes with He or N_2.

TABLE II. SECOND-ORDER RATE CONSTANTS, K_2, AND ACTIVATION PARAMETERS FOR THE OXIDATION OF C_4-NAH, C_8-NAH and C_{12}-NAH DERIVATIVES BY METHYLENE BLUE

Compound	Temp. ^oC	k_2 ℓ $M^{-1}min^{-1}$	$E_{act.}$ $KJ.M^{-1}$	$\Delta H^{\#}$ $KJ.M^{-1}$	$\Delta S^{\#}$ $JK^{-1}min^{-1}$
C_4-NAH	22	$2,14 \times 10^4$ *			
C_8-NAH	22	$1,76 \times 10^4$ *	44,7	39,8	-208,5
"	40	0,1455			
C_{12}-NAH	22	$0,54 \times 10^4$*	19,6	14,7	-77,0
	30	0,03040			

*in O_2-purged solution.

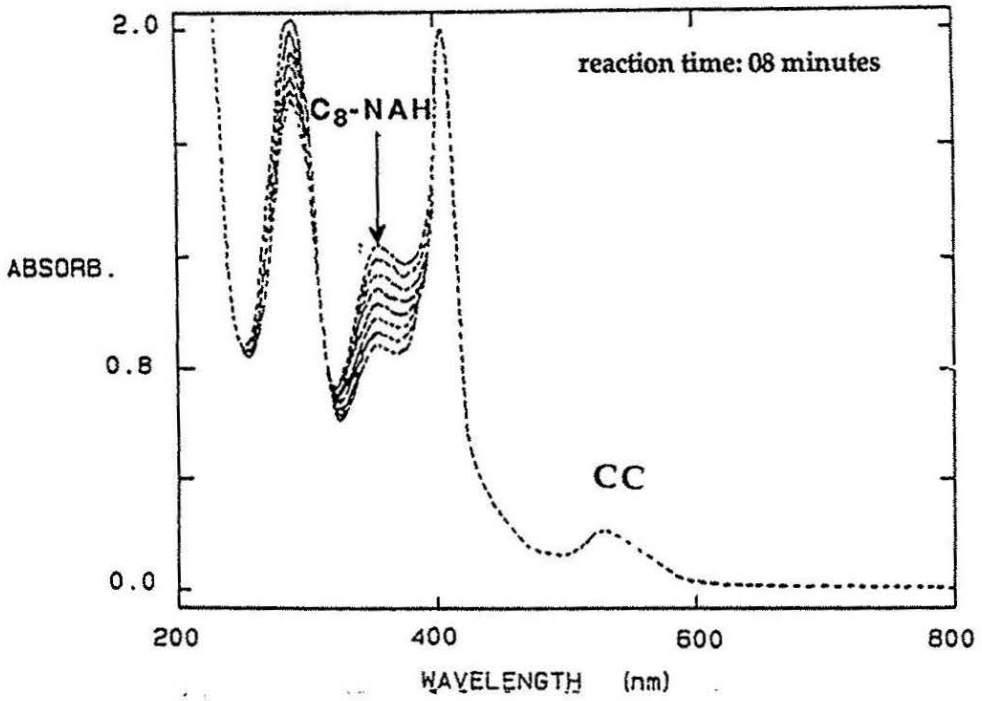

FIGURE 7. SPECTRAL CHANGES OBSERVED DURING THE REDUCTION OF CYTOCHROME-C BY C_8-NAH IN MICELLAR SOLUTIONS OF SDS. CONDITIONS: [C_8-NAH]= 11.06 x 10^{-5} M in SDS, ε = 6350; [CC] = 2.05 x 10^{-5} M IN BUFFER SOLUTION. Δt FOR EACH SPECTRUM IS 1 MINUTE; 1/10 V/V - [SDS] = 10^{-2} M, PHOSPHATE BUFFER, pH = 7.41 AND T = 30 °C.

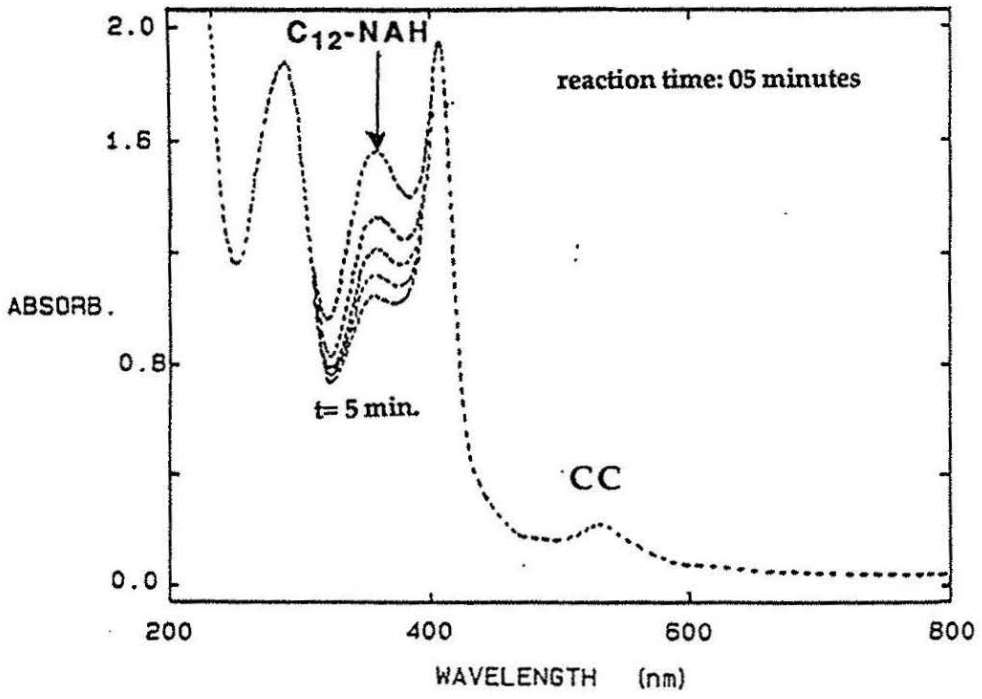

FIGURE 8. SPECTRAL CHANGES OBSERVED DURING THE REDUCTION OF CYTOCHROME-C BY C_{12}-NAH IN MICELLAR SOLUTIONS OF SDS. CONDITIONS: [C_{12}-NAH] = 25.22 x 10^{-5} M IN [SDS] = 10^{-2} M, ε = 4000, [CC] = 2.05 x 10^{-5} M IN BUFFER SOLUTION . Δt FOR EACH SPECTRUM IS 1 MINUTE; 1/10 V/V - SDS SOLUTION (10^{-2}M); PHOSPHATE BUFFER, pH = 7.41 AND T = 22 °C.

Table I - III presents rate data for the reduction of methylene blue and cytochrome-C with different R-NAH (R= C_4, C_8, C_{12}), under various conditions: concentration of R-NAH, temperature, oxygen presence and variation of number of SLS micelles.Table II presents data on the sencond order rate constants (k_2) and the activation parameters for the reaction of C_4, C_8 and C_{12} derivatives with MB.

The second order rate constant derived from the concentration dependence of MB is enhanced once, stacked dimers are known to be formed at high MB concentration [14]. Data from Table I and II for different R-NAH compounds indicate that dimers exhibit greater reactivity on the oxidation of R-NAH substrate as compared to the monomers.

The rate of reduction of CC is much less sensitive to the R-NAH concentration. High concentration of the donor leads to decrease the observed rate constant K_{obs}. One possibility would be formation of micelles when R-NAH+ concentration increases. Due to experimental limitations, the second order constant for CC reduction could not be determined.

Temperature dependence of the reduction was studied over the range of 22-38 °C. (A thermal decomposition of R-NAH coumpounds was observed when temperature rises to 40-45 °C. At temperatures below 15 °C non-reproducible results were obtained). The classical expression for the rate constant for a non-adiabatic electron exchange reaction contains a pre-exponential term which considers essentially the electron frequency, assuming that the reaction proceeds via thermal excitation [9]. According values presented in the Tables I - III, we can conclude that MB systems are much more thermally influenced with the additional variable of the chain length favouring the electron transfer processes in all systems.

For CC reduction, a slight increase on the reaction rate was observed with increasing temperature, which is in accordance to the idea that most biological electron-transfer processes are non-adiabatic [9].

TABLE III. RATE CONSTANTS (K_1) FOR R-NAH AND CYTOCHROME-C; WITH VARIED CONCENTRATIONS AND TEMPERATURES; LISTED BELLOW:

Experiment	C_4NAH M, (x 10^{-5})	Cyt.C M, (x 10^{-5})	Temp. °C	Conditions#	k (min^{-1})
1	10,18	2,05	22	1	0,0592
2	23,86	2,05	30	1	0,0439
3	19,09	2,05	22	1,4	0,0443
4	20,82	2,05	22	3	0,0303
5	16,21	2,05	30	3	0,0330
6	18,28	2,05	22	3	0,0468

#Conditions: (1) Buffer: 0,03 M Na_2HPO_4; 0,0087 M KH_2PO_4; (2) MeOH; (3) SLS= 0,01 M - (3a) SLS=0,1 M; (4) Irradiation: 300 to 400 nm (filter solution: 2 $CoSO_4$ + 1 $CuSO_4$); Xe arc lamp - 140 mW/ cm^2; (5) Degassing: 15 minutes with N_2 or He.

TABLE III. RATE CONSTANTS (K_1) FOR R-NAH AND CYTOCHROME-C; WITH VARIED CONCENTRATIONS AND TEMPERATURES; LISTED BELLOW:

Experiment	RNAH M, (x 10^{-5})	Cyt.C M, (x 10^{-5})	Temp. ^{o}C	Conditions#	k (min^{-1})
C8NAH					
7	12,0	2,05	15	2	0,0462
8	11,99	2,05	30	2	0,0780
9	12,11	2,05	22	2,4	0,0763
10	21,46	2,05	22	2,4	0,0318
11	13,16	2,05	22	2,4	0,0646
12	10,55	2,05	22	2,5	0,0445
13	16,2	3,76	22	2	0,0340
14	15,6	8,36	22	2	0,0355
15	10,75	2,05	22	3	0,0327
16	11,06	2,05	30	3	0,0513
C12NAH					
17	25,88	2,05	22	2	0,0349
18	16,81	2,05	22	2	0,0376
19	16,44	2,05	30	2	0,0353
20	25,22	2,05	22	3	0,0834
21	26,14	2,05	30	3	0,0633
22	30,02	2,05	22	3,4	0,1466
23	13,08	4,91	30	2	0,0805
24	14,32	4,91	22	2,4	0,8486
25	13,02	4,91	22	2,4	0,7945
26	55.8	8,36	22	3a,4	no reaction
27	42.5	4,91	22	3a	no reaction
28	56.2	8,36	30	3a	no reaction

#Conditions : (1) Buffer: 0,03 M Na_2HPO_4; 0,0087 M KH_2P0_4;(2) MeOH; (3) SLS= 0,01 M - (3a) SLS=0,1 M; (4) Irradiation: 300 to 400 nm using a filter solution of $CoSO_4$ + $CuSO_4$ (2:1);Xe arc lamp, 140 mW/cm^2;(5) Degassing: 15 minutes with N_2 or He.

As described in the literature [8] solubilization of donor and/or acceptor molecules in micellar assemblies provides control on solute distribution generating mainly monomers and as consequence enhancing efficiencies of photoredox processes. Data on MB reduction in the presence of SLS micelles confirm such possibilities.Table I shows (exp. 30-32) that k_{obs} decreases with increasing SLS concentration. For CC case, compartimentalization has also a negative effect. As shown in Table III (exp. 26 to 28) in the presence of SLS (concentration 10^{-1} M), no reduction is observed. The reaction may be blocked because of solubilization of the electron donor in the micellar assemblies.

The majority of the photochemical conversion schemes are based on light-induced electron-transfer reactions. When a molecule absorbs a photon of suitable energy, an electronically excited state is obtained that is a better oxidant and reductant than the ground-state [1-c, 9]. An electron-transfer reaction between such an excited state and a suitable reaction partner may convert a fraction of the absorbed light into chemical energy. Experimentally, the reduction of MB by R-NAH is enhanced upon photolysis. By comparison of the extend of reduction of two similar solutions (one kept in the dark and one irradiated) , an increase of approximately 80% of reaction yield by photolysis has been estimated. Photolysis by CC containing solutions however leads to non-reproducible results and first order kinetics is observed no longer due to decomposition of the central heme.

We may conclude that the reduction of methylene blue and cytochrome-C by the dihydronicotinamides follows first order kinetics in all systems. The electron transfer process is enhanced in the presence of MB (sensitized reaction), under irradiation and by increasing the chain length ($C_{12}>C_8>C_4$). The slow electron transfer of CC is due to restrictions of reorientation of its dipoles, the molecule shows differences in the equilibrium structure when the heme changes from ferric to ferrous state.

Aknowledgements : CNPq (Brazilian National Research Council) for financial support.

REFERENCES

1 . (a) J. Everson, B. Anderson, Eds. K.S. You, *The Pyridine Nucleotide Enzymes*, Academic Press, New York, 1982 ;(b) G.K. Vemulapalli, *Physical Chemistry*, Prentice-Hall, Inc., 1993; (c) K. Kalyanasundaram in *Photochemistry in Confined Media*, V. Ramamurthy ed., VCH Publishers, New York, 1991; (c) G. Lappin, *Redox Mechanisms in Inorganic Chemistry*, Prentice-Hall, London, 1994; (d) K.Kalyanasundaram, *Photochemistry in Microheterogenous Systems*, Ac. Press Inc., London, 1987.

2. (a)R.J. Kill, D.A. Willowson, in *Bioinorganic Chemistry*, Academic Press New York, Volume IV, Chapter 8, 1991; (b) D. S. Sigman, J. Hijdu and D.J. Creighton, *ibid*, chapter 14.

3 . J. Handman, A. Harriman and G. Porter, *Nature*, *307*, 534 (1984).

4 . K. Kalyanasundaram, *J. Photochem. Photobiol.*, *42A*, 87 (1988).

5 . (a)F. M. Martens , J. W. Verhoeven, *Recl. Trav. Chim. Pays-Bas*, 228 (1981); (b) C. Cilento, D.L. Sanioto, *Arch. Biochem. Biophys.*, *110*, 133 (1965).

6 . S.K. Chung, S.U. Park, *J. Org. Chem.*, *47*, 3197, (1982).

7 . S. Aono, T. Kita, I. Okura, A. Yamada, *Photochem. Photobiol.*, *43*,1 (1986).

8 . S. Shinai, T. Tsuno, O. Manabe, *J. Chem. Soc., Perkin Trans. II*, 1533 (1983).

9 . K. Kalyanasundaram, T. Colassis, R. Humphry-Baker, *J. Am. Chem. Soc.*, *111*, 3300 (1989).

10 . T. Colassis, Diploma Dissertation, EPF-Lausanne, Switzerland (1989).

11 . P. Karrer, G. Schwartzenbach, U. Solmssen, *Helv. Chim. Acta*, *19*, 811 (1936).

12 . K. Wallenfels, H. Schully, *Justus Liebigs Ann. Chem.*, *621*, 178 (1959).

13 . S.L. Murov, *Handbook of Photochemistry*, Marcel Dekker Inc., New York, 1973.

14 . M.S. Chang, J.R. Bolton, *Solar Energy*, *24*, 561 (1980).

15 . P. Karrer, G. Schwartzenbach, G.E. Utzinger, *Helv. Chim. Acta*, *20*, 72, (1937).

16 . J.F.J. Engbersen, A. Koudjis, H.C. van der Plas, *Recl. Trav. Chim. Pays-Bas*, *104*, 131 (1985).

17 . F. M. Marten, J. W. Verhoeven, P. Bergwerf, *J. Photochem.*, *22*, 99 (1983).

18 . N.A. Wiederkehr, Thèse de Doctorat, EPF-Lausanne, Switzerland (1991).

SOUTHERN BRAZILIAN JOURNAL OF CHEMISTRY

Vol. 2, No.2, 1994

AUTHOR INDEX / ÍNDICE DE AUTORES

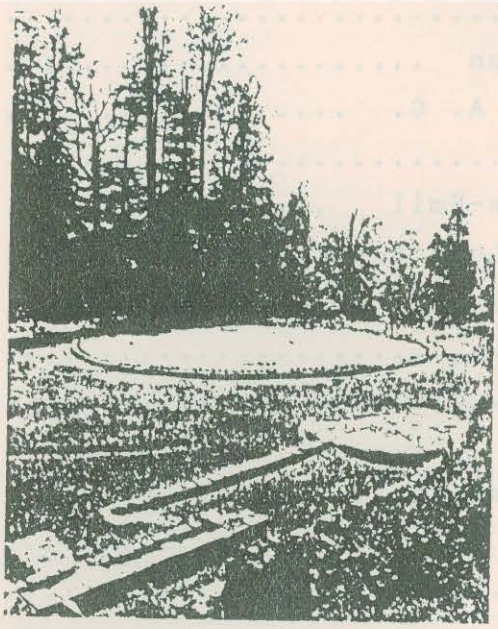

SANTUÁRIO DÁCICO DE SARMISEGETUSA, ROMÊNIA

DACIAN SANCTUARY IN SARMISEGETUSA, ROMANIA

ISSN 0104-5431

SOUTHERN BRAZILIAN JOURNAL OF CHEMISTRY

The *SOUTHERN BRAZILIAN JOURNAL OF CHEMISTRY* is an international forum for the rapid publication of original scientific articles dealing with chemistry and related areas. At the present there are no page charges and the authors will receive twenty five free reprints of their papers.

SPECIAL COMBINATION OFFER FOR NEW SUBSCRIBERS!

SUBSCRIPTION INFORMATION

PRICE: Brazil and Latin America: US$ 35.00 per issue.

Other Countries: US$ 50.00 per issue, including air mail delivery.

Persons or institutions outside Brazil should send subscription fee payable to Dr. L. G. Ionescu, c/o SBJC 8532 Howard Circle, Huntington Beach, California, USA 92647

ORDER FORM

☐ Please enter my subscription for _____ issues of Southern Brazilian Journal of Chemistry.

☐ Please send me _____ copies of the Southern Brazilian Journal of Chemistry (Vol. 1, Nº 1, 1993).

☐ I enclose a check or money order in the amount of $_____

☐ Please send me a Pro Forma Invoice for the above order.

NAME OR INSTITUTION: .....

ADDRESS: .....

.....

SOUTHERN BRAZILIAN JOURNAL OF CHEMISTRY

Lavinel G. Ionescu, B.S., M.S., Ph.D.,Editor
C.P. 15032, Agronomia
Porto Alegre, RS BRAZIL 91501-000
TEL. (051) 485-1820 FAX. (051) 339-1564

INFORMATION FOR AUTHORS

The Southern Brazilian Journal of Chemistry - SBJC will publish review articles, original research papers and short communications dealing with chemistry and interdisciplinary areas such as materials science, biotechnology, bioengineering and other multidisciplinary fields.

Articles report the results of a complete study. They should include an Abstract, Introduction describing the known art in the field Experimental or Materials and Methods, Results and Discussion, Acknowledgments (when appropriate) and References.

Short Communications should be limited to 1500 words, including the equivalent space for figures and/or tables and should include an Abstract and concise Experimental.

Manuscripts may be submitted on-line or in triplicate (original and two copies by registered mail) and are received with the understanding that the original has not been submitted for publication elsewhere. It is implicit that all the persons listed as authors have given their approval for the submission of the paper and that permission has also been granted by the employer, when necessary.

Manuscripts must be written in American or British English, single spaced, on A4 sheets (21 cm x 29.5 cm) and one side only and should be numbered beginning with the title page. Type must be 12 Arial or Times New Roman.

Margins of at least 3 cm should be left at the top and bottom and both sides of each page. The first page of the paper should contain only the title of the paper, the name(s) and addressees) of the author(s), an abstract of not more than 250 words and 4-8 keywords. We reserve the right to translate the abstract in Portuguese. Abstracts are required of all papers including reviews and short communications.

Figures and Tables with short explanatory titles, each on a separate sheet, should be adequate for direct reproduction and identified in pencil on the back of each page by Arabic numerals, corresponding to the order they appear in the manuscript. Tables and Figures (BMP or JPG format) may also be included directly in the text when convenient and the article may submitted in a quasi-final form in order to facilitate editorial work.

References should be numbered in the sequence they appear in the text, cited by superior numbers and listed at the end of the paper in the reference section in the numerical order they appear in the text. The style for references is shown below:

1. L. G. Ionescu and D. S. Fung, *J. Chem. Soc. Faraday Trans. I, 77*, 2907-2912 (1981).
2. K. L. Mittal, Ed., "*Solution Chemistry of Surfactants*", Plenum Press, New York (1984), Vols. 1-3, pp. 1-2173.

IUPAC Rules should be used for the name of chemical compounds and preference should be given to 51 units.

Authors are invited to send manuscripts by registered air mail to the EDITOR - SBJC, C.P. 15032, Agronomia, Porto Alegre, RS BRASIL 91501, or by e-mail to **lavinel@ibest.com.br** or **lavinel@pop.com.br**.

VISIT OUR SITE: http://www.sbjchem.he.com.br

SCIENCO
SOUTHERN BRAZILIAN JOURNAL OF CHEMISTRY

ISSN 0104-5431

The *SOUTHERN BRAZILIAN JOURNAL OF CHEMISTRY - SCIENCO* publishes original research articles in chemistry and related interdisciplinary areas and is intended to fill a gap in terms of scientific information for Southern Brazil.

Occasionally the journal will include review papers and articles dealing with chemical education and philosophy and history of science. It will be published mainly in English, with abstracts in Portuguese and only occasional papers in other languages. At the present there are no page charges and the authors will receive twenty five reprints of their papers free of charge.

We have set high standards for the articles to be published by ensuring strong but fair refereeing by at least two reviewers. We hope that this journal will provide a forum for dissemination of high quality research in chemistry and related areas and are open to any questions and suggestions.

The Editor

SUBSCRIPTION INFORMATION

Brazil and Latin America:
US$ 35.00 per issue.

Other Countries: US$ 50.00 per issue, including air mail delivery. Persons or institutions outside Brazil should send subscription fee payable to Dr. L. G. Ionescu, c/o SBJC, 8532 Howard Circle, Huntington Beach, California, USA 92647

MAILING ADDRESS

SOUTHERN BRAZILIAN JOURNAL OF CHEMISTRY - SBJC
Lavinel G. Ionescu, B.S., M.S., Ph.D., Editor
C.P. 15032, Agronomia
Porto Alegre, RS BRASIL 91501-000
Tel. (051) 485-1820 FAX (051) 339-1564

Endless Column, 1937, cast iron
CONSTANTIN BRÂNCUSI

FINANCIAL SUPPORT

SARMISEGETUSA RESEARCH GROUP

SANTA FE, NEW MEXICO, U.S.A.